School of Electrical Engineering, Computing, and Mathematical Sciences

Optimal Control of Microalgae for Maximum Lipid Production

Todd Michael Hurst

0000-0003-4654-7039

This thesis is presented for the Degree of

Doctor of Philosophy

of

Curtin University

May 2021

Declaration

To the best of my knowledge and belief this thesis contains no material previously published by any other person except where due acknowledgement has been made.

This thesis contains no material which has been accepted for the award of any other degree or diploma in any university.

Signature: .....

Name: Todd Michael Hurst

Date: 05-05-2021

Publications

Published papers related to this thesis

T. Hurst and V. Rehbock, "Optimal control for micro-algae on a raceway model," *Biotechnology Progress*, 2017, ISSN: 1520-6033. DOI: 10.1002/btpr.2532. [Online]. Available: https://aiche.onlinelibrary.wiley.com/doi/abs/10.1002/btpr.2532.

T. Hurst and V. Rehbock, "Optimizing micro-algae production in a raceway pond with variable depth," *Journal of Industrial & Management Optimization*, 2021. DOI: 10.3934/jimo.2021027. [Online]. Available: https://www.aimsciences.org/article/doi/10.3934/jimo.2021027.

Papers related to this thesis, accepted, but not yet published

T. Hurst and V. Rehbock, "Optimizing a micro-algae raceway model with periodic boundary conditions," *DCDIS Series B: Applications & Algorithms*, to appear.

Attribution Statement

The thesis is largely based on the results of the three papers listed above. As required by the Curtin University Higher Degree by Research Policies and Procedures here are the Attribution Statements for each paper. The relative attributions of the authors are thus also reflective of the entire thesis.

"Optimal control for micro-algae on a raceway model" [47]					
	Conception and Design	**Construct of Optimisation Model**	**Implementation and Numerical Results**	**Analysis of Results**	**Interpretation and Discussion**
Co-Author 1 Todd Hurst	90	95	100	95	95
Co-Author 1 Acknowledgment: I acknowledge that these represent my contribution to the above research output and I have approved the final version. Signed:					
Co-Author 2 Volker Rehbock	10	5	0	5	5
Co-Author 2 Acknowledgment: I acknowledge that these represent my contribution to the above research output and I have approved the final version. Signed:					

"Optimizing micro-algae production in a raceway pond with variable depth" [48]					
	Conception and Design	**Construct of Optimisation Model**	**Implementation and Numerical Results**	**Analysis of Results**	**Interpretation and Discussion**
Co-Author 1 Todd Hurst	95	95	100	95	95
Co-Author 1 Acknowledgment: I acknowledge that these represent my contribution to the above research output and I have approved the final version. Signed:					
Co-Author 2 Volker Rehbock	5	5	0	5	5
Co-Author 2 Acknowledgment: I acknowledge that these represent my contribution to the above research output and I have approved the final version. Signed:					

"Optimizing a micro-algae raceway model with periodic boundary conditions" [46]					
	Conception and Design	**Construct of Optimisation Model**	**Implementation and Numerical Results**	**Analysis of Results**	**Interpretation and Discussion**
Co-Author 1 Todd Hurst	95	95	100	95	95
Co-Author 1 Acknowledgment: I acknowledge that these represent my contribution to the above research output and I have approved the final version. Signed:					
Co-Author 2 Volker Rehbock	5	5	0	5	5
Co-Author 2 Acknowledgment: I acknowledge that these represent my contribution to the above research output and I have approved the final version. Signed:					

Abstract

This thesis is concerned with the use of computational optimal control methods to determine optimal strategies for operating raceway ponds in order to maximise the lipid yield of microalgae grown therein. The idea of using lipids from microalgae as a base for biofuels to mitigate the worlds dependence on crude oil has been considered by researchers over several decades. This strategy of generating biofuels is not currently considered to be cost competitive with fuels generated from crude oil. At the same time, incremental yield improvements of both biomass and lipids produced in bioreactors are continually being made and it is not yet clear if or when we will reach a point where this process is as or more economical then generating fuels from crude. Thus the main purpose of this thesis is to explore a variety of strategies by which lipid yield from microalgae may be improved in order to get a better understanding of the ultimate potential of this technology. Our background is in mathematics and computing and we hence choose to work with mathematical models of algal growth rather than trying to test strategies on actual raceway ponds. While this leads to obvious limitations in the direct applicability of our results, it also allows us to employ powerful numerical optimisation tools to develop strategies rather trying to incrementally develop these strategies by a long sequence of time consuming experiments on actual ponds. Although the optimal strategies developed in this manner may not perform as well in practice as they do for a mathematical model, they will give practitioners a useful guide to improving the algal growth process and may even lead to new insights into the growth process itself.

We start by briefly describing the human use of microalgae over history with a particular focus on biofuel production. Next, we examine a variety of mathematical models of algal growth, both in a general setting and in the context of raceway ponds. Microalgae growth can be influenced by temperature, light, nutrient availability, CO_2 availability, and pH level. All of these processes have been analysed and modelled mathematically, starting with simple Michaelis-Menten-Monod kinetics, concerned only in a single substrate, and leading to complex systems of differential and algebraic equations which track various combinations of light intensity, chlorophyll, temperature,

intra and extracellular nutrients, lipid biomass, and total biomass. We consider the suitability of various models towards the aim of optimising lipid production and then choose the most appropriate one for the basis of our computational studies. This model combines a Droop growth model, a Michaelis-Menten-Monod type model of light intensity, and a temperature effect model for the total growth of microalgae where nitrogen, light intensity, and temperature are all limiting factors of growth. The setting of the model is a raceway pond bioreactor that assumes a completely mixed medium.

The problem of maximising biomass or lipid growth can be formulated as an optimal control problem. We give a brief review of this general class of mathematical optimisation problems and the necessary conditions for a locally optimal solution. As most practically orientated problems in this class are too complex to solve analytically, we review a range of existing numerical solution methods, particularly those which are used in this thesis.

Next, we describe in detail the mathematical model which forms the basis of the numerical studies in this thesis. We give an open loop optimal control formulation for maximising either biomass or lipid yield. We then transform the system of differential algebraic equations in the model to a system of ordinary differential equations in order to make the problem suitable for solution by the MISER optimal control package we intend to use. This introduces dynamics for average light intensity and chlorophyll, yielding a total of seven state variables. We then use MISER to determine the optimal inflow rates to maximise either biomass or lipids and compare these results to those published previously with the original model. Our results yield a 10% improvement in biomass and a 20% improvement in lipids and are very close to satisfying the first order conditions of optimality. For the remainder of the thesis, we are focussed on lipid production only and we measure any further lipid yield improvements with respect to this base case lipid result.

Next, we modify the original optimal control formulation of the model to allow for variable nutrient concentration of the inflow (as a second control variable) as well as making the initial nutrient concentration of the pond a decision variable. For modest increases in nutrient concentration, we show that lipid yield can be improved by about 28% over the that in the base case. Higher upper bounds on the nutrient concentrations lead to further improvements still. We test the robustness of the corresponding optimal controls with respect to various disturbances of the dynamics and we also formulate and solve a feedback optimal control version of the problem. Both the open loop and feedback optimal controls appear to be quite robust with respect to these disturbances.

We next consider the possibility of variable raceway depth. In the first instance, we assume the depth to be constant over the time horizon and model it as a decision variable within the problem

formulation. If we maintain the same pond volume, the solution generated demonstrates that lipid yield can be improved by over 40% with a very shallow pond at the expense of a much larger surface area. If instead we choose to fix the surface area and allow volume to vary with the chosen depth, the resulting lipid yield improvement is about 8% over that of the base case (assuming the same amount of initial nutrients and biomass as for the base case model). As a second variation, we also consider the case where the pond depth is allowed to vary over the time horizon. This requires an additional state variable to model depth as well as an additional control to allow for variable outflow. The modified dynamics are again transformed into a system of ordinary differential equations and the resulting problem is solved with MISER. Numerical results show that the lipid yield can be increased by 67% compared to that obtained with the base case when pond depth is allowed to vary over the time horizon.

The open loop control results generated thus far have the common feature of a washout period, i.e. high flow rates are imposed near the end of the time horizon in order to maximise the algae harvest. This is consistent with the batch process nature of the optimal control formulation but it also leaves a pond largely depleted of algae at the end if the process. As preparing the pond for the next batch may be quite costly, we also consider a modified optimal control model which allows for a continuous operation of the pond. This is done by imposing terminal constraints on the state variables of the model such that the terminal states are equal to their values at the start of the time horizon. At the same time, we allow the initial and final values of the state variables to be decision variables. This turns out be a more challenging numerical problem to solve and the best solution obtained by MISER proved to be somewhat suboptimal. However, we are able to use another computational method to derive an optimal solution to this problem. Both solutions give an improvement of around 45% in lipid yield over that obtained for the base case problem. However, we also show that the optimal periodic boundary conditions are difficult to reach in finite time from arbitrary initial conditions. Nevertheless, the optimal periodic solution provides a useful benchmark which can inform the design of more practical control algorithms for the system in the future.

We conclude the thesis by outlining the main shortcomings of the existing model and optimal control formulations and suggest a variety of ideas for future numerical studies in this area.

Acknowledgements

Formally, I obligedly acknowledge that the research for this thesis is and was supported by an Australian Government Research Training Program (RTP) Scholarship.

Then, I acknowledge that this research is and was done on Aboriginal land and recognise the strength, resilience, and capacity of the Noongar people of southern Western Australia.

I thank Professor Kok Lay Teo for his teachings and support as one of my supervisors as part of the time for creation of this thesis. He has been a brilliant person to consult for access of his broad and deep knowledge.

I thank Professor Yong-Hong Wu for his guidance through the bureaucratic forest as well as being the chair of my thesis committee. He has been one of the best people to show the correct route when hiking through this greenwood.

I thank Professor Helmut Maurer for his encouragement to use the AMPL package and his assistance with the implementation of our model therein.

I keenly thank Doctor Ian Van Loosen for his constant guidance and assistance as a co-supervisor over the entire time for the creation of this thesis. Ian has been a great comfort, able to answer questions and push me in the right direction when others have been unavailable.

I deeply thank Associate Professor Volker Rehbock for his enormous support and for being an extremely sturdy mentor throughout these long years. I also thank him for his friendship after retirement, yet continuance as an Adjunct Professor as a co-supervisor. Volker has been a truly wonderful person to guide me on this research as well as to quell my anxiety any time it arose, helping me avoid falling down the rabbit hole.

Yarr, I thank me wench 'n beauty, Natalie Hurst, fer her emotional 'n social support, bein' at the helm o' this ole ship (meself) durin' the sail through dark waters.

I thank the entire staff of ENT, Physiotherapy, Speech-pathology, Radiation, and Medical Oncology of Sir Charles Gairdner Hospital for their life extending procedures through the cancerous times.

Contents

List of Figures

List of Tables

Chapter 1

Introduction

1.1 Microalgae and their role in the World

Algae is the name given to a range of aquatic organisms which are capable of carrying out photosynthesis (the process of converting the energy in sunlight to generate carbohydrates). Common examples of algae familiar to most of us are seaweeds and pond scum which often make aquatic environments less attractive to humans. In fact, there exists a huge variety of algae. Many of these have the potential for human use while many more are actually critical to human existence.

Algae differ from higher level plants in that they lack features such as roots, stems, leaves, and a vascular system to circulate water and nutrients through their bodies. Some algae are multicellular and take on a leafy appearance such as giant kelp which can grow as long as 60 metres. Most, however, are unicellular and exist as single, microscopic cells, and are hence referred to as microalgae. Even microalgae can exist in a chain or group structure, thereby making them visible to the naked eye. Their sizes can be measured in terms of micrometres and they are specially adapted to a fluid environment dominated by viscous forces. Microalgae in both freshwater and marine environments are essential to maintain life on the planet. They are estimated to contribute about half of our planets oxygen production and simultaneously consume large amounts of carbon dioxide. In addition, microalgae are considered the basis of the marine food web, being the primary food source of many marine species such as molluscs, filtering bivalves, and the larval stages of fish and crustaceans.

The variety of microalgae is huge with an estimated 200,000 - 800,000 species inhabiting the planet. Only about 50,000 of these have been identified so far. More than 15,000 distinct chemical compounds originating from algal biomass have been isolated. These include carotenoids, antioxi-

dants, fatty acids, enzymes, polymers, peptides, toxins, and sterols [82]. Human use of microalgae has a long history with the first documented incidence being the consumption of the Nostoc genus of blue-green algae as a food source during famine by the Chinese 2000 years ago. The Aztec of middle America are reported to have harvested microalgae from natural lakes for human consumption as far back as the 1600s [14, 26]. Today, microalgae are grown and harvested commercially in many countries of the world, yielding a range of products that can be used for pharmaceuticals, food supplements, cosmetics, animal feed and feed for aquaculture operations [12, 82, 103, 128]. The worlds largest microalgae production plant consisting of a 250 hectare series of artificial ponds is located in the Hutt Lagoon, about 450 km north of the Western Australian state capital Perth. The main product is β-carotene, used as a food colouring and vitamin A supplement.

In many parts of the world, microalgal blooms occur in freshwater lakes and rivers, often due to human influence. An algal bloom results from excess availability of nutrients (often due to release of untreated waste-water or fertiliser run-off from intensive farming operations) combined with high water temperatures and slow water flow. Algal cells can multiply rapidly in these conditions leading to high biomass loads, low oxygen levels, and release of toxins. This often results in the mass death of other aquatic species. However, the same algal species involved in these algal blooms can also be used in a targeted way to treat waste-water and extract excess nutrients. Indeed, there are many publications which examine the dynamics of algal blooms and many others looking at the use of algae in water purification [88, 113, 124].

1.2 Biofuel and Microalgae

As the earth's supply of easily accessible crude oil depletes, various substitutes of have been considered. Among these are biofuels which can be classed into four distinct generations. First generation biofuels are made from edible high energy crops grown on arable land where their sugar, starch, and vegetable oils are converted to ethanol or biodiesel with yeast fermentation or transesterification, respectively. However, growing these crops has an obvious negative impact on global food production, thus sparking research into further areas. Second generation biofuels are created from non-edible waste plant or animal biomass. The main fuel produced in this way is methane which is used mainly for power generation, but it is not a very useful substitute for crude oil. Third generation biofuels use microalgae with a large lipid concentration as a feedstock which can be grown on non-arable land. A major advantage of microalgae over terrestrial plants is that they can grow 20-30 times faster. Fourth generation biofuels refer to genetically modified versions of

micro-organisms to improve the hydrogen to carbon yield as well as providing an artificial carbon-sink. This promotes absorption of carbon dioxide from the atmosphere, thereby reducing the worlds overall carbon-footprint [1].

The composition of microalgae is by no means uniform but varies considerably between different species and even within the same species when exposed to different environments. Many microalgae can endure in a wide variety of environments. It is possible to concentrate various desirable products in these species by changing environmental conditions such as temperature, illumination, pH, carbon dioxide supply, salinity, and nutrient concentration. Nutrient availability can effect microalgae growth in a number of ways. In the context of biofuel production, it is interesting to note that when starved of nutrients, some species will accumulate lipids more rapidly thanks to photosynthesis and respiration [12, 66, 116].

The first documented proposals to grow microalgae as a source of lipids for food or fuel appeared in 1942 [41, 42] in Germany. In the early 1950s efforts were made in the US, England, Germany, Japan, and Israel to grow and process algae on a larger scale [19] with little to no success. Renewed efforts in the area appeared in the 1970s as a consequence of crude oil shortages due to political instability in the Middle East. The US Department of Energy established the Aquatic Species Programme (ASP) in 1978 with the aim of developing liquid transportation fuel from algae which could compete with crude oil. It examined a large variety of algal species as well as a range of growth and production systems over an 18 year period until its closure in 1996 due to record low oil prices. While the program demonstrated that large scale production of fuel from algae grown in outdoor ponds was possible, the cost of production could not compete with that of crude oil [116].

Although not directly concerned with the growth of algae for fuel, Japan's research institute of Innovative Technology for the earth (RITE) started a research programme with the aim of CO_2 sequestration via the growth of microalgae. It was shown that microalgae could be grown successfully using power plant flue gas as a CO_2 source [92] and this has had a significant influence on subsequent algal biofuel research [82, 128]. Note that CO_2 sequestration was also a focus of the ASP [115, 116]. More recently the US National Renewable Energy Laboratory (NREL) has continued the ASP's work in biofuel production from microalgae [115].

In the early 2000s, rising crude oil prices led to a renewed interest in algal biofuels with numerous research projects funded in the US, Europe, the Middle East, and Australia among many other places [98]. Several companies started selling algae derived fuel from 2012, but this did not continue very long and most of them either no longer exist or they have switched to producing higher valued lipids for human consumption [36, 127].

1.2.1 Cultivation of Microalgae

Farming of microalgae combines the growth of biomass with different methods of harvest and extraction [82, 105, 128]. Microalgae growth occurs in a 'bioreactor' which is either a closed or open system. Biomass harvest is usually done through centrifugal or flocculation methods. Lipid extraction is performed with cell disruption or cell rupture and the subsequent application of solvents, if needed. We discuss these briefly below.

Bioreactors

Bioreactor is the general term for various biological production systems and these can be either industrial plants or ponds [17]. More specifically, a photo-bioreactor is a system for growing microbial, algal or plant cells in which these carry out a photo-biological reaction. A bioreactor system can be closed, open, or a hybrid of both. Closed systems are those where the culture is sealed from the environment; open systems are those where the culture is directly exposed to it. Note that the term photo-bioreactor is commonly understood to describe a closed system [82].

Closed Systems

For algal growth, closed system photo-bioreactors usually consist of a set of containers containing a mixture of water, microalgae, and CO_2. Closed system photo-bioreactors allow for a set environment of temperature and light for the culture to grow in. This environment is usually managed in such a way as to provide the optimal growth conditions for the algae [12, 82, 132].

This flexibility allows for the cultivation of many algal species which would not survive in an open pond. Closed systems are often made of transparent containers and pipes which allows for greater light penetration into the culture, although the light does first have to cross the reactor walls.

Closed systems have a number of obvious advantages.

- The growth environment can be well controlled in terms of nutrient concentrations, temperature, and light exposure.
- Atmospheric contamination can be kept to a minimum.
- Evaporation can be minimised.

As a consequence of these advantages, closed systems are capable of growing algae to much higher densities than open systems. This subsequently leads to more efficient harvesting of the algae.

Unfortunately, closed systems also suffer from many limitations:

- High capital costs, especially with the use of glass for vessels or tubing. Less expensive materials such as plastics can reduce the cost significantly but these also need to be renewed more frequently. Costs also increase significantly with scale.
- Biofouling of the vessels or tubing frequently occurs and can be expensive to correct.
- Cooling is often required and artificial lighting is also frequently employed. Both of these can lead to very high energy costs.

As a consequence the cost of biomass production in closed systems is estimated to be one order of magnitude higher than that of corresponding open systems. Thus, commercially viable closed systems are currently only used for high value products such as pharmaceuticals and cosmetics.

Open systems

Open systems can take various forms such as a shallow lagoon/pond, an inclined system, a circular central-pivot pond, or a raceway pond [12, 14]. Shallow ponds are of varying sizes and have been used with microalgae as simple waste-water treatment systems for thousands of years. Shallow ponds are also often fertilised with manure as a means for the growth of algal biomass.

Inclined systems have the cultures flow down an angled surface. It is collected at the bottom and then pumped back to the top of the inclined surface. This circulation is maintained during daylight while at night the culture is aerated and mixed in a large tank to reduce pumping costs and maintain its temperature.

Circular central-pivot ponds can be up to 50 metres in diameter and are mixed with a rotating arm mounted at the centre of the pond [14]. These are some of the oldest pond types used for commercial algae production. One of their disadvantages is uneven mixing due to the arm travelling over a greater distance at the periphery.

Raceway ponds are easily scalable and generally the most economical to create and operate. They are the most widely used system for microalgae production commercially. The simplest type of these ponds is a ditch dug from the ground with appropriately sloped sides. Viewed from the top, the shape of a raceway pond is usually an oval. A paddle usually drives water around the raceway to keep the culture mixed. The flow rate is typically between 20 and 30 $\mathrm{cm\,s^{-1}}$ [14]. Commercial algae raceway ponds are plastic lined using materials such as HDPE textile or PVC. The lining, although expensive, results in less resistance to water circulation. When correctly installed, these

liners can last around 20 years [14]. Ponds can be directly dug into the ground and lined, or they may be built up from the ground with concrete blocks or concrete cast in situ, after which lining is usually also installed. Concrete is not suitable with seawater unless it is epoxy coated which adds significantly to the expense.

The main advantages of open systems compared to closed ones are as follows:

- They have much lower capital and maintenance costs.
- They require far less energy to operate.
- They can be easily scaled up to handle large volumes which is especially important in waste water treatment.
- Although they are not suitable for all algae species, they mimic the natural environment of many of them.

Open systems do have a wide range of disadvantages:

- They are directly influenced by weather conditions. Evaporation and rain make it difficult to control the water level and therefore algal and nutrient concentrations. Artificial heating and cooling are usually not viable so the temperature can fluctuate significantly. Seasonal variations and unpredictable cloud cover result in inconsistent insolation.
- They are easily contaminated by other algae and bacteria.
- They occupy a significant area.

Note that the last of these disadvantages is less of a problem in remote locations such as the north west coast of Western Australia where large tracts of land as well as seawater and consistent sunlight are readily available [15, 115].

It is also possible to partially or fully cover raceway ponds to limit contamination and evaporation. In colder climates, covers can help to maintain a suitable temperature, while temperatures may become excessive when covers are used in warmer locations. Finally note that for most raceway pond operations, the only source of CO_2 required for algae growth is from the atmosphere. Since only about 0.04% of the atmosphere is CO_2, this situation can lead to a significant restriction on algal growth. It is possible (and often desirable if a pond is situated close to a power plant with CO_2 emissions) to enrich the CO_2 supply by aerating the water directly with CO_2 [62]. Despite their many disadvantages, most researchers currently consider raceway ponds as the only viable

option for producing large volumes of lipid biofuels from algae. The algae growth model we consider throughout this thesis assumes growth in a raceway pond.

1.2.2 Post-growth Treatment

Although we do not address the harvesting aspect of farming algae in this thesis, it is worth noting that the greatest efficiency and cost uncertainties in the overall production of biofuels from algae are related to harvesting and processing of the biomass. For algal biomass to be converted to biofuel the following processes are required:

- Harvesting the algae.
- Disruption of the cells.
- Extraction of the lipids.

Harvesting Options

For large volume cultures and a wide variety of algal species, centrifugation is most commonly used. Although effective, this process required expensive equipment and high energy inputs [128].

Flocculation, sometimes in combination with centrifugation or dissolved air flotation, is another widely used method for harvesting algal biomass. Flocculation is the aggregation of particles in suspension to form clusters which can then increase the settling rate. This reduces or avoids altogether the need for centrifugation. However, the efficiency of flocculation depends greatly on the species type and its growth stage [128].

Extraction of Lipids

Most species of algae accumulate lipids inside their cell walls. Thus the main focus of extraction methods is to break open the cell wall first. This can be achieved with physical (e.g. freezing and thawing), mechanical (crushing, blending, ultrasonic vibrations, etc.), chemical (e.g. solvents) or enzymatic methods (enzymes to decompose walls).

Pretreatments such as drying the biomass are desirable but often are not viable due to high energy requirements. No one method has yet been adopted for a broad range of algae, since each species has different characteristics that require an adaptation of existing methods [128].

1.2.3 The aim of this thesis

The growth of microalgae can be changed by a large number of environmental factors. The most influential of these are temperature, light, nutrient availability, CO_2 availability, and pH level. Each species of microalgae has their own optimal temperature range, light intensity, and pH level, although only some of these can be controlled in an open raceway pond. Our aim in this thesis is to see how much the productivity of raceway ponds can ultimately be improved in an idealised setting. While the results may not be directly applicable to the operation of actual raceway ponds, it is important to better understand the ultimate potentials of this technology if it is to ever become a viable alternative to crude oil.

We investigate several different approaches of operating a raceway pond so that the total algal lipids produced are maximised. Rather than implementing a variety of strategies on actual ponds which we don't have the means to do, we are going to work with a mathematical model of algal lipid growth in a raceway pond setting. A range of such models with varying levels of complexity is available in the literature and reviewed in the next section.

1.2.4 Microalgae growth models

There is a long history of modelling the growth of microalgae mathematically with the first studies appearing in the 1940s [89, 90]. Most of the early publications are aimed at better understanding of the basic contributors to algal growth and adopt features of other kinds of biological growth. Some models consider algal growth from an environmental point of view in order to better understand how to limit algal blooms in natural lake and river systems [18, 61]. These often concentrate on the movement of algae in the water column and its light exposure. Models which concern themselves with the production of microalgae tend to assume a well mixed pond or closed production system, so more emphasis is placed on the actual growth of cells and their main contributors such as nutrients and light.

A basic growth model is the Monod equation [89, 90] where growth is defined as

$$\mu = \mu_{\max} \frac{S}{K_s + S}. \tag{1.2.1}$$

Here, $\mu_{\max}$ is the maximum growth rate, S is the concentration of a limited substrate, and K_s is the half saturation constant for S. It should be noted that K_s and $\mu_{\max}$ are empirical coefficients. The equation has the same form as the Michaelis-Menten kinetics equation used widely in biology.

The model is thus sometimes referred to as the Michaelis-Menten-Monod model.

Another basic growth model is the Droop model which describes the algal growth rate as dependant on the total level of nutrients in the cell. Nutrient levels are described by what is known as the intracellular quota which is the ratio of nutrient concentration to biomass concentration [29–31]. The growth rate equation is given by

$$\mu = \mu_{\max}\left(1 - \frac{Q_0}{Q}\right), \tag{1.2.2}$$

where $\mu_{\max}$ is the maximum possible growth rate, Q is the intracellular quota, and Q_0 is the minimal cell quota (below which growth will cease). This model is well widely used for nutrient limited environments and has been shown to predict microalgae growth more accurately than the Monod equation [24, 119].

Liebig's law of the minimum (proposed in 1840 by Carl Sprengel and popularised subsequently by Justus von Liebig) was first applied to plant or crop growth where it was found that an unlimited supply of nutrients could only increase the rate of plant growth to a certain point, and also that only increasing the supply of the most limited nutrient would increase the rate of growth. Thus, the growth rate is given by

$$\mu = \min\left(F_1, F_2, \ldots, F_n\right), \tag{1.2.3}$$

where $F_1, \ldots, F_n$ are terms representing growth limiting functions. Note that the non-smooth nature of Liebig's law can cause problems with numerical simulation and optimisation tools.

Below, we consider a range of algal growth models in the literature.

"A model of phytoplankton growth on multiple nutrients based on the Michaelis-Menten-Monod uptake, Droop's growth and Liebig's law"[65]

This simple model involves the extracellular concentration of multiple nutrients, the intracellular concentration of multiple nutrients within the microalgae, and the algae cell density. It is assumed that nutrients are independent of each other in regards to their uptake and incorporation paths into the algal cells. The model uses the Liebig's law of the minimum in determining the growth rate. There is no consideration of light, temperature or CO_2 and the model also only looks at the total biomass, so lipid growth is difficult to determine.

"Phytoplankton growth and stoichiometry under multiple nutrient limitation"[60]

This model looks at two inorganic nutrients represented by two intracellular nutrient cell quotas as well as the total microalgae biomass. The overall environment is a simple bioreactor where fresh medium is continuously added while the culture liquid is removed at the same rate to keep the volume constant, known as a chemostat. The model assumes a single supply rate and two different input nutrient concentrations. Nutrient uptake is assumed to depend on inorganic nutrient concentrations, but not on the intracellular nutrient stores. Nutrient cell quotas increase based on Michaelis-Menten kinetics and decrease due to dilution based on growth. The microalgae biomass is modelled to grow based on Droop's formulation combined with Liebig's law of the minimum for multiple-nutrient-limited growth and decrease due to density-independent mortality. It is also assumed, for simplicity, that the microalgae has the same hypothetical infinite quota growth rate for both nutrients. This model also has no consideration of light, temperature, or CO_2, and again only looks at a total biomass, so it is not suitable for the optimisation of lipid growth.

"Growth and neutral lipid synthesis in green microalgae: a mathematical model"[95]

Algal biomass concentration (excluding neutral lipids), neutral lipid concentration, chlorophyll content of biomass, and the extracellular nitrogen concentration are modelled dynamically here. Biomass growth is either nitrogen limited or light-limited represented by Liebig's law of the minimum. Nitrogen limited growth is modelled using the cell quota model. Light limited growth is modelled by the Poisson single-hit model of algae photosynthesis which has the general form of

$$p(I) = p_m \left[1 - exp\left(\frac{-aI\Phi}{p_m}\right)\right],$$

where p_m is the light-saturated photosynthesis rate, a is the optical cross section of chlorophyll, I is irradiance, and Φ is quantum efficiency. Note that $-aI\Phi$ thus represents the light-limited rate. The total biomass quota is defined as

$$\tilde{Q} = \frac{AQ}{A+L},$$

where Q is the nitrogen quota of non-lipid biomass, L is the neutral lipid concentration, and A is the algal biomass concentration excluding neutral lipids. Self-shading and depth of the reactor are incorporated by using the Lambert-Beer law. Briefly, this relates the absorption of light to a material it is travelling through. The value of irradiance at a specific depth, x, is related to the

surface irradiance I_0 by

$$I(x) = I_0 \exp(-aHAx), \tag{1.2.4}$$

where HA is chlorophyll density as H is chlorophyll content. It is assumed that biomass density from mixing is homogeneous and as such, (1.2.4) can be integrated by a total bioreactor depth of z to give

$$I(A, H) = \frac{I_0}{aHAz}(1 - \exp(-aHAz)). \tag{1.2.5}$$

This model ignores temperature and CO_2, but it does separate lipids from the total biomass and does consider light intensity.

Views on Liebig's Law.

The use of Liebig's law was questioned in [94], where different growth models were fitted to a wide range of microalgae datasets with the aim of minimising residual mean squares. It was found that growth models based on the product of multiple Michaelis-Menten-Monod terms resulted in a superior fit. Most of the more recent models are also using Michaelis-Menten-Monod terms for growth in preference to Liebig's law. The Michaelis-Menten-Monod products also lead to smooth dynamics which are easier to simulate and optimise. Due to these disadvantages as well as the non-smoothness of Liebig's Law, we have opted to not implement any models that use it.

"Modeling microalgal growth in an airlift-driven raceway reactor"[58]

This model considers the dependence of growth on CO_2. The raceway is equipped with an airlift system instead of a standard raceway paddle. It is a complex model based on a well-mixed system that looks at dissolved CO_2 transfer with mass balance equations between the rate of transfer to the surface atmosphere, from sparging air, from the supplemental supply in the down-flow, and the rate of consumption by microalgae. The model also considers the dependence of growth on light, temperature, and nitrogen. Unfortunately, it only calculates a total biomass, thus making it unsuited to the optimisation of lipid growth.

"Optimal strategies for biomass productivity maximization in a photobioreactor using natural light"[39]

This model looks at a photobioreactor that allows light to be included when calculating the rate of growth, although, the effect of temperature is ignored. Optimal control is used in this model using the dilution rate of biomass as a control variable, however this model only represents a closed

system. It is also unfortunate that it is only nitrogen concentration and total biomass growth that are considered in the overall model, making it difficult to identify and optimise total lipid growth.

Optimising microalgal production in raceway systems [91]

A comprehensive model that combines many of the key drivers of growth and the influences of temperature and light is given by Muñoz-Tamayo *et al.* [91]. This raceway model is based on a combination of the Bernard [8] biomass model and the Mairet *et al.* [79, 80] lipid production model. It should be noted that both of these are themselves extensions of the Droop model [29]. In this new model, it is assumed that nitrogen, temperature, and light are the key limiting factors for the growth of microalgae. Temperature is assumed to have a homogeneous effect on uptake, growth, and respiration rates and, along with light, it also influences the ratio of chlorophyll and nitrogen. The absorption of light is described by the Lambert-Beer law and light also affects the growth rate. The model is presented in detail in Chapter 2. A novel feature of [91] is the use of optimal control methods to optimise both biomass and lipid contents of the raceway pond. Prior to [91], [39] was the only other publication to take this approach. However, the model in [39] is purposely kept simple to allow the use of analytic tools in optimal control to determine an optimal solution. The model in [91] has enough added complexity to then require numerical methods to determine an optimal control solution as the analytic approach becomes too difficult. As we shall show in Chapter 2, the numerical solutions obtained in [91] are some way off from being truly optimal. It was this observation which initially sparked our interest in the problem and we set out to find an improved optimal control for the raceway pond operation. This model forms the basis of most of the work in this thesis as it has sufficient flexibility to explore a wide range of operational changes to the raceway pond. In the next section, we review the basic formulation of an optimal control problem, solution methods, and optimality criteria.

1.3 Optimal Control

1.3.1 Basics of Optimal control theory

In this thesis, we are concerned with maximising the growth of algal lipids in a raceway pond. As we shall see, this problem can be cast in the form of an optimal control problem and solved with numerical methods specifically developed for such problems. In this section we give a brief review of a general class of optimal control problems and associated numerical solution methods.

A general optimisation problem consists of an objective function which must be either maximised or minimised subject to a set of constraints. In a static optimisation problem (also called a mathematical programming problem), the objective and constraints depend on a finite number of variables and the constraints are purely algebraic. In contrast, in a dynamic optimisation problem (also known as an optimal control problem), the objective depends on variables which are themselves functions (known as control functions or simply controls, typically depending on time) and there are dynamic constraints in the form of differential equations. Optimal control problems arise in a wide variety of disciplines, such as power generation [107], submarine movement [125], cancer chemotherapy [81], spacecraft control [37, 44, 45, 67], process control [9, 27, 72, 76, 129], and many others [122].

1.3.2 General Optimal Control Problem

A general class of optimal control problems can be written as follows. Find a function $\mathbf{u}$ which maps the interval $[0, t_f)$ to a set $U \in \mathbb{R}^r$ so as to minimise

$$g_0(\mathbf{u}) = \Phi_0(\mathbf{x}(t_f)) + \int_0^{t_f} \psi_0(t, \mathbf{x}(t), \mathbf{u}(t))dt, \tag{1.3.1}$$

subject to dynamic constraints

$$\frac{d\mathbf{x}}{dt} = \mathbf{f}(t, \mathbf{x}(t), \mathbf{u}(t)), \qquad t \in [0, t_f) \tag{1.3.2}$$

with initial conditions

$$\mathbf{x}(0) = \mathbf{x}_0 \in \mathbb{R}^n, \tag{1.3.3}$$

subject to the canonical constraints

$$g_i = 0, \qquad i = 1, 2, \ldots, N_e \tag{1.3.4a}$$

$$g_i \leq 0, \qquad i = N_e + 1, N_e + 2, \ldots, N, \tag{1.3.4b}$$

with

$$g_i(\mathbf{u}) = \Phi_i(\mathbf{x}(t_f)) + \int_0^{t_f} \psi_i(t, \mathbf{x}(t), \mathbf{u}(t))dt, \qquad i = 1, \ldots, N, \tag{1.3.4c}$$

Note that

$$\mathbf{x}(t) = [x_1(t), x_2(t), \ldots, x_n(t)]^\top \tag{1.3.5a}$$

and

$$\mathbf{u}(t) = [u_1(t), u_2(t), \ldots, u_r(t)]^\top \tag{1.3.5b}$$

are the state variables and control variables, respectively [122]. $[0, t_f]$ is referred to as the time horizon of the problem with t_f known as the terminal time. Here n and r are the dimensions of state and control functions, respectively. g_0 is known as the objective functional while g_i, $i = 1, \ldots, N$, are called constraint functionals. U is the control restraint set defined as

$$U = \{\mathbf{u} = [u_1, \ldots, u_r]^\top \in \mathbb{R}^r | u_{i,\min} \leq u_i \leq u_{i,\max}, \quad i = 1, \ldots, r\}, \tag{1.3.6}$$

where $u_{i,\min}$ and $u_{i,\max}$, $i = 1, \ldots, r$, are given lower and upper bounds of the individual control components.

Note that most mathematical literature on optimisation defines problem classes in terms of minimising an objective as we have done here. There is no loss of generality with this approach since maximising a particular objective g is equivalent to minimising $-g$. Problems in later chapters which require an object to be maximised can thus still be considered to belong to the class defined here.

It is assumed that:

1. Φ_i is a continuously differentiable function for $i = 0, 1, \ldots, N$.
2. ψ_i is continuously differentiable with respect to $\mathbf{x}$ and $\mathbf{u}$ as well as piecewise continuous with respect to t for $i = 0, 1, \ldots, N$.
3. $\mathbf{f} = [f_1, \ldots, f_n] \in \mathbb{R}^n$ are continuously differentiable functions with respect to all of their arguments.
4. $\mathbf{u}$ is piecewise continuous.

1.3.3 Pontryagin Minimum Principle

Consider the basic unconstrained problem ($U = \mathbb{R}^r$):

$$\min_{\mathbf{u}} \left\{ g(\mathbf{u}) = \Phi(\mathbf{x}(t_f)) + \int_0^{t_f} \psi(t, \mathbf{x}(t), \mathbf{u}(t)) dt \right\}, \tag{1.3.7}$$

subject to

$$\frac{d\mathbf{x}}{dt} = \mathbf{f}(t, \mathbf{x}(t), \mathbf{u}(t)), \qquad t \in [0, t_f) \tag{1.3.8}$$

$$\mathbf{x}(0) = \mathbf{x}_0 \in \mathbb{R}^n. \tag{1.3.9}$$

The dynamic constraints can be added to the objective functional using $\boldsymbol{\lambda}(t) \in \mathbb{R}^n$ as a Lagrange multiplier, which is often referred to as the costate. The appended objective functional is

$$g^*(\mathbf{u}) = \Phi(\mathbf{x}(t_f)) + \int_0^{t_f} \left[\psi(t, \mathbf{x}(t), \mathbf{u}(t)) + (\boldsymbol{\lambda}(t))^\top \left(\mathbf{f}(t, \mathbf{x}(t), \mathbf{u}(t)) - \frac{d\mathbf{x}(t)}{dt} \right) \right] dt \tag{1.3.10}$$

which is equivalent to $g(\mathbf{u})$ as long as the dynamic equations hold.

We define the Hamiltonian function as

$$H(t, \mathbf{x}, \mathbf{u}, \boldsymbol{\lambda}) = \psi(t, \mathbf{x}, \mathbf{u}) + (\boldsymbol{\lambda}(t))^\top \mathbf{f}(t, \mathbf{x}, \mathbf{u}). \tag{1.3.11}$$

In the classical calculus of variations which assumes an unconstrained control, the first order optimality conditions for an optimal control are known as the Euler-Lagrange equations [122]. In addition to the state dynamics (1.3.8) and initial conditions (1.3.9) being satisfied, they prescribe dynamics and terminal conditions for the costate,

$$\frac{d\boldsymbol{\lambda}(t)}{dt} = -\left[\frac{\partial H(t, \mathbf{x}, \mathbf{u}, \boldsymbol{\lambda})}{\partial \mathbf{x}} \right]^\top, \tag{1.3.12a}$$

$$\boldsymbol{\lambda}(t_f) = \left[\frac{\partial \Phi(\mathbf{x}(t_f))}{\partial \mathbf{x}} \right]^\top, \tag{1.3.12b}$$

and they require that the derivative of the Hamiltonian with respect to the control must vanish along an optimal trajectory, i.e.

$$\left[\frac{\partial H(t, \mathbf{x}, \mathbf{u}, \boldsymbol{\lambda})}{\partial \mathbf{u}} \right]^\top = 0, \quad \forall t \in [0, t_f]. \tag{1.3.12c}$$

In the more general situation the controls are constrained by upper and lower bounds, i.e. $\mathbf{u}(t) \in$

$U, t \in [0, t_f]$, where U is defined by (1.3.6). In this case, the Euler-Lagrange equations are replaced by the well known Pontryagin Minimum Principle [101]. This states that for an optimal control $\mathbf{u}^*$ and the corresponding optimal state $\mathbf{x}^*$ and costate $\boldsymbol{\lambda}^*$ it is necessary that

$$\frac{d\mathbf{x}^*(t)}{dt} = \left[\frac{\partial H(t, \mathbf{x}^*, \mathbf{u}^*, \boldsymbol{\lambda}^*)}{\partial \boldsymbol{\lambda}}\right]^\top = \mathbf{f}(t, \mathbf{x}^*(t), \mathbf{u}^*(t)), \tag{1.3.13a}$$

$$\mathbf{x}^*(0) = \mathbf{x}_0, \tag{1.3.13b}$$

$$\frac{d\boldsymbol{\lambda}^*(t)}{dt} = \left[\frac{\partial H(t, \mathbf{x}^*, \mathbf{u}^*, \boldsymbol{\lambda}^*)}{\partial \mathbf{x}}\right]^\top, \tag{1.3.13c}$$

$$\boldsymbol{\lambda}(t_f) = \left[\frac{\partial \Phi(\mathbf{x}(t_f))}{\partial \mathbf{x}}\right]^\top, \tag{1.3.13d}$$

and

$$\min_{\mathbf{v} \in U} H(t, \mathbf{x}^*, \mathbf{v}, \boldsymbol{\lambda}^*) = H(t, \mathbf{x}^*, \mathbf{u}^*, \boldsymbol{\lambda}^*), \forall t \in [0, t_f], \tag{1.3.13e}$$

except possibly on a finite subset of $[0, t_f]$. In other words, the control at almost every instant is chosen so that the Hamiltonian is minimised at that instant.

Also, if we add the terminal condition $\mathbf{x}^*(t_f) = \mathbf{x}_f$ then, if $\mathbf{u}^*$ is an optimal control, $\mathbf{x}^*$ and $\boldsymbol{\lambda}^*$ are the corresponding optimal state and costate variables, then it is necessary that [101]

$$\frac{d\mathbf{x}^*(t)}{dt} = \left[\frac{\partial H(t, \mathbf{x}^*, \mathbf{u}^*, \boldsymbol{\lambda}^*)}{\partial \boldsymbol{\lambda}}\right]^\top = \mathbf{f}(t, \mathbf{x}^*(t), \mathbf{u}^*(t)), \tag{1.3.14a}$$

$$\mathbf{x}^*(0) = \mathbf{x}_0, \tag{1.3.14b}$$

$$\mathbf{x}^*(t_f) = \mathbf{x}_f, \tag{1.3.14c}$$

$$\frac{d\boldsymbol{\lambda}^*(t)}{dt} = \left[\frac{\partial H(t, \mathbf{x}^*, \mathbf{u}^*, \boldsymbol{\lambda}^*)}{\partial \mathbf{x}}\right]^\top, \tag{1.3.14d}$$

and

$$\min_{\mathbf{v} \in U} H(t, \mathbf{x}^*, \mathbf{v}, \boldsymbol{\lambda}^*) = H(t, \mathbf{x}^*, \mathbf{u}^*, \boldsymbol{\lambda}^*), \forall t \in [0, t_f], \tag{1.3.14e}$$

except possibly on a finite subset of $[0, t_f]$. Clearly, the only change in this case is the replacement of the terminal costate constraint with the terminal state constraint.

We shall make use of both of these results to analyse solutions of various versions of the raceway optimal control in later chapters.

In optimal control problems where both the objective and dynamics are linear with respect to

the control variables, the Hamiltonian equation can be written as

$$H = \left[\sum_{1}^{r} K_i(t, \mathbf{x}^*, \boldsymbol{\lambda}^*) u_i^*\right] + K_{r+1}(t, \mathbf{x}^*, \boldsymbol{\lambda}^*). \tag{1.3.15}$$

Here, K_i for $i = 1, \ldots, r$ are coefficients for each control and K_{r+1} is a term not involving any of the controls. Given the control bounds, (1.3.6), the sign of K_i for $i = 1, \ldots, r$ (which is referred to as a switching function) then determines the choice of the control. Clearly, minimisation of H requires

$$u_i^*(t) = \begin{cases} u_{i,\min}^*, & \text{if } K_i(t) > 0, \\ u_{i,\max}^*, & \text{if } K_i(t) < 0, \\ \text{undetermined}, & \text{if } K_i(t) = 0, \end{cases} \tag{1.3.16}$$

for $i = 1, \ldots, r$. If the third case does not arise, we have a so-called bang-bang solution. If the third case does come into play over a non-trivial interval in $[0, t_f]$, we say that the control is singular on this interval. In some fortuitous situations, the first order necessary conditions stated above can be used to determine an analytic form of the optimal control. For the vast majority of practical problems, this is not possible and numerical solution methods are required instead.

1.3.4 Numerical Solution Methods for Optimal Control Problems

The Pontryagin Minimum Principle briefly outlined in the previous section can be used to derive analytical solutions for a variety of relatively simple optimal control problems when the number of states and controls is small and the dynamics take certain basic forms. A well known example is the linear quadratic regulator (LQR) problem where an optimal linear feedback control can be readily derived and which has many applications in engineering [3]. Other examples occur in the study of economics and management where optimal control solutions of various basic problems lead to important principles applied in these disciplines [53].

However, most real world problems arising in science and engineering are considerably more complex in terms of dimension and nonlinearity and analytic solutions are generally not feasible for these [9, 11, 22, 25, 43, 44, 49, 67, 69, 73, 78, 81, 121, 123, 130, 131]. Consequently, a wide variety of computational algorithms has been developed to find numerical solutions for optimal control problems and we give a brief review of these in this section.

It must be noted that designing and coding a generic algorithm for solving a broad class of

optimal control problems numerically is a challenging task. Many of the successful algorithms in existence have taken years of development, testing, and continual improvement to reach their current form. The individuals and teams behind these algorithms thus have had limited time and incentive to concern themselves with someone else's algorithm. As a consequence, there are very few, if any, publications which give a detailed comparison of algorithms in terms of their performance or efficiency. Furthermore, the usage of any one algorithm tends to be largely confined to the team which designed it and their associates.

Dynamic Programming and Iterative Dynamic Programming

Dynamic Programming is an optimisation technique which is useful for problems which can be broken down into simpler sub-problems in a recursive manner. It was proposed in the 1950s by Richard Bellman [7] and relies on the so-called Principle of Optimality. Optimal path finding problems in networks are an obvious application of the method but it is also used widely for a range of other discrete optimisation problems [28]. In the context of optimal control problems, the method can be applied to discrete approximations of these problems. However, it suffers from the so-called Curse of Dimensionality. This arises in problems with multiple state variables due to the large number of approximated points needed in the multidimensional state space to apply the method. Thus, direct applications of dynamic programming to optimal control problems are limited to problems with a small number of states and controls.

A variation is known as Iterative Dynamic Programming (IDP) was proposed by Rein Luus in 1989 [75] in order to overcome the curse of dimensionality. In its original form, IDP allows for piecewise constant controls over a chosen partition of the time horizon. Over each interval of this partition, a finite set of control values is considered. The dynamics of the problem are integrated numerically over each interval for each value of the control in turn to generate a set of accessible points in the state space, thereby limiting the number of points needing to be considered in that space and avoiding the curse of dimensionality. A coarse optimal solution can then be determined by dynamic programming. Successive refinements around this coarse trajectory can then be generated until they converge to a satisfactory solution. The method was later extended to allow for piecewise linear continuous controls and a variety of constraints could be included via the use of penalty methods [77]. IDP has been successfully applied to many challenging optimal control problems, particularly in the area of chemical engineering [76, 78]. Its developers claim it to be robust and capable of avoiding local optima since the underlying optimisation process avoids the use of gradients with respect to control parameters [77]. A novice user may find it difficult to

choose values for the various tuning parameters of the method. These include the region contraction factor, number of allowable control values at each stage, initial region size and restoration factor.

Indirect Methods

It can be seen that the various versions of the Pontryagin minimum principle (see (1.3.13) and (1.3.14) in Section 1.3.3) constituting the first order necessary conditions for an optimal solution essentially yield a two point boundary value problem (TPBVP) with the combined state-costate dynamics needing to be solved subject to conditions given at both the initial and terminal time. The traditional approach for solving a TPBVP is known as a shooting method [102]. This considers the TPBVP in the form of an initial value problem with the unknown components of the initial conditions assumed to be variables. Guesses are made for the values of these variables and the dynamics are integrated forward in time. The resulting terminal values of the state and costate are then compared with the terminal conditions of the TPBVP and the differences are recorded. The aim is to then adjust the variables successively until these differences are reduced to zero. The problem with this approach is that the forward integration of the dynamics is often unstable, particularly for the costate component. An improvement of the shooting method is known as multiple shooting, where conditions are fixed at several points in the interior of the time horizon and integration proceeds between these points. In the context of optimal control problems, the multiple shooting approach also allows for additional constraints to be imposed in the interior of the time horizon. The software BNDSCO [93] implements an extended version of multiple shooting to solve a general class of optimal control problems.

The Leapfrog method [57] is another approach for solving the TPBVP arising in optimal control. Like multiple shooting, the time horizon is partitioned and local optimal controls are found separately over each subinterval. Starting with a feasible trajectory, improvements are made iteratively by determining piecewise optimal trajectories over pairs of subintervals (defined by three successive time points) and updating the optimal state at the middle time point. As the algorithm progresses, it is possible to eliminate time points which in turn improve its efficiency. Under some broad assumptions, the algorithm is shown to converge to a solution which satisfies the Pontryagin minimum principle.

Another indirect approach is to solve the TPBVP by means of collocation methods. Collocation methods, more advanced versions of which are also known as pseudo spectral methods, involve a partition of the time horizon and assume a piecewise polynomial form for both the controls, states, and costates. By enforcing requirements of state and costate values and derivatives at

the knot points of the partition, the differential equations defining the dynamics are replaced by corresponding algebraic equations. Controls can then be chosen so that the optimality conditions are satisfied at the so-called collocation points (the midpoints of the intervals defined by the chosen partition). The objective can be approximated using appropriate quadrature formulae consistent with the given partition of the time horizon. It can be shown that collocation methods are, in fact, special cases of Runge-Kutta numerical integration methods. As noted in [32], this indirect approach can lead to a situation where the resulting control does not converge to the true optimal control unless the partition, integration scheme and quadrature rule are chosen in a consistent manner.

Direct Methods

As the name would suggest, direct methods attempt to solve an optimal control problem directly and without invoking the optimality conditions prescribed by the minimum principle. As optimal control problems by their very nature are infinite dimensional optimisation problems, direct methods require some form of finite dimensional representation of the control. In addition, the dynamical system defining the state variables needs to be solved numerically using some form of Runge-Kutta integration scheme. Within the class of direct methods, we distinguish between the full discretisation methods and control parameterisation. In full discretisation approaches the discretised dynamics are viewed as algebraic constraints and the state as well as control values at the knot points of the discretisation scheme are both treated as variables. Control parameterisation, to be discussed in more detail below, expresses only the controls in terms of a finite number of variables and the resulting states are calculated numerically but not treated as variables themselves.

The simplest direct approach is to choose a partition of the time horizon, replace the differential equations describing the dynamics by a Runge-Kutta scheme consistent with the knot points of the partition and replace any integral terms in the objective by a quadrature formula also consistent with the partition. The state and control values at all knot point are treated as variables and the resulting discretised problem now consists minimising an objective function subject to a large number of algebraic constraints (resulting from the Runge-Kutta scheme). Both the objective and constraints are generally nonlinear. To ensure a reasonable degree of accuracy for most practical problems, the partition of the time horizon needs to be quite fine. This, in turn, mean a large number of knots and generally leads to a large scale nonlinear programming problem (NLP) to be solved. This approach was simply not feasible up until the 1990s due to constraints in computing power and a lack of suitable NLP solvers. However, large scale NLP solvers such as SNOPT [35]

and IPOPT [126] are now available which can take advantage of the sparse nature of the NLP resulting from discretisation (due to the nature of the Runge-Kutta schemes). A popular recent approach [114] has been to interface these NLP solvers with a mathematical modelling environment such as AMPL [33] where the discretised problem can be coded with relative ease and gradients of objective and constraints are determined by automatic differentiation [38]. This is one of the computational approaches we use to solve several versions of the algae growth problems described in this thesis.

A lot of variations of the basic approach outlined in the last paragraph exist in the literature. Many practitioners prefer the use of a simple Euler method with a uniform partition of the time horizon instead of higher order Runge-Kutta schemes due to the ease of implementation. A comprehensive Fortran based package which employs a 4th order Runge-Kutta method with automatic partition refinement is NUDOCCCS [20, 21].

As noted above, collocation methods are effectively special cases of Runge-Kutta schemes. Nevertheless, many publications specifically use the term direct collocation when these methods are applied to optimal control problems in the direct sense. A variety of such methods exists, differing in the order of approximation of both the control and dynamic approximation and using both fixed and adjustable partitions of the time horizon. Two well known softwares that belong to this class of solution methods are DIRCOL [120] and GPOPS [104].

In most direct methods, the NLP resulting from the discretisation of the original optimal control problem is solved directly by one of a range of existing NLP solvers. An alternatively approach is to apply a more elaborate method to solve the NLP. One such method is known as the Inexact Restauration (IR) method [10] which is itself an extension of a much earlier method known as the Sequential Gradient Restauration algorithm [85–87]. Each step of an IR algorithm consists of a restoration phase where infeasibility is reduced and an optimality phase where an appended objective is minimised approximately subject to a linear approximation of the constraints. Both phases involve the solution of a much simpler NLP which can again be solved by any one of a range of generic NLP solvers. The main advantage of IR is improved convergence to optimal solutions compared to the straightforward use of a generic NLP solver. For optimal control problems, this approach has been successfully reported in [4, 55, 56].

Once a solution for an optimal control problem has been attained, it is desirable to check whether it satisfies the necessary and sufficient conditions for optimality. While this task has often been neglected in the past, it is shown in [23] that it can be achieved for the full discretisation approach. For the necessary conditions (minimum principle), it is necessary to first determine the

costates corresponding to the optimal solution. These can be calculated using the optimal Lagrange multipliers of the NLP. The sufficient conditions are more difficult to verify directly, but they can be checked numerically by considering the corresponding sufficient conditions of the discretised NLP.

As was the case for indirect methods, in the full discretisation approach there is a need to match the choice of time horizon partitions, quadratures, and numerical integrations schemes carefully so that the resulting sequence of discrete approximations of the original problem are consistent in the sense that their solutions converge to that of the original problem [99, 100]. The RIOTS optimal control toolbox [111, 112] available in MATLAB [83] follows this requirement.

Control Parameterisation

Figure 1.3.1: A piecewise constant parameterisation of k^{th} control

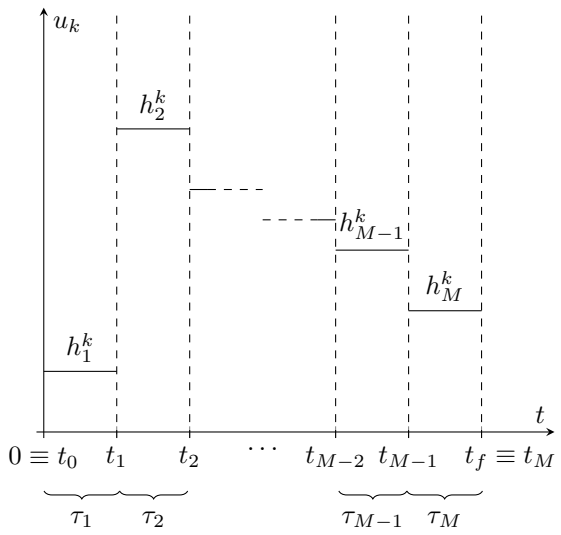

As we have noted previously, an optimal control problem is an infinite dimensional optimisation problem which requires some form of discretisation before one can attempt to solve it numerically so we again need to partition the time horizon. In the control parameterisation approach, the control functions are expressed in terms of a finite number of variables, often referred to as control parameters. For example, one can express the control as a linear combination of low order basis splines with finite support which is equivalent to defining them as being piecewise polynomial over one or more subintervals of the chosen partition. The variables (control parameters) are then effectively just the coefficients of these polynomials. For each instance of the control parameters, one can then substitute the corresponding controls into the dynamics of the problem and integrate these to obtain the corresponding states. The integration of the dynamics needs to be performed numerically using some type of Runge-Kutta scheme and the partition of the time horizon for

this integration is typically much finer than that chosen for the parameterisation of the controls. The objective and any constraints of the problem are then also evaluated using a quadrature scheme consistent with this fine partition. In this way we obtain a NLP approximation of the original problem, but it has far fewer variables than the corresponding NLP obtained in the full discretisation approach and it is thus much less time consuming to solve. However, this saving in computational time is offset by the additional time required to numerically integrate the dynamics at each iteration of the NLP solver. In addition, if one wishes to supply the gradients of the objective and constraints with respect to the control parameters (see [122] for the appropriate formulae for these gradients) to the NLP solver, one is required to set up and solve a separate costate dynamical system for the objective and each one of the constraints. While this further increases the overall computational time required, it will speed up the converge of the NLP solution.

One of the simplest yet often used forms of control parameterisation is to allow each component of the control, u_k, $k = 1, \ldots, r$, to be a piecewise constant function consistent with a given partition of the time horizon with M intervals, as shown in Figure 1.3.1. The control parameters to be optimised in this case are the heights, h_i^k, $i = 1, \ldots, M$, in the individual subintervals of the partition. As many practical optimal control problems are such that their Hamiltonian is linear in the control, leading to the optimal control being either bang-bang or bang-singular, this seemingly naive choice actually lends itself reasonably well to their numerical solution. If a piecewise linear continuous approximation is required for the control, one can easily generate this by defining it as the integrand of another piecewise constant control function (which then requires a simple additional equation in the system dynamics). This process can be repeated for still higher order piecewise polynomial continuous approximations if required (see Chapter 9 of [122]).

The accuracy of the solution obtained by solving an approximate problem obtained by control parameterisation can be improved by increasing the number of time points in the partition defining the control. If one considers a sequence of partitions with increasingly smaller subintervals, convergence of the resulting approximate optimal objective values to the true objective has been established in [117], although convergence of the corresponding controls to the true optimal control has only been demonstrated for problems involving linear dynamics [122]. Nevertheless, the controls typically end up sufficiently close to the true optimal control for practical purposes.

Note that in the above description of control parameterisation, the partition of the time horizon is assumed to be fixed. For the case of a piecewise constant control as shown in Figure 1.3.1, the durations, τ_i, $i = 1, \ldots, M$, for which each control stays constant is thus also assumed to be fixed. It would be preferable to consider these to be variables to be optimised along with the control values

over each interval so that exact switching times for a bang-bang control could be determined, for example. The gradients of objective and constraints with respect to these time durations can be determined either in terms of the Hamiltonian of the problem [122] or by introducing a sequence of auxiliary systems integrated forward in time [74]. The latter approach is similar to the switching time computation (STC) method introduced in [54]. In the context of control parameterisation with piecewise constant controls, however, a more convenient way to allow for variable time durations is to introduce a new time scale and an auxiliary piecewise constant control function consistent with a uniform fixed partition on that time scale. The piecewise constant values of this auxiliary control are the time durations of the partition in the original time scale. The link between the two time scales is that the derivative of time in the original scale with respect to time in the transformed scale is simply this auxiliary control. Time in the original scale can then be treated as an auxiliary state of the problem. The transformed problem thus has a fixed partition with one additional state and one additional piecewise constant control and the standard control parameterisation approach with piecewise constant controls can be used to solve it. This idea was originally proposed in [63] and has been widely used to solve a variety different classes of optimal control problems [64, 68, 71, 72].

A general purpose optimal control software known as MISER [51] implements the control parameterisation approach as described above for the general class problems defined by in Section 1.3.2. It is used to solve the majority of the computational models considered in this thesis. MISER is written in FORTRAN and capable of solving a wide range of optimal control problems with many types of constraints [51]. We do not give detailed discussion of all these capabilities here as most of algal growth models examined in this thesis are either unconstrained or only involve relatively simple terminal state constraints. One feature worth mentioning is that MISER will allow the formulation of problems involving individual decision variables other than those associated with the controls. These are referred to as system parameters and may appear in any term of the generic problem in Section 1.3.2, including the right hand side of the initial conditions of the dynamics. For instance, they can be used to model unspecified initial conditions which often feature in application problems.

MISER requires the user to specify the functional form of their problem via a set of FORTRAN subroutines. There are separate subroutines for:

- the objective and constraint integral and nonintegral terms,
- the initial conditions of the dynamics,

- the right hand sides of the system dynamics,
- the derivatives of all of these functions with respect to system parameters, states, and controls.

These subroutines are to be completed by user and then compiled with the rest of the MISER software into an executable program. Other features of a problem, such as:

- the dimensions of state, control, and system parameter vectors,
- the start and end point of the time horizon,
- the partition of the time horizon for the piecewise constant control,
- the upper and lowers bounds for controls and system parameters,
- the number of constraints and their type

are specified in a text file to be completed by the user. In addition, the text file allows the user to specify optional parameters for the integration of the state and costate dynamics as well as for the optimisation subroutine used within MISER. MISER allows for several different NLP solvers to be invoked for the discretised problem resulting from control parameterisation. It is supplied with the sequential quadratic programming subroutine NLPQL [110] but allows for 3 other packages to be used subject to availability of these to the user. Integration of the state and costate dynamics in MISER is handled by the subroutine LSODA [97] which uses an adaptive 6th order Runge-Kutta method. Note that LSODA is invoked successively over a series of subintervals of a partition of the time horizon which is much finer than that used to define the piecewise constant controls. Instead of the original NLPQL supplied with MISER, we have modified MISER to use NLPQLP [109], an updated version of NLPQL.

The availability of many software packages for the numerical solution of optimal control problems might suggest that solving them is a trivial exercise. Indeed, relatively simple problems can be coded by proficient practitioners in a matter of minutes and solutions obtained in a matter of seconds thereafter. Many realistic problems display a much higher degree of complexity and therefore present a range of challenges. For example, the right hand sides of the dynamic equations may be defined by several layers of algebraic equations rather than simple expressions, making it very difficult to determine their derivatives [118]. The dynamics of the states or costates may be stiff (some components change much more rapidly with time than others), requiring excessive computational time for their solution or failing to integrate altogether. Due to limited computational accuracy, gradients with respect to system or control parameters may be fuzzy and lead to slow

convergence of the NLP solver or even failure to find a solution at all. More challenging problems can have an underlying nonsparse NLP with many hundreds of variables requiring hundreds or thousands of iterations to solve. As a guide, for the algal growth models considered in this thesis, the computational time to determine an individual optimal solution on a personal computer is in the order of days.

1.4 Thesis Outline

We briefly outline the contents of the thesis below.

In Chapter 2 we apply numerical optimal control methods to the existing algae growth model [91] with the aim to determine the best performance of the model under known conditions using a variety of decision variables. To allow the use of the MISER optimal control package, we first transform the system of differential algebraic equations (DAEs) in the existing model to a system of ordinary differential equations (ODEs) which introduces dynamics for average light intensity and chlorophyll. In addition we allow for variable nitrogen concentration of the inflow as well as variable initial nitrogen concentration of the raceway. Our main focus is on optimising of the production of lipids and we show that yield can be improved significantly over previous results. We calculate both open and closed loop optimal controllers and test their robustness. Finally we also consider raceway depth as a decision variable which results in a further yield improvement.

In Chapter 3 we present a modified model of the algae growth model with the additional feature of variable pond depth. This requires an additional state variable to model depth as well as additional control to allow for variable outflow. We once again convert the modified system of DAEs into an equivalent system of ODEs and apply MISER to solve the resulting problem. We show that the lipid yield of the process can be increased by 67% compared to that obtained with a fixed pond depth.

In Chapter 4 we allow for variable periodic boundary conditions on the states of the problem to allow for an ongoing, rather than a batch operation. We show that significant improvements in lipid yield can be achieved with this approach compared to those outlined earlier in the thesis. However, we also show that the optimal periodic boundary conditions are difficult to reach in finite time from arbitrary initial conditions. Nevertheless, the optimal periodic solution provides a useful benchmark which can inform the design of more practical control algorithms for the system in the future. Some formulations of the problem in this Chapter are quite difficult to solve and we use two distinct numerical solution methods.

In Chapter 5, we summarise the findings of this thesis. We also point out the shortcomings of the models used in this thesis and we suggest a number of ideas to be tested in the future numerical studies.

Chapter 2

Optimal Control for Microalgae on a Raceway Model

2.1 Introduction

A comprehensive algae growth model that combines many of the key drivers of growth and the influences of temperature and light is given by Muñoz-Tamayo *et al.* [91]. This raceway model is based on a combination of the Bernard [8] biomass model and the Mairet *et al.* [79, 80] lipid production model. In this new model, it is assumed that nitrogen and light are the key limiting factors for the growth of microalgae.

While the focus in Muñoz-Tamayo *et al.* [91] is on determining a quasi-optimal closed loop control for the purposes of online implementation, we are more interested in investigating the potential performance of the system by calculating open loop optimal controls. The open loop optimal control formulation allows for the inclusion of a variety of system and control constraints, the combined optimisation of certain system parameters and controls, and the formulation of many different objectives [70]. Although we only consider some minor variations of the original model, there are other practical variations which are investigated in Chapters 3 and 4. While open loop optimal controls generally lack robustness with respect to uncertainties, we show that there is only a minor degradation of the performance of the optimal control when various disturbances are introduced.

We use the computational optimal control package MISER 3.3 [51] to optimise the performance of the existing model [91]. The dynamics in this model are described by a system of differential

algebraic equations (DAEs), but, like many computational optimal control packages, MISER is only able to solve problems involving ordinary differential equations (ODEs). Hence, we first transform the DAEs in the model to an equivalent system of ODEs.

The original dynamic model [91] includes just one control variable, the input flow rate. We also allow the influent nitrogen concentration to vary over time and consider the initial extracellular nitrogen concentration to be a decision variable (both of these were assumed constant in Muñoz-Tamayo *et al.* [91]). Numerical results show that optimal yields of biomass and lipids can be easily determined with this approach and that significant improvement in lipid yields can be achieved. As practical considerations often favour a continuous operation of the raceway, we also formulate and solve an optimal feedback control problem and test the performance of the resulting closed loop control. Finally, we show that further improvements in yield are possible if raceway depth is also considered as a decision variable. This chapter is largely based on [47].

2.2 Existing Model

Table 2.1: State Variable, Control Variable, System Parameter and Function Definitions

Variables	Definition	Units
s	Nitrogen concentration	gN m^{-3}
q_n	Nitrogen quota	gN $(gC)^{-1}$
x	Carbon biomass concentration	gC m^{-3}
x_l	Lipid carbon concentration	gC m^{-3}
x_f	Functional carbon concentration	gC m^{-3}
L	Pond depth	m
$\bar{I}$	Average light intensity	µmol photons m^{-2} s^{-1}
C_{hl}	Chlorophyll concentration	gC_{hl} m^{-3}
I_0	Incident light intensity	µmol photons m^{-2} s^{-1}
T	Raceway temperature	°C
ϕ_T	Temperature factor affecting growth kinetics	
λ	Optical depth	
μ	Growth rate	h^{-1}
ρ	Nitrogen uptake rate	gN $(gC\ h)^{-1}$
θ_N	Chl:N ratio	gC_{hl} $(gN)^{-1}$
ξ	Attenuation factor	m^{-1}
R	Overall respiration rate	h^{-1}
f_{in}	Feeding flow rate	m^3 h^{-1}
f_{out}	Extraction flow rate	m^3 h^{-1}
η_L	Efficiency of light absorption	
t_f	final time point	h

The model proposed by Muñoz-Tamayo *et al.* [91] is given by the mass balance equations for a

completely mixed reactor at a constant volume V below.

$$\begin{aligned}
\dot{s} &= f_{in}s_{in}/V - f_{in}s/V - \rho x, \\
\dot{q}_n &= \rho - (\mu - R)q_n, \\
\dot{x} &= (\mu - f_{in}/V - R)x, \\
\dot{x}_l &= \beta q_n \mu x - \gamma \rho x - r_0 \phi_T x_l - f_{in}x_l/V, \\
\dot{x}_f &= (\alpha + \gamma)\rho x - r_0 \phi_T x_f - f_{in}x_f/V,
\end{aligned} \tag{2.2.1}$$

where s is the extracellular nitrogen concentration and q_n is the internal nitrogen quota. The concentration of total carbon biomass x is the sum of three carbon pools: storage lipids x_l, functional pool x_f, and carbohydrates x_g [79, 80, 91]. Only x, x_l, and x_f are modelled in the dynamics since

Table 2.2: Parameter Definition and Values

Parameters	Definition	Units	Value
α	Protein synthesis coefficient	gC(gN)^{-1}	3.0
β	Fatty acid synthesis coefficient	gC(gN)^{-1}	3.80
ϵ_I	Dissociation light constant	µmol photons m^{-2} s^{-1}	50
φ	Biosynthesis cost coefficient	gC(gN)^{-1}	1.30
γ	Fatty acid mobilisation coefficient	gC(gN)^{-1}	2.90
v	Reduction factor of nitrogen uptake during night		0.19
$\tilde{\mu}$	Theoretical maximum specific growth rate	h^{-1}	8.7916×10^{-2}
$\bar{\rho}$	Maximum uptake rate	gC(gN h)^{-1}	4.16×10^{-3}
a	Light attenuation due to chlorophyll	m^2 $(\text{g } C_{hl})^{-1}$	2.0
b	Light attenuation due to background turbidity	m^{-1}	0.087
g_1	Coefficient (2.2.16)	$\text{gN } (\text{g}C_{hl})^{-1}$	16.74
g_2	Coefficient (2.2.16)	$\text{gN } (\text{g}C_{hl}\ ^\circ\text{C})^{-1}$	0.39
g_3	Coefficient (2.2.16)	$\text{gN } (\text{g}C_{hl}\text{µmol photons m}^{-2}\ \text{s}^{-1})^{-1}$	1.4×10^{-3}
g_4	Coefficient (2.2.16)	$^\circ\text{C}^{-1}$	0.0015
K_s	Nitrogen saturation constant	gN m^{-3}	0.018
K_{sI}	Light saturation constant	µmol photons m^{-2} s^{-1}	1.5×10^2
m	Hill coefficient		3.0
Q_l	Saturation cell quota	gN(gC)^{-1}	0.20
Q_0	Minimum nitrogen cell quota	gN(gC)^{-1}	0.05
r_0	Maintenance respiration rate	h^{-1}	4.16×10^{-4}
T_{min}	Lower temperature for microalgae growth	$^\circ$C	-0.20
T_{max}	Upper temperature for microalgae growth	$^\circ$C	33.30
T_{opt}	Temperature at which growth rate is maximal	$^\circ$C	26.70
s_{in}	Influent nitrogen concentration	gN m^{-3}	50.0
T_a	Coefficient (2.2.3)	$^\circ$C	-5.75
T_b	Coefficient (2.2.3)	$^\circ$C	20.75
t_a	time point	h	3.733
t_b	time point	h	4.9
t_c	time point	h	19.1
t_d	time point	h	20.267
I_{0a}	Coefficient (2.2.4)	µmol photons m^{-2} s^{-1}	-3.890408560
I_{0b}	Coefficient (2.2.4)	µmol photons m^{-2} s^{-1}	-52.13043162
I_{0c}	Coefficient (2.2.4)	µmol photons m^{-2} s^{-1}	141.6278134
I_{0d}	Coefficient (2.2.4)	µmol photons m^{-2} s^{-1}	841.1792340
I_{0e}	Coefficient (2.2.4)	µmol photons m^{-2} s^{-1}	358.8207660
I_{0f}	Coefficient (2.2.4)	µmol photons m^{-2} s^{-1}	3.890411835
I_{0g}	Coefficient (2.2.4)	µmol photons m^{-2} s^{-1}	-52.13042142
I_{0h}	Coefficient (2.2.4)	µmol photons m^{-2} s^{-1}	-141.6278049

x_g can always be calculated as $x - x_l - xf$. Derivatives are with respect to t, this being the time of day measured in hours where $t = 0$ corresponds to midnight. The influent nitrogen concentration is s_{in} and f_{in} is the inflow rate. Unlike Muñoz-Tamayo *et al.* [91], we consider both s_{in} and f_{in} to be control variables. The functions μ, ρ, R, ϕ_T represent the average growth rate, nitrogen uptake rate, overall respiration rate and temperature effect, respectively. These are described in more detail below. α, β, r_0, and V are model constants whose values are given in Table 2.2. We assume that the initial value of s is to be optimised, so

$$s(0) = z_1, \tag{2.2.2}$$

where z_1 is a decision variable. In Muñoz-Tamayo *et al.* [91], z_1 was fixed to the value 2. The initial values of q_n, x, x_l, and x_f can also be found in Table 2.2.

Outdoor microalgae raceway systems are strongly influenced by temperature and light. In this model, these effects are implemented via homogeneous effects on uptake, growth, and respiration as well as by setting the C_{hl}:N ratio to be dependent on temperature and light. The equations are given below.

To describe temperature, $T(t)$, following the information in Muñoz-Tamayo *et al.* [91], we use

$$T(t) = T_a \cos(t\pi/12) + T_b, \tag{2.2.3}$$

where T_a, and T_b are given in Table 2.2. $I_0(t)$ (incident light intensity) is described in Muñoz-Tamayo *et al.* [91] as a truncated wave function. The graph given for $I_0(t)$ [91] is non-smooth at sunrise and sunset. Since MISER works best with smooth functions, we use a smoothed version given by

$$I_0(t) = \begin{cases} 0, & (t \bmod 24) \le t_a, \\ I_{0a}((t \bmod 24) - t_a)^5 + I_{0b}((t \bmod 24) - t_a)^4 + I_{0c}((t \bmod 24) - t_a)^3, & t_a < (t \bmod 24) \le t_b, \\ I_{0d} \sin(((t \bmod 24) - 6)\pi/12) + I_{0e}, & t_b < (t \bmod 24) \le t_c, \\ I_{0f}((t \bmod 24) - t_d)^5 + I_{0g}((t \bmod 24) - t_d)^4 + I_{0h}((t \bmod 24) - t_d)^3, & t_c < (t \bmod 24) \le t_d, \\ 0, & (t \bmod 24) > t_d. \end{cases} \tag{2.2.4}$$

where $[t_a, t_b]$ and $[t_c, t_d]$ can be interpreted as the dawn and dusk periods respectively, mod represents the remainder function (modulo operation), and $I_{0a}, \ldots, I_{0h}$ are constants which are chosen

so that they result in a continuous second derivative. The values for these constants are given in Table 2.2. For ease of notation, $T(t)$ and $I_0(t)$ are referred to below as T and I_0 respectively.

The light intensity at reactor depth z ($z = L$ corresponds to the bottom of the reactor), I_z, is then given by

$$I_z = I_0 \exp(-\xi z), \tag{2.2.5}$$

where

$$\xi = aC_{hl} + b \tag{2.2.6}$$

is the light attenuation factor, C_{hl} represents the concentration of chlorophyll, and a as well as b are constants whose values are also given in Table 2.2 [91].

On this basis, the growth rate at depth z with a hypothetical infinite nitrogen quota is given as

$$\mu_z = \tilde{\mu}\frac{I_z}{I_z + K_{sI}}. \tag{2.2.7}$$

Integration of (2.2.7) over the raceway depth gives us

$$\bar{\bar{\mu}} = \frac{\tilde{\mu}}{\xi \mathrm{L}} \ln \frac{I_0 + K_{sI}}{I_0 \exp(-\xi L) + K_{sI}}, \tag{2.2.8}$$

which leads to the overall growth rate of

$$\mu = \bar{\bar{\mu}}\phi_T \left(1 - \frac{Q_0}{q_n}\right), \tag{2.2.9}$$

where

$$\phi_T = \begin{cases} 0, & T < T_{\min}, \\ \dfrac{(T - T_{\max})(T - T_{\min})^2}{(T_{\mathrm{opt}} - T_{\min})[(T_{\mathrm{opt}} - T_{\min})(T - T_{\mathrm{opt}}) - (T_{\mathrm{opt}} - T_{\max})(T_{\mathrm{opt}} + T_{\min} - 2T)]}, & T \in [T_{\min}, T_{\max}], \\ 0, & T > T_{\max} \end{cases} \tag{2.2.10}$$

represents the temperature effect. Furthermore, $\tilde{\mu}, Q_0, L, K_{sI}, T_{\min}, T_{\max}$, and T_{opt} are constants whose values are listed in Table 2.2.

The respiration rate is given by

$$R = r_0\phi_T + \varphi\rho, \tag{2.2.11}$$

where ρ is the nitrogen uptake rate given by

$$\rho = \bar{\rho}\phi_T \frac{s}{s + K_s}\left(v + (1-v)\frac{\bar{I}^m}{\bar{I}^m + \epsilon_I^m}\right)\left(1 - \frac{q_n}{Q_l}\right). \tag{2.2.12}$$

Here φ, $\bar{\rho}$, K_s, v, m, ϵ_I, and Q_l are constants whose values can be found in Table 2.2. $\bar{I}$ is defined as average irradiance and can be found by the integration of (2.2.5) along the raceway depth (z), averaged by the total depth (L). This gives

$$\bar{I} = \frac{\int_0^L I_z dz}{L} = \frac{I_0}{\xi L}(1 - \exp(-\xi L)). \tag{2.2.13}$$

By substituting (2.2.6) into (2.2.13) we get

$$\bar{I} = \frac{I_0}{(aC_{hl} + b)L}(1 - \exp(-(aC_{hl} + b)L)). \tag{2.2.14}$$

The C_{hl} to nitrogen ratio is given as

$$\theta_N^{-1} = (g_1 - g_2 T) + g_3 \bar{I}\exp(-g_4 T), \tag{2.2.15}$$

where g_1, g_2, g_3, and g_4 are constants (see Table 2.2) and C_{hl} is assumed to correlate to particulate nitrogen (xq_n) [91]. From this, we have

$$C_{hl} = \frac{xq_n}{(g_1 - g_2 T) + g_3 \bar{I}\exp(-g_4 T)}. \tag{2.2.16}$$

(2.2.1)–(2.2.16) constitutes a system of differential algebraic equations (DAEs).

2.3 DAEs to ODEs

We intend to use MISER [51] to find optimal controls for the model defined in Section 2.2. MISER is designed to solve problems involving ordinary differential equations (ODEs) only and it cannot directly accommodate the system of DAEs defined by (2.2.1)–(2.2.16). However, it is possible to transform a system of DAEs to an equivalent system of ODEs. A general approach is to differentiate

the original system k times until the derivatives for all variables appear (where k is the so called index of the DAE) [16, 52]. The system (2.2.1)–(2.2.16) is a DAE of index of 1 and there are only two states, $\bar{I}$ and C_{hl}, for which we require derivatives with respect to time t.

A general DAE system can be written in the form

$$\mathbf{E}_1\dot{\mathbf{x}}_1(t) = \mathbf{f}_1(t, \mathbf{x}_1(t), \mathbf{x}_2(t)) \tag{2.3.1}$$

$$\mathbf{0} = \mathbf{f}_2(t, \mathbf{x}_1(t), \mathbf{x}_2(t)), \tag{2.3.2}$$

where $\mathbf{x}_1(t) \in \mathbb{R}^{n_1}$ and $\mathbf{x}_2(t) \in \mathbb{R}^{n_2}$ are the state variables, $\mathbf{f}_1 : \mathbb{R} \times \mathbb{R}^{n_1} \times \mathbb{R}^{n_2} \to \mathbb{R}^{n_1}$ and $\mathbf{f}_2 : \mathbb{R}\times\mathbb{R}^{n_1}\times\mathbb{R}^{n_2} \to \mathbb{R}^{n_2}$ are given functions, and $n_1+n_2 = n$. For the remainder of this thesis, we adopt the convention that for a real valued function of a vector variable, $h(\mathbf{y})$, $\mathbf{y} = [y_1, y_2, \ldots, y_l]^\top \in \mathbb{R}^l$, the gradient with respect to $\mathbf{y}$ is defined as a row vector.

Using the approach in Jennings *et al.* [52], we differentiate (2.3.2) with respect to time t to yield

$$\frac{\partial \mathbf{f}_2}{\partial t} + \frac{\partial \mathbf{f}_2}{\partial \mathbf{x}_1}\dot{\mathbf{x}}_1 + \frac{\partial \mathbf{f}_2}{\partial \mathbf{x}_2}\dot{\mathbf{x}}_2 = \mathbf{0}, \tag{2.3.3}$$

which gives

$$\frac{\partial \mathbf{f}_2}{\partial \mathbf{x}_1}\dot{\mathbf{x}}_1 + \frac{\partial \mathbf{f}_2}{\partial \mathbf{x}_2}\dot{\mathbf{x}}_2 = -\frac{\partial \mathbf{f}_2}{\partial t}. \tag{2.3.4}$$

Combining (2.3.4) with (2.3.1), we have

$$\begin{bmatrix} \mathbf{E}_1 & 0 \\ \frac{\partial \mathbf{f}_2}{\partial \mathbf{x}_1} & \frac{\partial \mathbf{f}_2}{\partial \mathbf{x}_2} \end{bmatrix} \begin{bmatrix} \dot{\mathbf{x}}_1 \\ \dot{\mathbf{x}}_2 \end{bmatrix} = \begin{bmatrix} \mathbf{f}_1 \\ -\frac{\partial \mathbf{f}_2}{\partial t} \end{bmatrix}. \tag{2.3.5}$$

If we assume the system of DAEs (2.3.1) and (2.3.2) is of index 1, then the matrix $\frac{\partial \mathbf{f}_2}{\partial \mathbf{x}_2}$ is of full and constant rank n_2.

For our application, we have $\mathbf{E}_1 = \mathbf{I}$ and we let

$$\mathbf{x}_1 = [s, q_n, x, x_l, x_f]^\top, \tag{2.3.6}$$

$$\mathbf{x}_2 = \left[\bar{I}, C_{hl}\right]^\top, \tag{2.3.7}$$

$$\dot{\mathbf{x}}_1(t) = \mathbf{f}_1(t, \mathbf{x}_1(t), \mathbf{x}_2(t)), \tag{2.3.8}$$

$$\mathbf{f}_1(t, \mathbf{x}_1(t), \mathbf{x}_2(t)) = [\dot{s}, \dot{q}_n, \dot{x}, \dot{x}_l, \dot{x}_f]^\top, \tag{2.3.9}$$

$$\mathbf{f}_2(t, \mathbf{x}_1(t), \mathbf{x}_2(t)) = [f_{21}, f_{22}]^\top, \tag{2.3.10}$$

and, from (2.2.13) and (2.2.16) respectively,

$$f_{21} = \frac{I_0}{\xi L}(1 - \exp(-\xi L)) - \bar{I}, \tag{2.3.11}$$

$$f_{22} = \frac{x q_n}{(g_1 - g_2 T) + g_3 \bar{I} \exp(-g_4 T)} - C_{hl}. \tag{2.3.12}$$

In this context, (2.3.5) may be written as

$$\begin{bmatrix} \mathbf{I} & 0 \\ \frac{\partial \mathbf{f}_2}{\partial \mathbf{x}_1} & \frac{\partial \mathbf{f}_2}{\partial \mathbf{x}_2} \end{bmatrix} \begin{bmatrix} \dot{\mathbf{x}}_1 \\ \dot{\mathbf{x}}_2 \end{bmatrix} = \begin{bmatrix} \mathbf{f}_1 \\ -\frac{\partial \mathbf{f}_2}{\partial t} \end{bmatrix}. \tag{2.3.13}$$

Since $\frac{\partial \mathbf{f}_2}{\partial \mathbf{x}_2}$ is of full rank, the matrix in (2.3.13) is invertible and we may write

$$\begin{bmatrix} \dot{\mathbf{x}}_1 \\ \dot{\mathbf{x}}_2 \end{bmatrix} = \begin{bmatrix} \mathbf{I} & 0 \\ \frac{\partial \mathbf{f}_2}{\partial \mathbf{x}_1} & \frac{\partial \mathbf{f}_2}{\partial \mathbf{x}_2} \end{bmatrix}^{-1} \begin{bmatrix} \mathbf{f}_1 \\ -\frac{\partial \mathbf{f}_2}{\partial t} \end{bmatrix}. \tag{2.3.14}$$

Letting $\mathbf{x}(t) = [\mathbf{x}_1(t), \mathbf{x}_2(t)]^\top$, (2.3.14) may be written as

$$\dot{\mathbf{x}}(t) = \begin{bmatrix} \mathbf{I} & 0 \\ \frac{\partial \mathbf{f}_2}{\partial \mathbf{x}_1} & \frac{\partial \mathbf{f}_2}{\partial \mathbf{x}_2} \end{bmatrix}^{-1} \begin{bmatrix} \mathbf{f}_1 \\ -\frac{\partial \mathbf{f}_2}{\partial t} \end{bmatrix}. \tag{2.3.15}$$

Note that, by virtue of (2.3.11) and (2.3.12), we have

$$\begin{bmatrix} \mathbf{I} & 0 \\ \frac{\partial \mathbf{f}_2}{\partial \mathbf{x}_1} & \frac{\partial \mathbf{f}_2}{\partial \mathbf{x}_2} \end{bmatrix} = \begin{bmatrix} 1 & 0 & 0 & 0 & 0 & 0 & 0 \\ 0 & 1 & 0 & 0 & 0 & 0 & 0 \\ 0 & 0 & 1 & 0 & 0 & 0 & 0 \\ 0 & 0 & 0 & 1 & 0 & 0 & 0 \\ 0 & 0 & 0 & 0 & 1 & 0 & 0 \\ 0 & 0 & 0 & 0 & 0 & -1 & \frac{\partial f_{21}}{\partial C_{hl}} \\ 0 & \frac{\partial f_{22}}{\partial q_n} & \frac{\partial f_{22}}{\partial x} & 0 & 0 & \frac{\partial f_{22}}{\partial \bar{I}} & -1 \end{bmatrix} \text{ and } \begin{bmatrix} \mathbf{f}_1 \\ -\frac{\partial \mathbf{f}_2}{\partial t} \end{bmatrix} = \begin{bmatrix} \dot{s} \\ \dot{q}_n \\ \dot{x} \\ \dot{x}_l \\ \dot{x}_f \\ -\frac{\partial f_{21}}{\partial t} \\ -\frac{\partial f_{22}}{\partial t} \end{bmatrix}.$$

Using Maple [34], we then find that (2.3.15) may be written as

$$\dot{\mathbf{x}}(t) = \begin{bmatrix} \dot{s} \\ \dot{q}_n \\ \dot{x} \\ \dot{x}_l \\ \dot{x}_f \\ \dfrac{-\left(\frac{\partial f_{21}}{\partial C_{hl}}\frac{\partial f_{22}}{\partial q_n}\dot{q}_n\right) - \left(\frac{\partial f_{21}}{\partial C_{hl}}\frac{\partial f_{22}}{\partial x}\dot{x}\right) - \frac{\partial f_{21}}{\partial t} - \left(\frac{\partial f_{21}}{\partial C_{hl}}\frac{\partial f_{22}}{\partial t}\right)}{\frac{\partial f_{21}}{\partial C_{hl}}\frac{\partial f_{22}}{\partial \bar{I}} - 1} \\ \dfrac{-\left(\frac{\partial f_{22}}{\partial q_n}\dot{q}_n\right) - \left(\frac{\partial f_{22}}{\partial x}\dot{x}\right) - \left(\frac{\partial f_{22}}{\partial \bar{I}}\frac{\partial f_{21}}{\partial t}\right) - \frac{\partial f_{22}}{\partial t}}{\frac{\partial f_{21}}{\partial C_{hl}}\frac{\partial f_{22}}{\partial \bar{I}} - 1} \end{bmatrix}. \tag{2.3.16}$$

As we now have just ordinary differential equations defining all state variables, we need to specify initial values for $\bar{I}$ and C_{hl}. By referring to the I_0 graph in Muñoz-Tamayo *et al.* [91] or considering (2.2.4), we can see that at $t = 0$, $I_0 = 0$. Substituting this value into (2.2.13), we have

$$\bar{I}(0) = \frac{0}{\xi L}(1 - \exp(-\xi L)) = 0. \tag{2.3.17}$$

With this, we can substitute $q_n(0)$ and $x(0)$ (the values given in Table 2.2), $T(0)$ (found from (2.2.3)), and (2.3.17) into (2.2.16) to find

$$C_{hl}(0) = \frac{x(0)q_n(0)}{(g_1 - g_2T(0)) + g_3\bar{I}(0)\exp(-g_4T(0))} = 9.091 \times 10^{-1}\text{g}C_{hl}. \tag{2.3.18}$$

Note that this transformation preserves the original dynamics and guaranties satisfaction of alge-

braic equations [52]. It is routinely used in the optimal control literature for a variety of applications [2]. The resulting system of ODE's is now suitable for implementation with MISER.

2.4 Problem Formulation

In this study, we are interested in optimising the performance of the raceway model by choosing the input flow rate (f_{in}), the inflow nitrogen concentration (s_{in}), and the initial extracellular nitrogen concentration ($s(0)$). Guided by the objectives in Muñoz-Tamayo *et al.* [91], the aim is to maximise either the biomass productivity or the lipid productivity. Both of these objectives can be incorporated in the following combined optimal control and optimal parameter selection problem

$$\max_{\substack{f_{in} \\ s_{in} \\ z_1}} \int_0^{t_f} \psi(t, \mathbf{x}(t), f_{in}(t))dt \tag{2.4.1}$$

subject to the dynamics (2.3.16), the initial conditions,

$$\begin{aligned} s(0) &= z_1, \\ q_n(0) &= 0.09, \\ x(0) &= 110, \\ x_l(0) &= 22, \\ x_f(0) &= 55, \\ \bar{I}(0) &= 0, \\ C_{hl}(0) &= 0.909, \end{aligned} \tag{2.4.2}$$

the control bounds

$$\begin{aligned} 0 \leq f_{in}(t) \leq 0.8333, \\ 0 \leq s_{in}(t) \leq 100 \end{aligned} \tag{2.4.3}$$

and the parameter bounds

$$0 \leq z_1 \leq 5.$$

Note that the initial conditions for q_n, x, x_l, and x_f are taken from [91].

The upper bound of f_{in} corresponds to a maximum rate of 20m^3 per day, chosen after personal consultation with the authors of the original model [91].

If the objective is to optimise lipid productivity then

$$\psi(t, \mathbf{x}(t), f_{in}(t)) = f_{in}(t)x_l(t) = f_{in}(t)x_l(t). \tag{2.4.4}$$

Alternatively, if the objective is to optimise biomass productivity, then

$$\psi(t, \mathbf{x}(t), f_{in}(t)) = f_{in}(t)x(t) = f_{in}(t)x(t). \tag{2.4.5}$$

MISER employs the control parameterisation technique which allows for a variety of different parametrised forms of the control functions [51]. We have chosen piecewise constant controls over the time horizon $[0, 720]$ (720 hours is equivalent to 30 days) with a uniform partition into 1 hour intervals. Note that MISER will only guarantee a locally optimal solution as it uses the sequential quadratic programming (SQP) method NLPQLP [109] to solve the underlying optimisation problem. Whilst using a standard home computer with an Intel core i7-7700K 4.2Ghz, convergence to solutions can take approximately 4-5 hours.

The Hamiltonian function of the problem, H, can be written in the general form

$$H = K_3 + (K_2 s_{in} + K_1) f_{in}, \tag{2.4.6}$$

where the terms K_1, K_2, and K_3 are functions of the various states. Note that the formulation of the problem in MISER means that K_1, K_2, and K_3 are readily computable within existing subroutines. If s_{in} is a fixed value (i.e. not a control variable), then this can be re-written as

$$H = M_1 f_{in} + M_2, \tag{2.4.7}$$

where M_1 and M_2 are functions of the states only. Maximisation of H then requires

$$f_{in}^* = \begin{cases} 0.8333, & \text{if } M_1 > 0, \\ 0, & \text{if } M_1 < 0, \\ \text{undetermined}, & \text{if } M_1 = 0. \end{cases} \tag{2.4.8}$$

If s_{in} is a control variable then H reverts back to the general form (2.4.6). Although H contains a product term of the controls, the non-negativity of f_{in} and s_{in} makes it relatively easy to analyse the optimality conditions. The switching function for f_{in} is $K_2 s_{in} + K_1$ and the switching function

for s_{in} is $K_2 f_{in}$. Thus maximisation of H requires

$$f_{in}^* = \begin{cases} 0.8333, & \text{if } K_2 s_{in} + K_1 > 0, \\ 0, & \text{if } K_2 s_{in} + K_1 < 0, \\ \text{undetermined}, & \text{if } K_2 s_{in} + K_1 = 0, \end{cases} \tag{2.4.9a}$$

and

$$s_{in}^* = \begin{cases} 100, & \text{if } K_2 f_{in} > 0, \\ 0, & \text{if } K_2 f_{in} < 0, \\ \text{undetermined}, & \text{if } K_2 f_{in} = 0. \end{cases} \tag{2.4.9b}$$

The switching functions will be plotted along with the corresponding controls to see if the optimality conditions given by (2.4.8) and (2.4.9) are satisfied.

2.5 Base Results

The results presented in this chapter have been previously published by the candidate in [47].

It is important to acknowledge several errors in the model as presented in [47]. Firstly, temperature should, of course, be in the units of °C and K_s should be in the units of gN m^{-3}. Next, all coefficients $I_{0a}, I_{0b}, \ldots, I_{0h}$ (due to confusion of the time units used), as well as L were reported incorrectly, the correct values (as actually used for the numerical result in [47]) are listed in Table 2.2. Also, there was a lack of accuracy in converting gC over 30 days to tons ha^{-1} a^{-1}. Finally, we discovered an error in our model code where the value of 5 µmol photonsm^{-2} s^{-1} instead of 50 µmol photonsm^{-2} s^{-1} was used for ϵ_I. For the results presented in this thesis, all of these errors have been corrected. Note that the revised results exhibit very similar behaviour to those presented in [47].

The first set of results assume that the influent nitrogen concentration, s_{in}, is set to 50 for the duration of the time horizon and that the initial extracellular nitrogen concentration, $s(0) = z_1$, is fixed to the value 2. This scenario corresponds to the open loop optimal control problem solved in Muñoz-Tamayo *et al.* [91]. We find that the resulting optimal objective function value for lipids (2.4.4) is 7584.4 gC (grams of carbon) and that for mass (2.4.5) is 48681 gC (we use MISER [51]

to solve the lipid scenario with the options of: number of knots in the partition for the control = 721, tolx = 10^{-9}, tolpsi = 10^{-7}, hmax = 10^{-2}, maxite = 1000, epsopt = 10^{-12}, epscon = 10^{-8}, imerit = 2, and ilql = 1 as well as using the NLPQLP optimiser [109]). The corresponding optimal control control f_{in} for each case is shown in Figures 2.5.1 and 2.5.2, respectively. In both cases, the control appears to be of bang-singular type and the signs of the switching functions appear to generally follow the required optimality conditions (2.4.8). Note that we don't expect exact satisfaction of optimality conditions here as the partition of the time horizon is fixed so that the exact switching instants of the optimal control could not be determined. We did attempt to solve these problems using the time scale transformations described in Section 1.3.4 in an attempt to optimise the switching times, but resulting transformed problems proved to be too difficult to solve numerically. Note that the figure displaying corresponding inflow rates for the results in [91] does not show a bang-singular pattern indicating that these solutions are far from optimal. Assuming, as in Muñoz-Tamayo *et al.* [91], that carbon contributes 56% of ash free dry weight, the yields are equivalent to 28.928 tons ha^{-1} a^{-1} and 185.67 tons ha^{-1} a^{-1}, respectively. They compare well to the corresponding results in Muñoz-Tamayo *et al.* [91] which are approximately 24 tons ha^{-1} a^{-1} and 168 tons ha^{-1} a^{-1}, respectively, and which themselves are noted to be consistent with other productivities reported in the literature. However, as pointed out in Muñoz-Tamayo *et al.* [91], we note that our results are also based on temperature and light profiles for the month of June, so cannot be extrapolated directly to an annual operation. Figure 2.5.3 combines the optimal inflow rates for both objectives. Note that the objective of maximum lipid yield results in higher inflow rates earlier in the time horizon and a 2-3 day period of zero flow towards the end of the time horizon. As can be seen in Figure 2.5.4, this zero flow period results in a zero extracellular nitrogen concentration between day 25 and day 27 which promotes the growth of lipids (see Figure 2.5.7). Also, both solutions involve a distinct period of maximum inflow at the end of the time horizon due to the need to harvest the microalgae. In the literature, this is sometimes referred to as a washout period. The extracellular nitrogen concentration and other state variables are shown in Figures 2.5.4–2.5.10. As in Muñoz-Tamayo *et al.* [91], we also present the neutral lipid quota, $\frac{x_l}{x}$, and the efficiency of light absorption, $\eta_L = 1 - \exp(-\xi L)$ in Figures 2.5.11 and 2.5.12, respectively. Note that the latter is simply a measure of how efficiently light is being absorbed in the pond. A value of 1 would indicate complete absorption.

We consider the above results for lipids to be a base case to which further results aimed at improving lipid production will be compared, both in this and in subsequent chapters.

Figure 2.5.1: Fixed s_{in} and $s(0)$. f_{in} and switching function (Lipids)

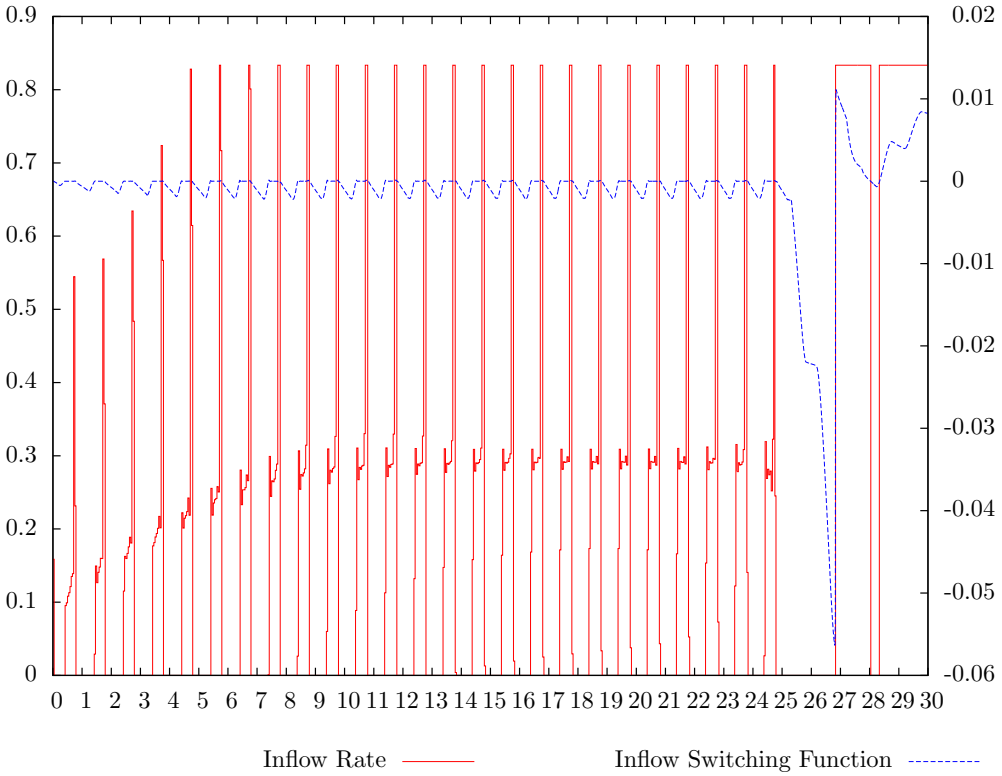

Figure 2.5.2: Fixed s_{in} and $s(0)$. f_{in} and switching function (Biomass)

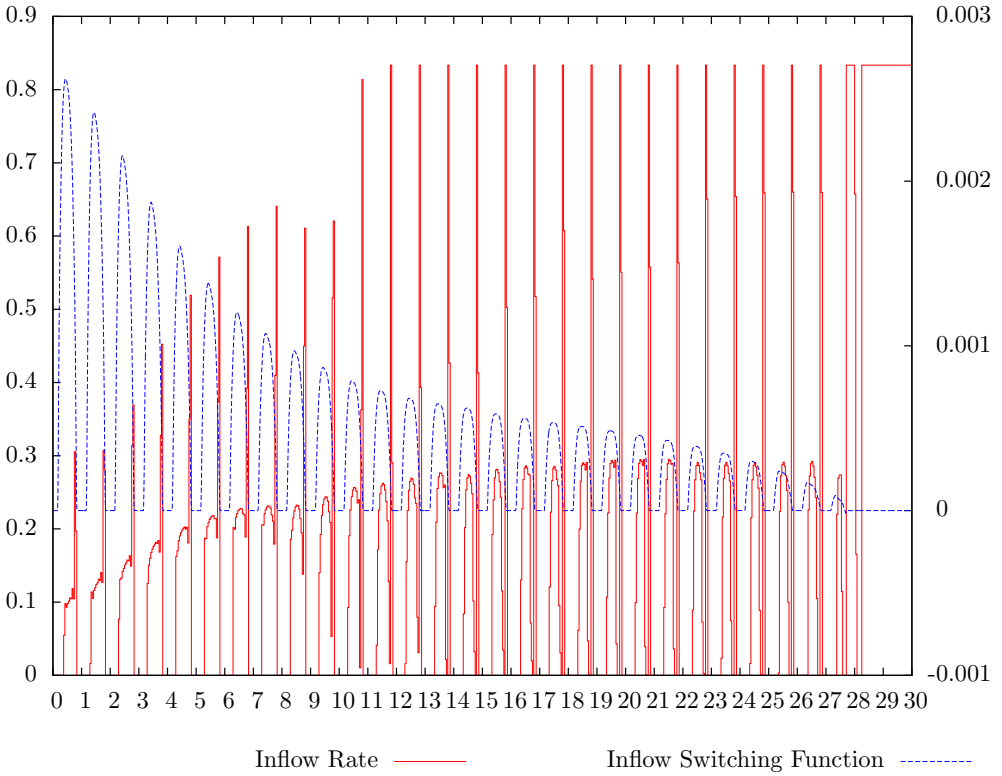

Figure 2.5.3: Fixed s_{in} and $s(0)$. f_{in} (Inflow rate)

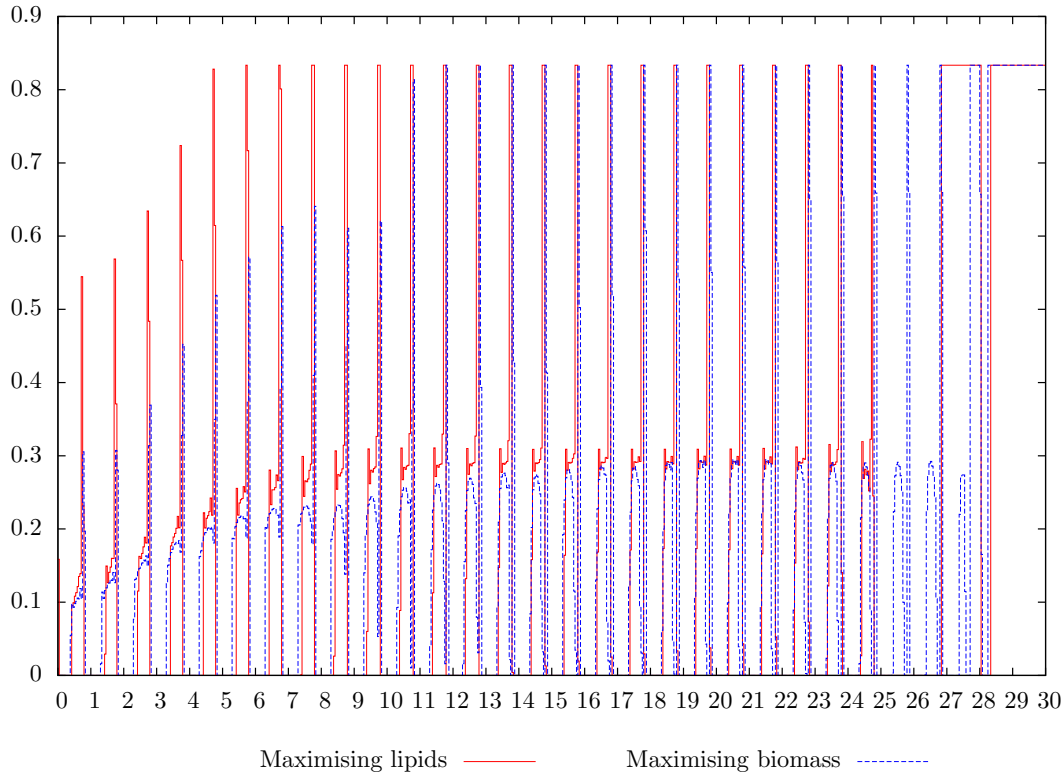

Figure 2.5.4: Fixed s_{in} and $s(0)$. s (Extracellular nitrogen concentration)

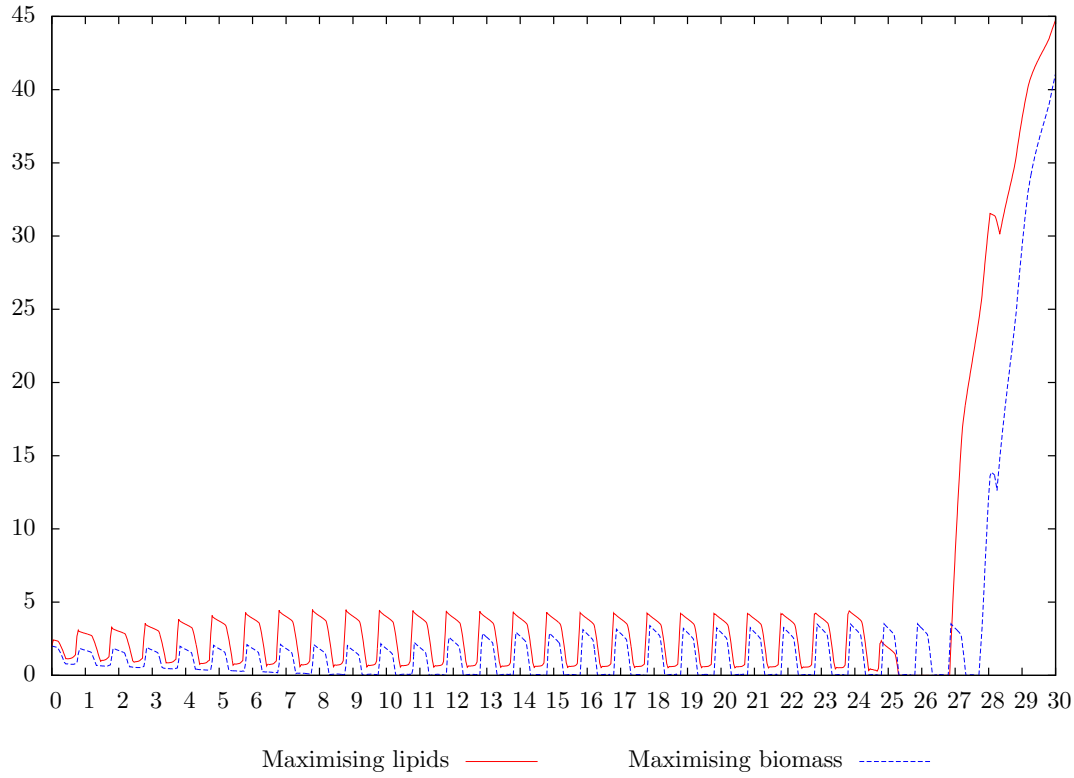

Figure 2.5.5: Fixed s_{in} and $s(0)$. q_n (Nitrogen quota)

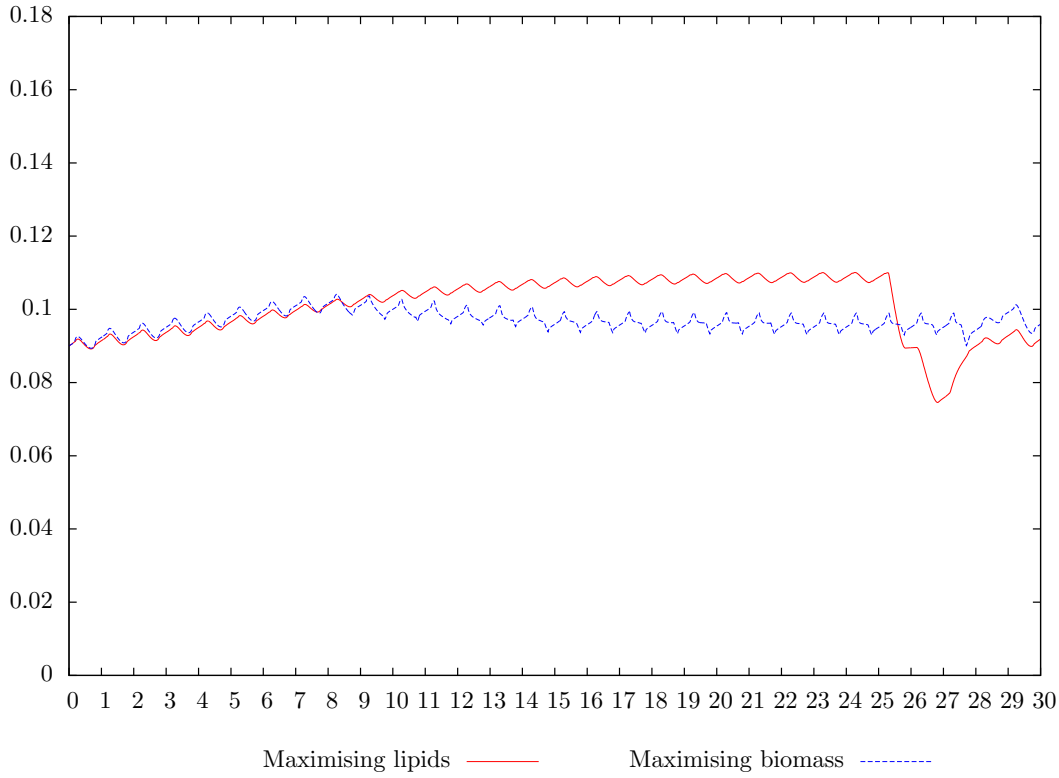

Figure 2.5.6: Fixed s_{in} and $s(0)$. x (Carbon biomass concentration)

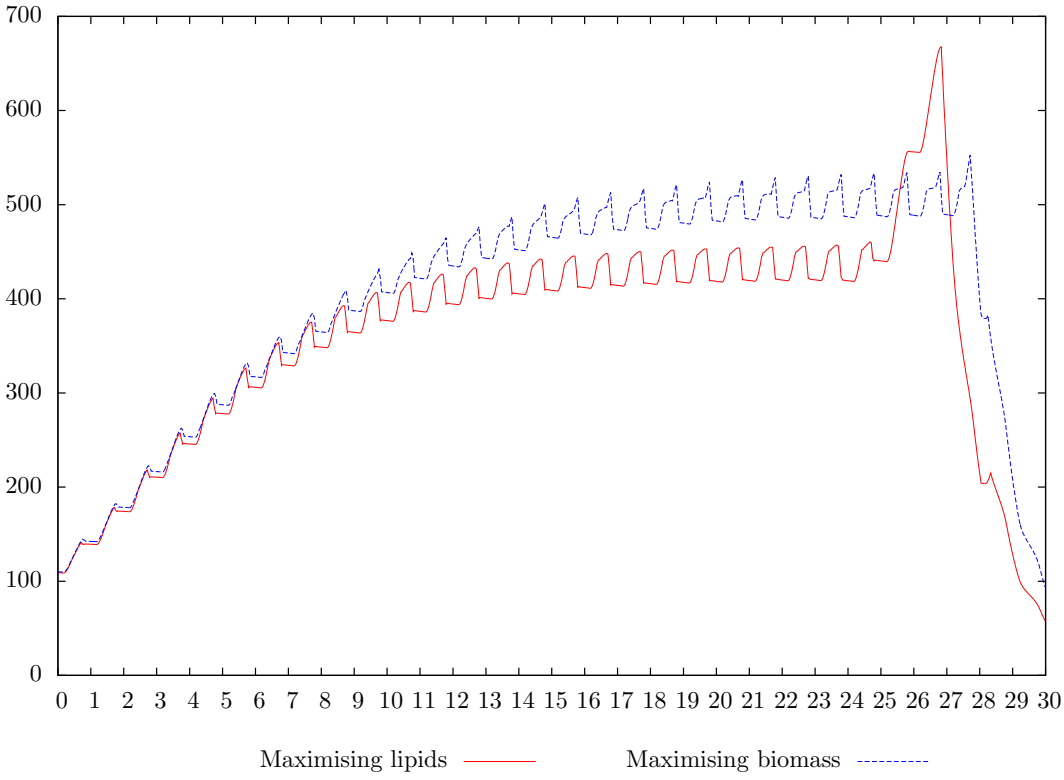

Figure 2.5.7: Fixed s_{in} and $s(0)$. x_l (Lipid carbon concentration)

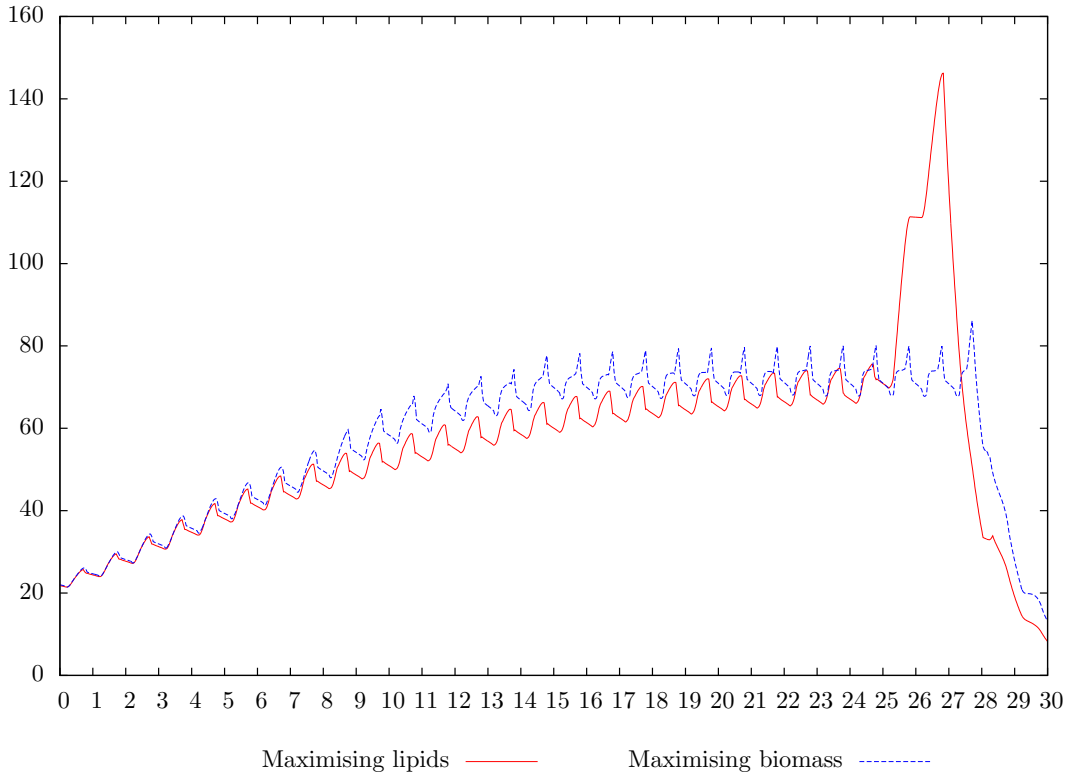

Figure 2.5.8: Fixed s_{in} and $s(0)$. x_f (Functional carbon concentration)

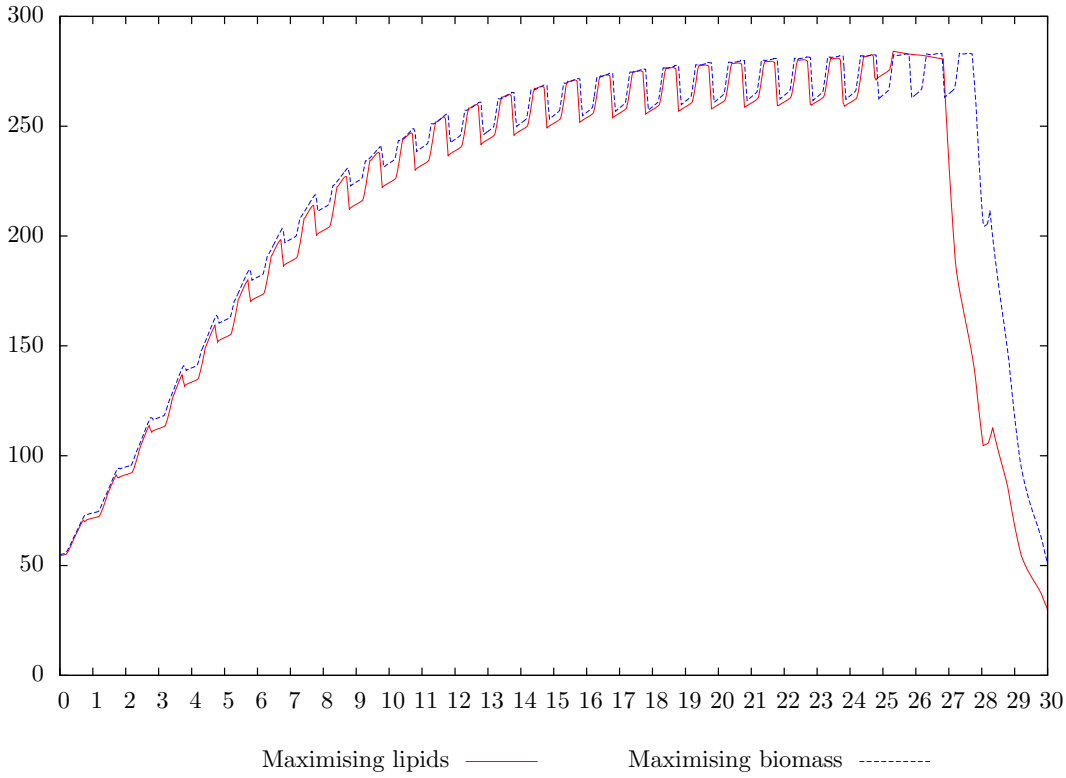

Figure 2.5.9: Fixed s_{in} and $s(0)$. $\bar{I}$ (Average light intensity)

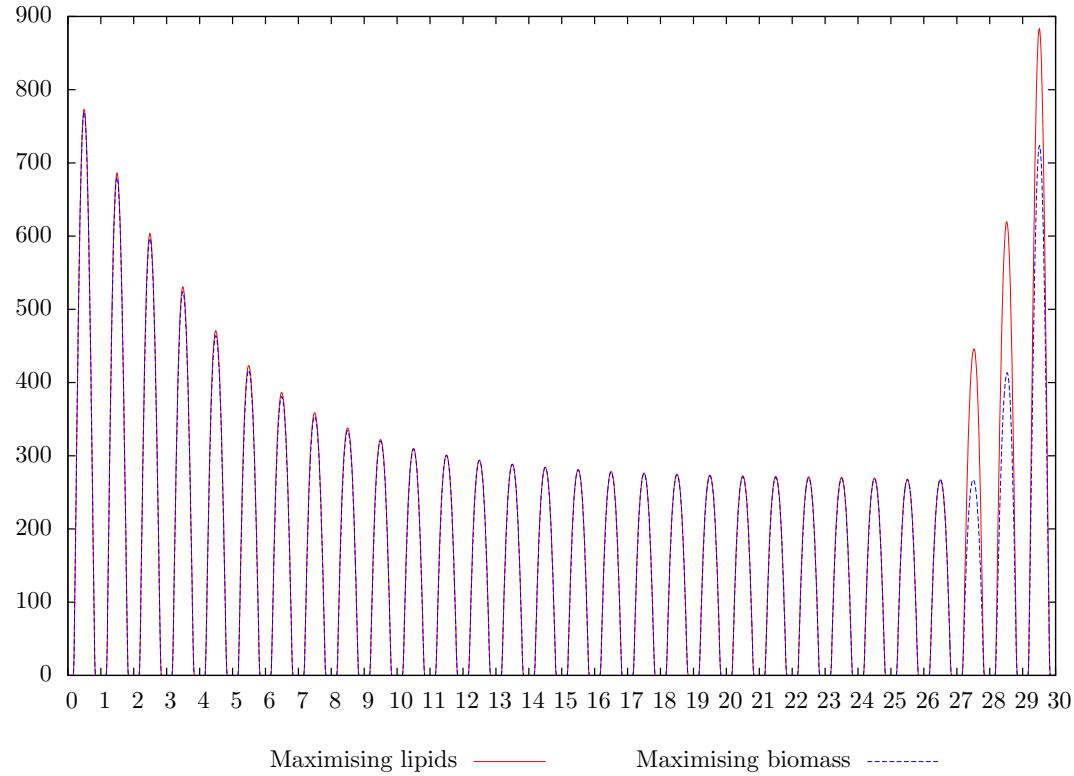

Figure 2.5.10: Fixed s_{in} and $s(0)$. C_{hl} (Chlorophyll concentration)

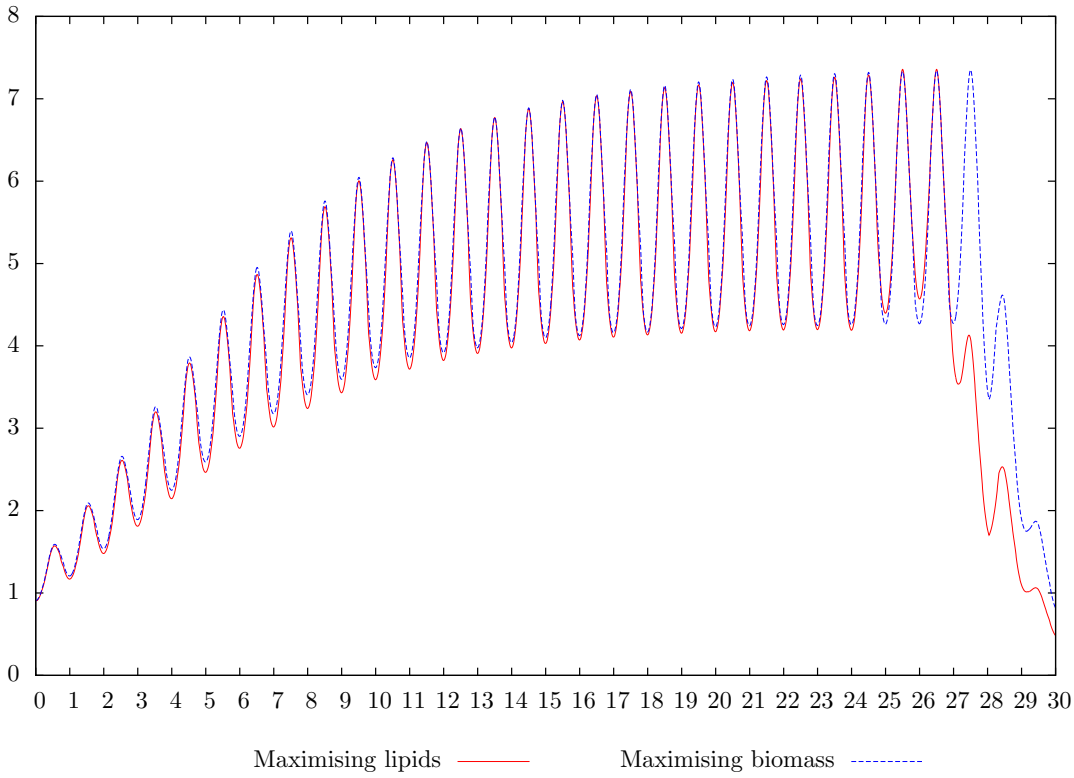

Figure 2.5.11: Fixed s_{in} and $s(0)$. $\frac{x_l}{x}$ (Lipid Quota)

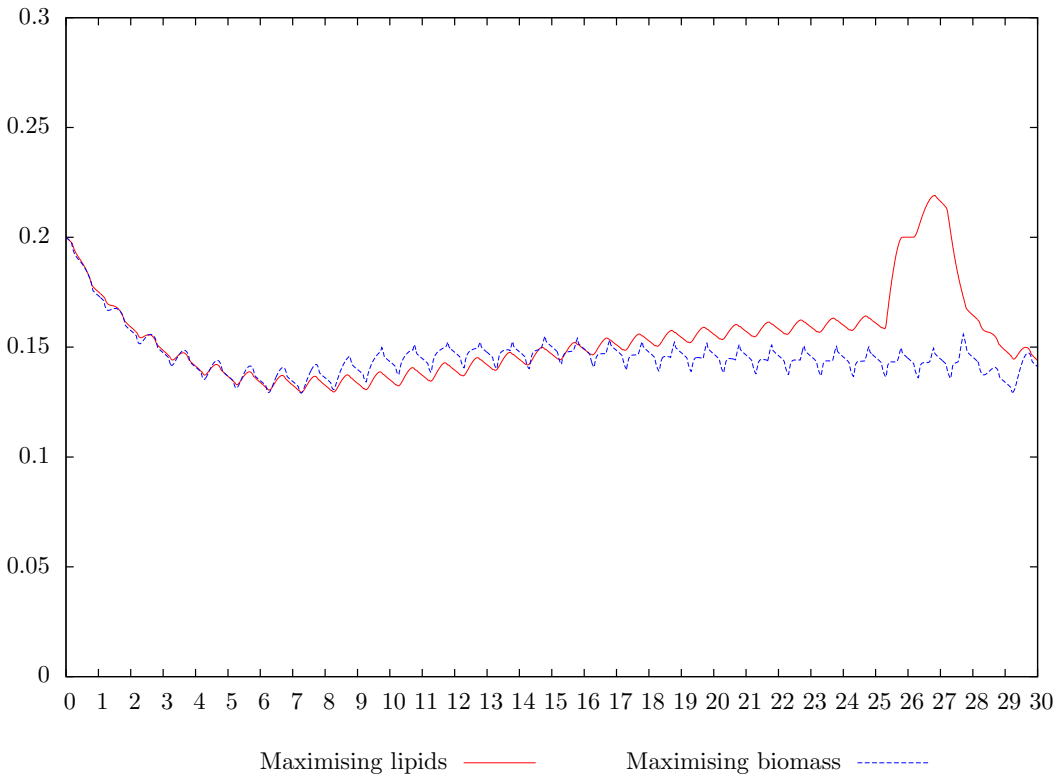

Figure 2.5.12: Fixed s_{in} and $s(0)$. η_L (Efficiency of light absorption)

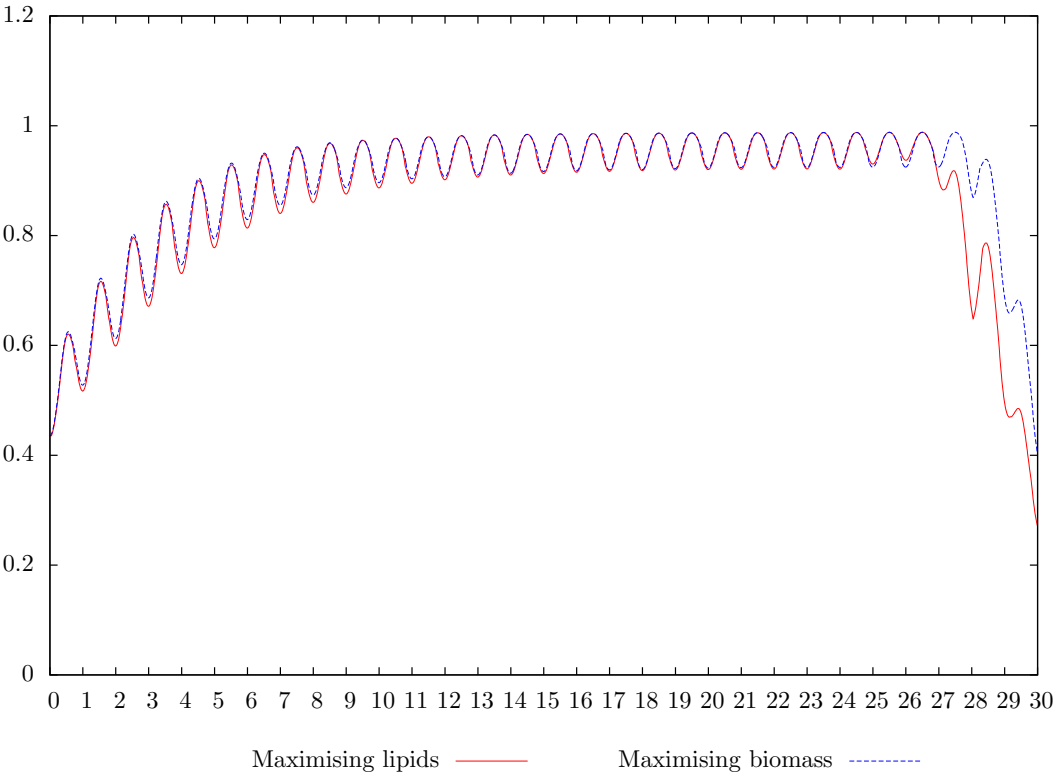

2.6 Varying Nitrogen Supply

We now allow a variable influent nitrogen concentration with the bounds

$$0 \leq s_{in} \leq 100, \ t \in [0, 720], \tag{2.6.1}$$

and we also allow $s(0) = z_1$ to be variable with

$$0 \leq z_1 \leq 5. \tag{2.6.2}$$

We consider only the objective (2.4.1) with integrand (2.4.4) from now on, i.e., the aim is to maximise the production of lipids. We denote this as Problem P for later reference. Optimisation of Problem P achieves a total yield of 9701.5 gC (37.003 tons ha^{-1} a^{-1}) which is a 27.91% improvement over the base case result in Section 2.5. We use MISER to solve Problem P with the options of: number of knots in the partition for the control = 721, tolx = 10^{-9}, tolpsi = 10^{-9}, hmax = 10^{-4}, maxite = 1000, epsopt = 10^{-8}, epscon = 10^{-9}, imerit = 2, and ilql = 1 as well as using the NLPQLP optimiser [109]. Graphs of the optimal controls, states, and efficiency of light absorption can be found in Figures 2.6.1–2.6.10. Similar to the results in Figures 2.5.4 and 2.5.7, it would appear that lipid production can be maximised by a combination of higher extracellular nitrogen concentration early on and a 'starvation period' of low or zero nitrogen concentration close to the end of the process (note the zero feeding flow rate between day 22 and day 27 in Figure 2.6.1). The optimal value of $s(0) = z_1 = 5$ and s_{in} is at its upper bound for most of the time horizon. Note that the efficiency of light absorption has increased over most of the time horizon (compare the solid lined curves in Figures 2.5.12 and 2.6.10).

The results for Problem P indicate that there is significant potential to increase yield if more nitrogen can be made available early. Indeed, if we increase the upper bounds on s_{in} and z_1 in (2.6.1) and (2.6.2) to 500 and 100, respectively, we finally see a limit of this potential with a resulting yield of 11735 gC (44.760 tons ha^{-1} a^{-1}) a 54.73% improvement over the base case result. The corresponding optimal $z_1 = 100$ and the optimal s_{in} barely reaches the upper bound of 500 in this case (at which point $f_{in} = 0$ and thus the s_{in} value there has no effect on nitrogen supply, see Figures 2.6.11 and 2.6.12). Note also that f_{in} is generally reduced compared to the original version of Problem P, since not much is inflow is required to raise the extracellular nitrogen concentration. In contrast, there are now also two distinct intervals of zero extracellular nitrogen concentration (see Figure 2.6.13) which lead to two rapid growth phases for lipids (see Figure 2.6.15). The efficiency

Figure 2.6.1: Variable s_{in} and $s(0)$. f_{in} (Inflow rate)

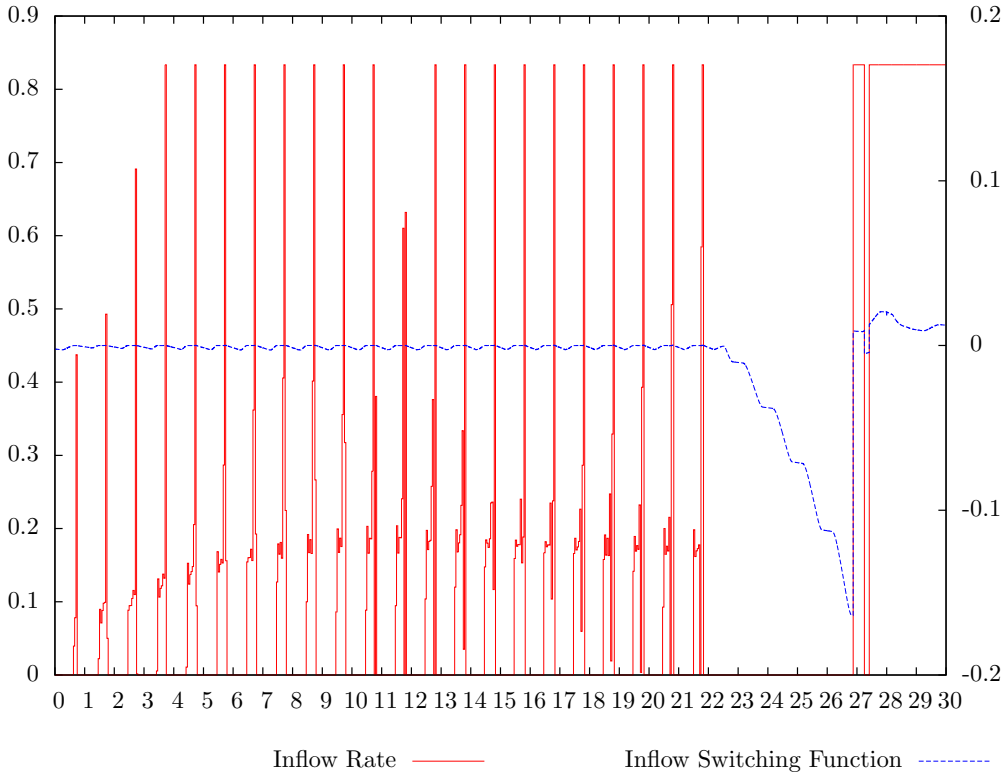

of light absorption (Figure 2.6.16) show excellent utilisation of insolation in this case. One must acknowledge that the high nitrogen concentration obtained with these results are unlikely to be reached in practice, though.

Figure 2.6.2: Variable s_{in} and $s(0)$. s_{in} (Influent Nitrogen Concentration)

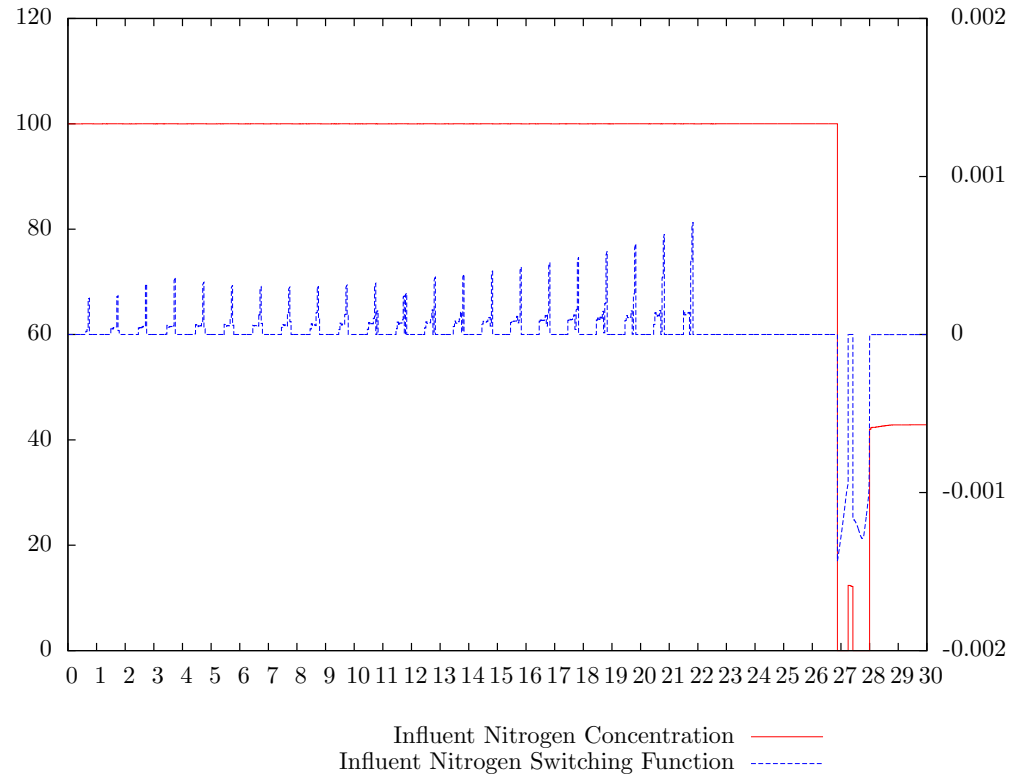

Figure 2.6.3: Variable s_{in} and $s(0)$. s (Extracellular Nitrogen Concentration)

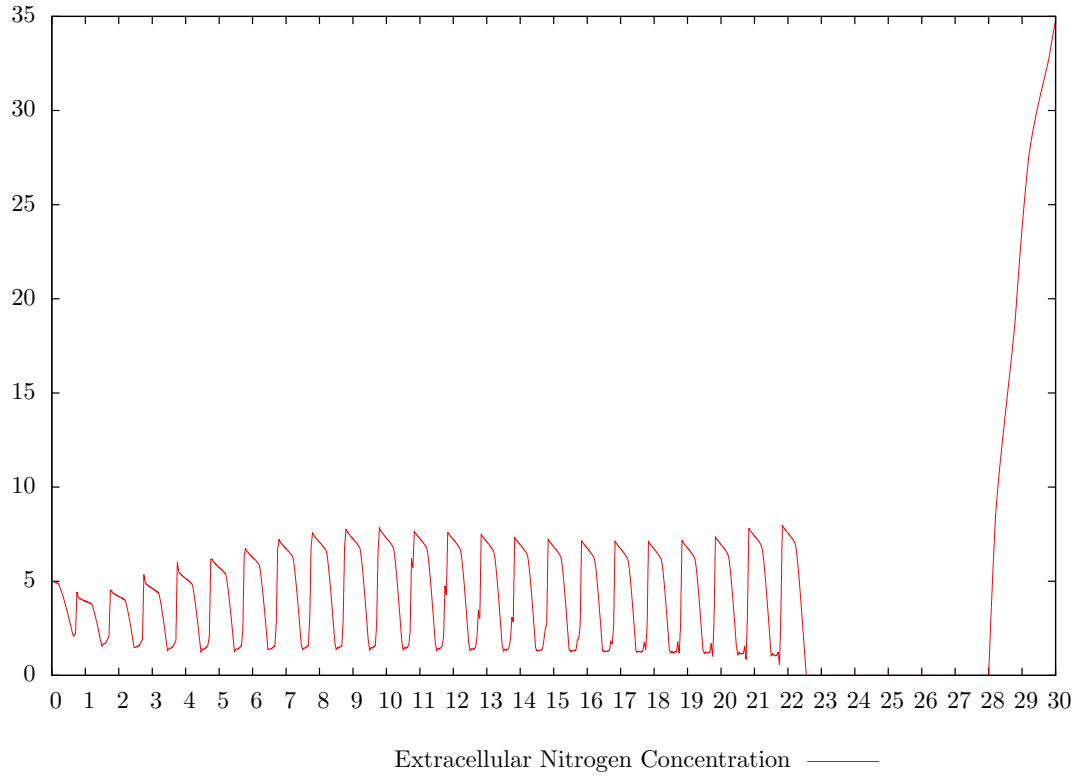

Figure 2.6.4: Variable s_{in} and $s(0)$. q_n (Nitrogen quota)

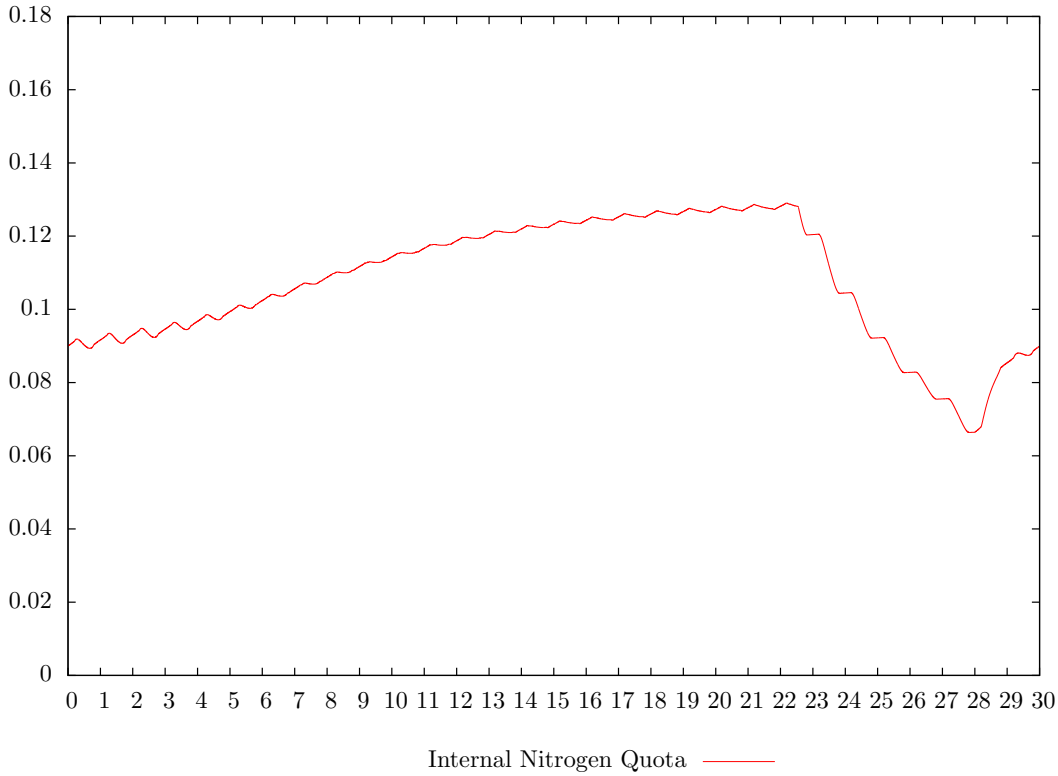

Figure 2.6.5: Variable s_{in} and $s(0)$. x (Carbon biomass concentration)

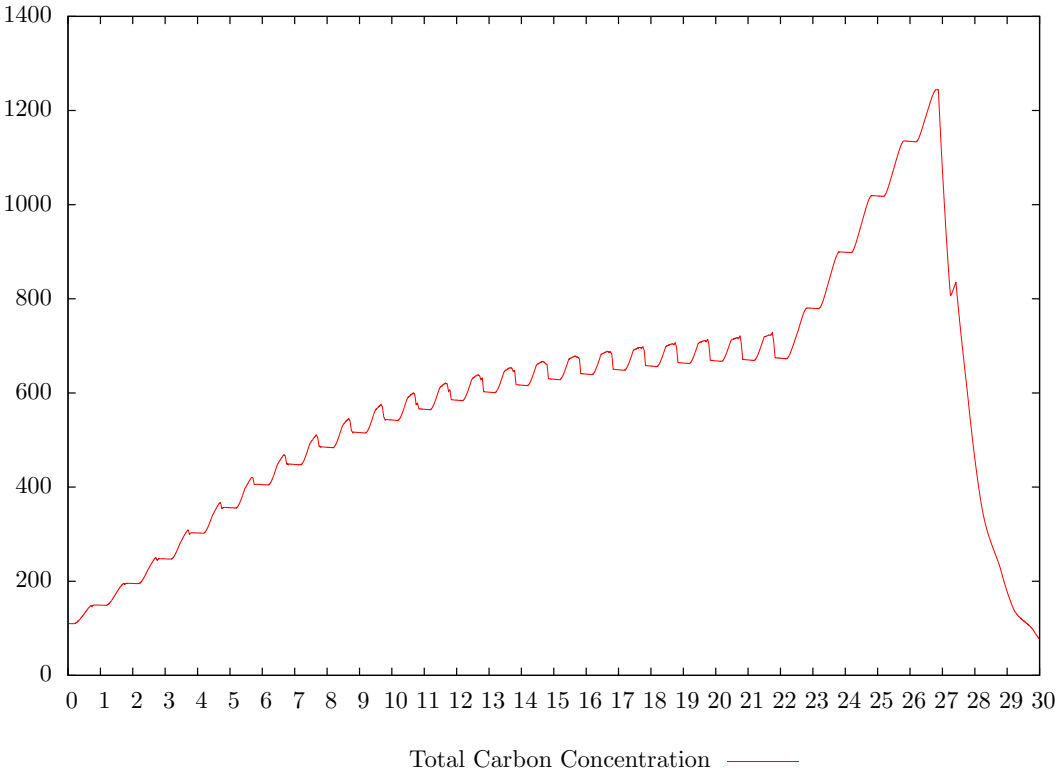

Figure 2.6.6: Variable s_{in} and $s(0)$. x_l (Lipid carbon concentration)

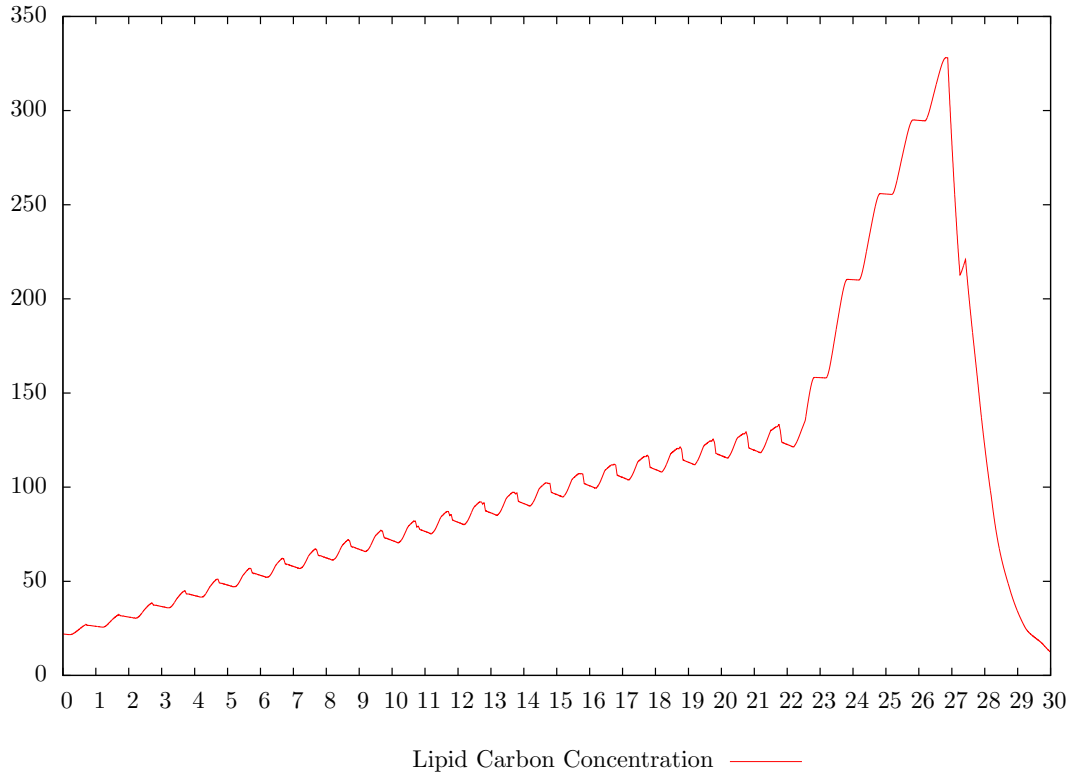

Figure 2.6.7: Variable s_{in} and $s(0)$. x_f (Functional carbon concentration)

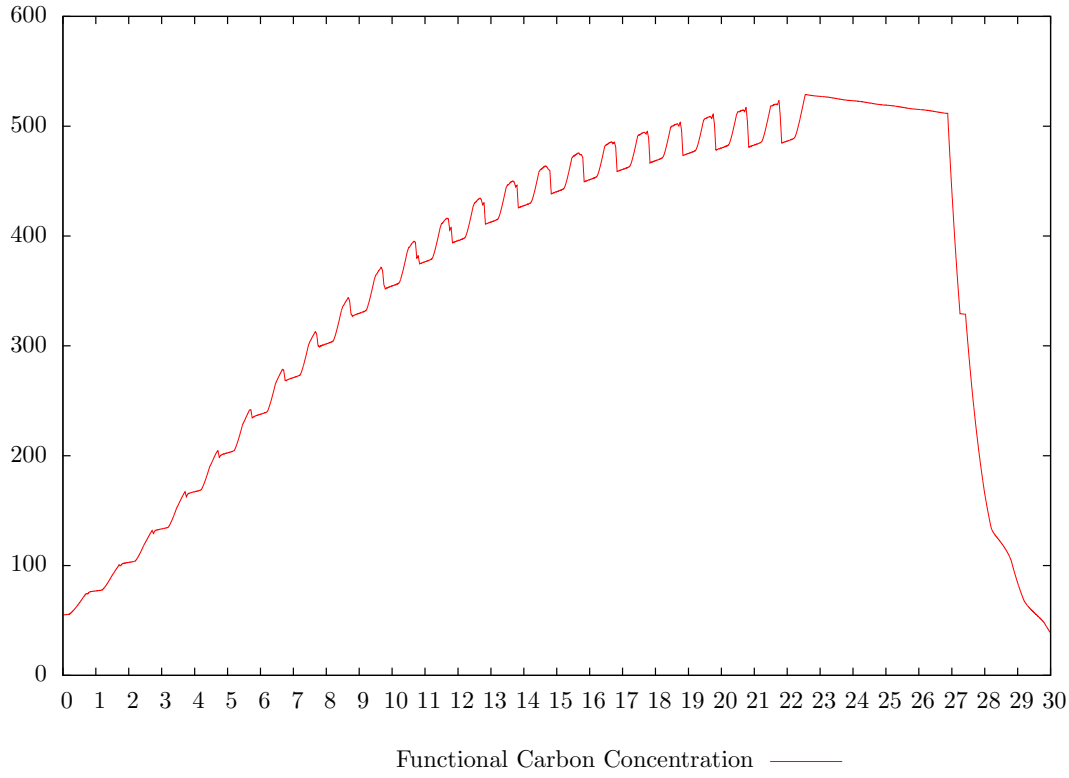

Figure 2.6.8: Variable s_{in} and $s(0)$. $\bar{I}$ (Average light intensity)

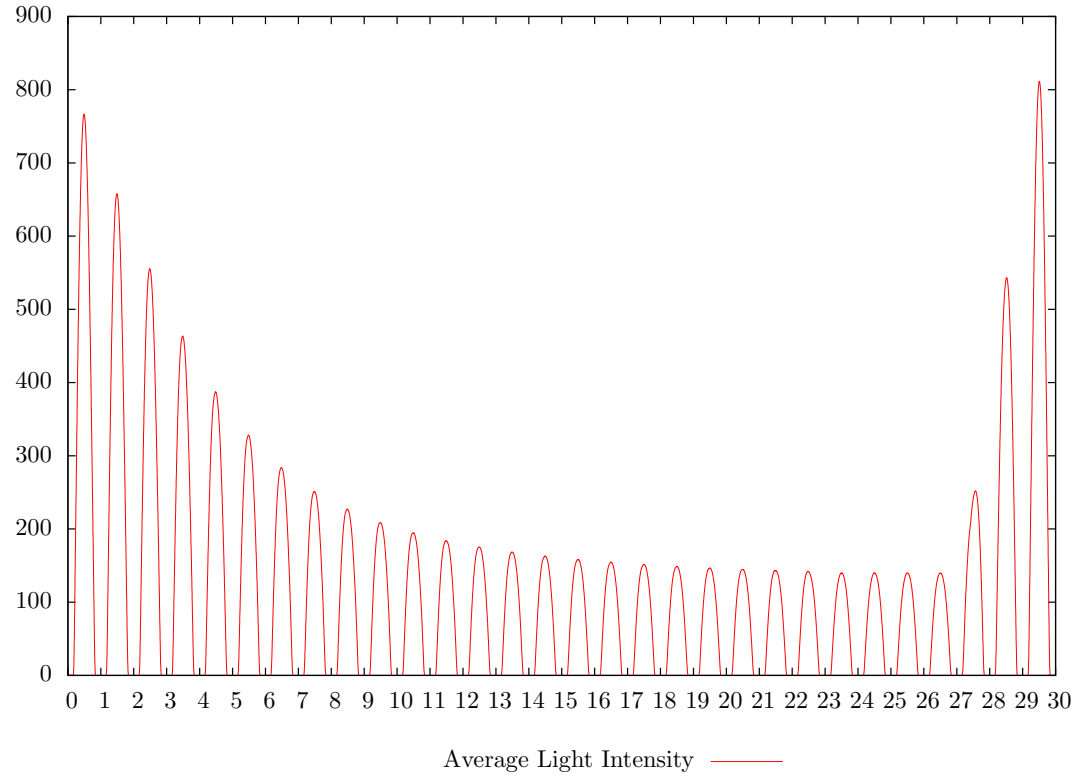

Figure 2.6.9: Variable s_{in} and $s(0)$. C_{hl} (Chlorophyll concentration)

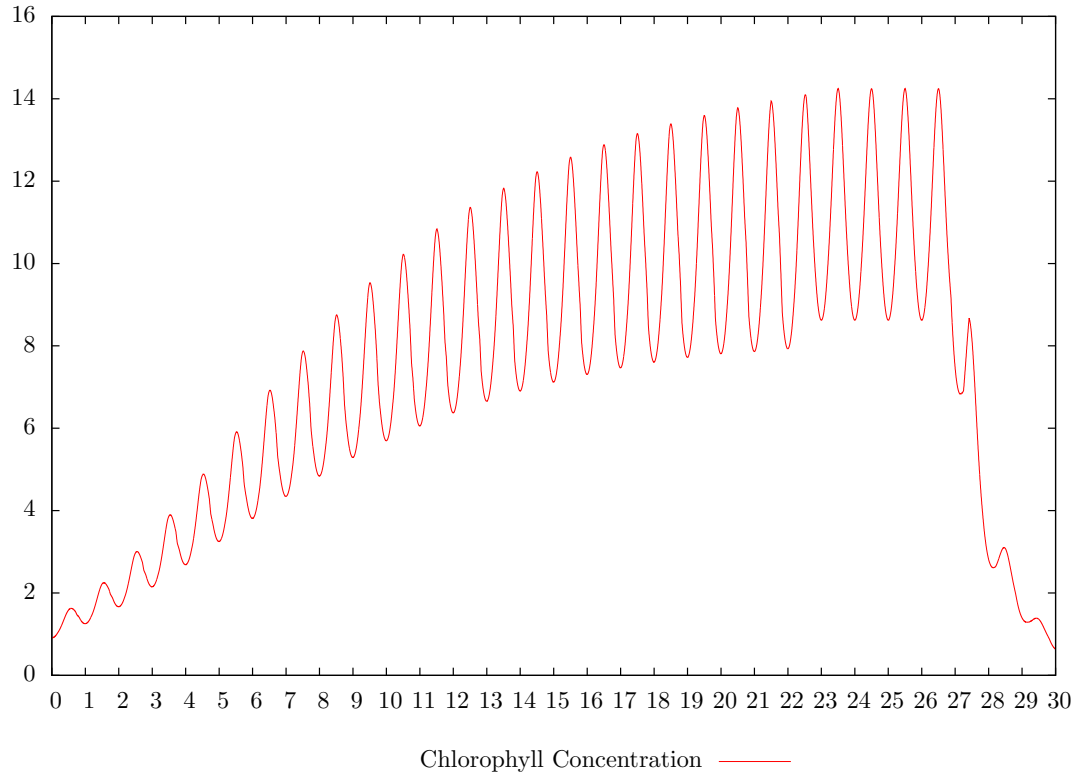

Figure 2.6.10: Variable s_{in} and $s(0)$. η_L (Efficiency of light absorption)

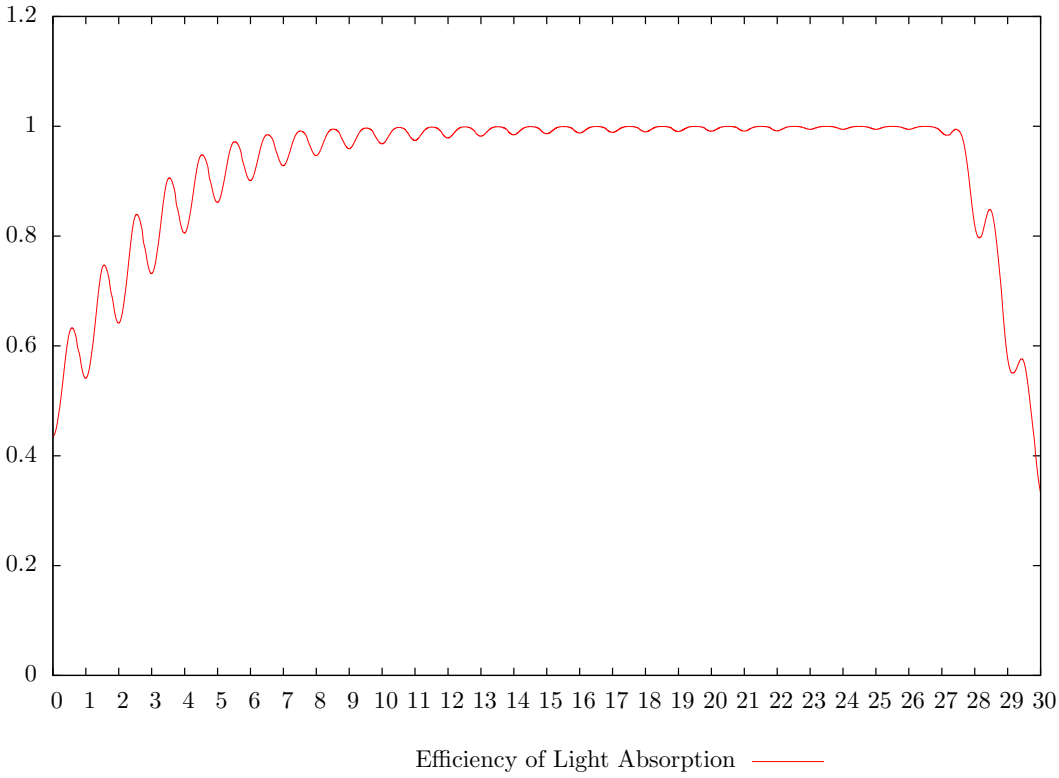

Figure 2.6.11: Extreme Nitrogen. f_{in} (Inflow Rate)

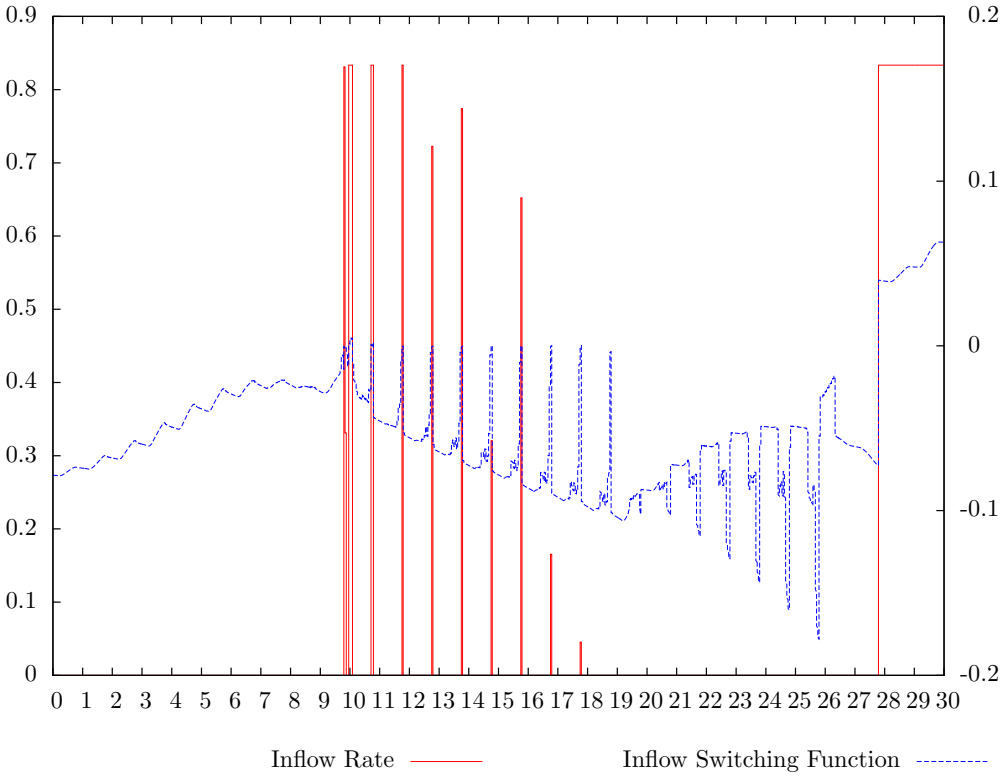

Figure 2.6.12: Extreme Nitrogen. s_{in} (Influent Nitrogen Concentration)

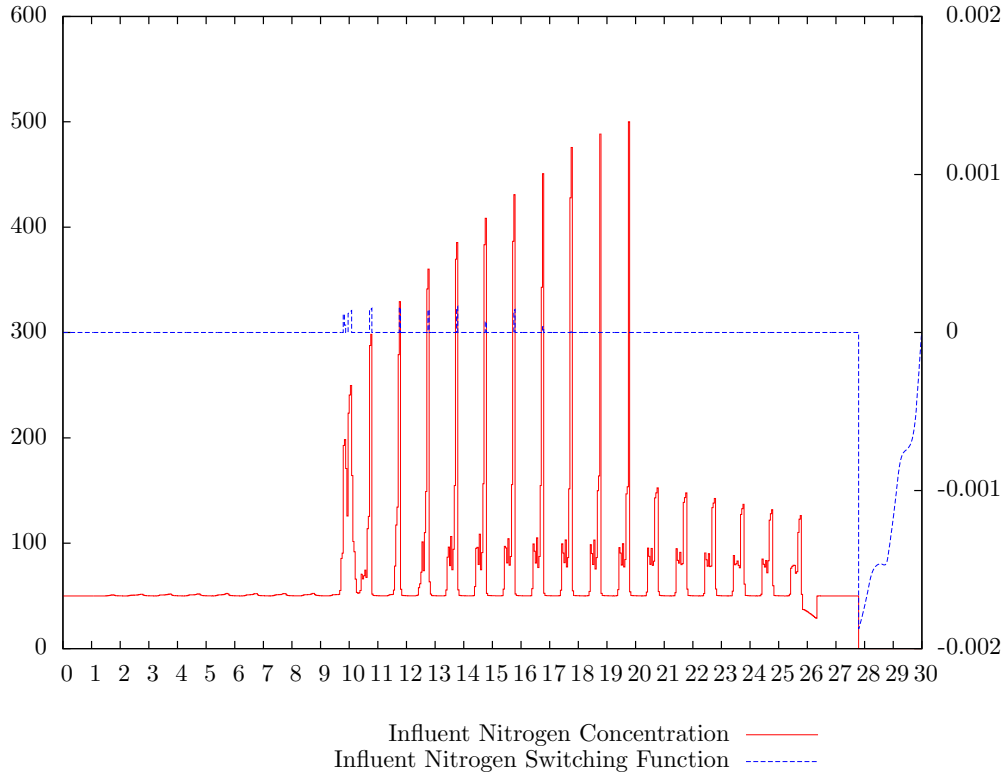

Figure 2.6.13: Extreme Nitrogen. s (Extracellular Nitrogen Concentration)

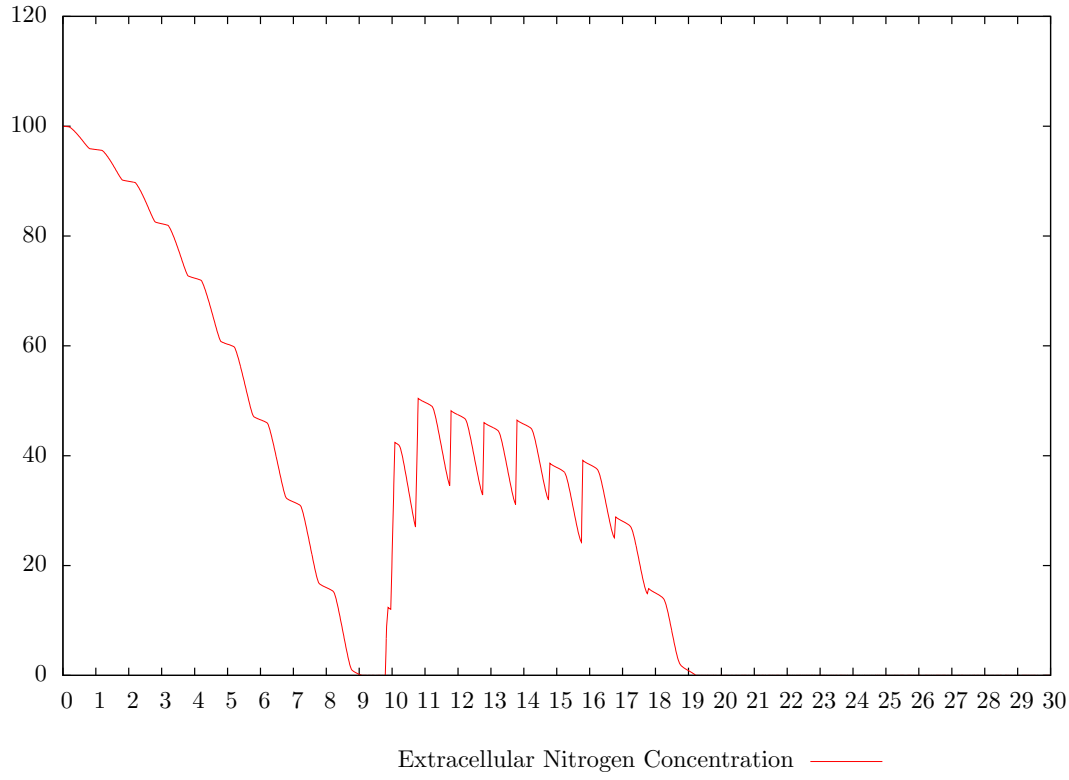

Figure 2.6.14: Extreme Nitrogen. x (Carbon biomass concentration)

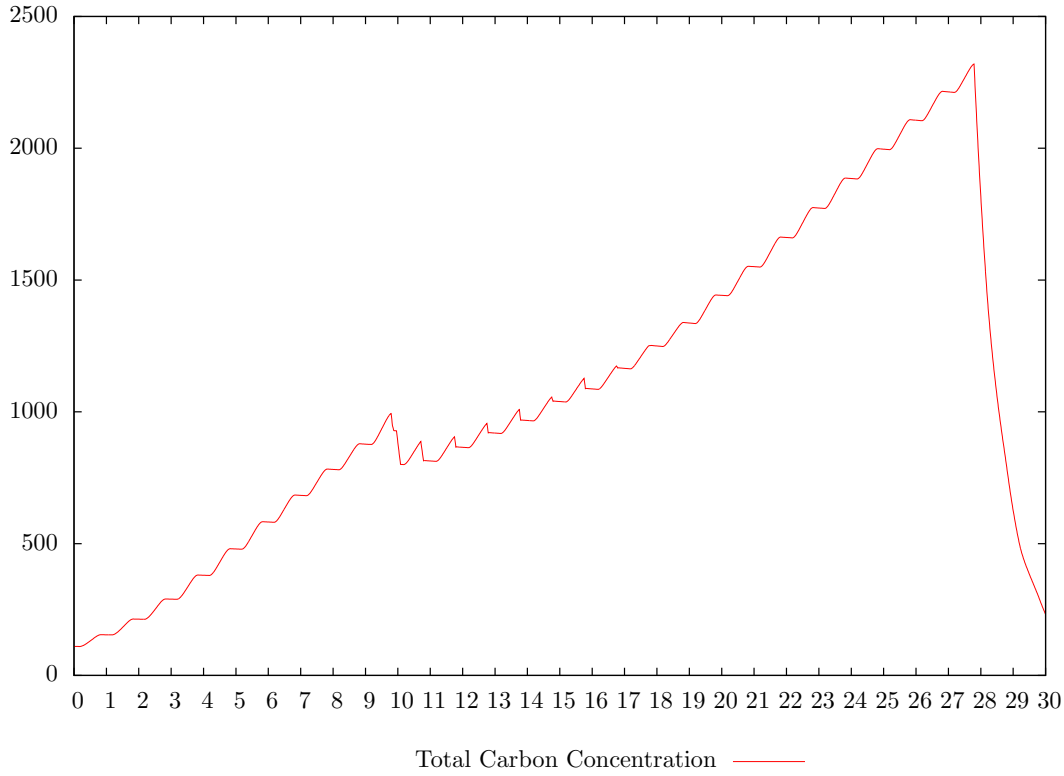

Figure 2.6.15: Extreme Nitrogen. x_l (Lipid carbon concentration)

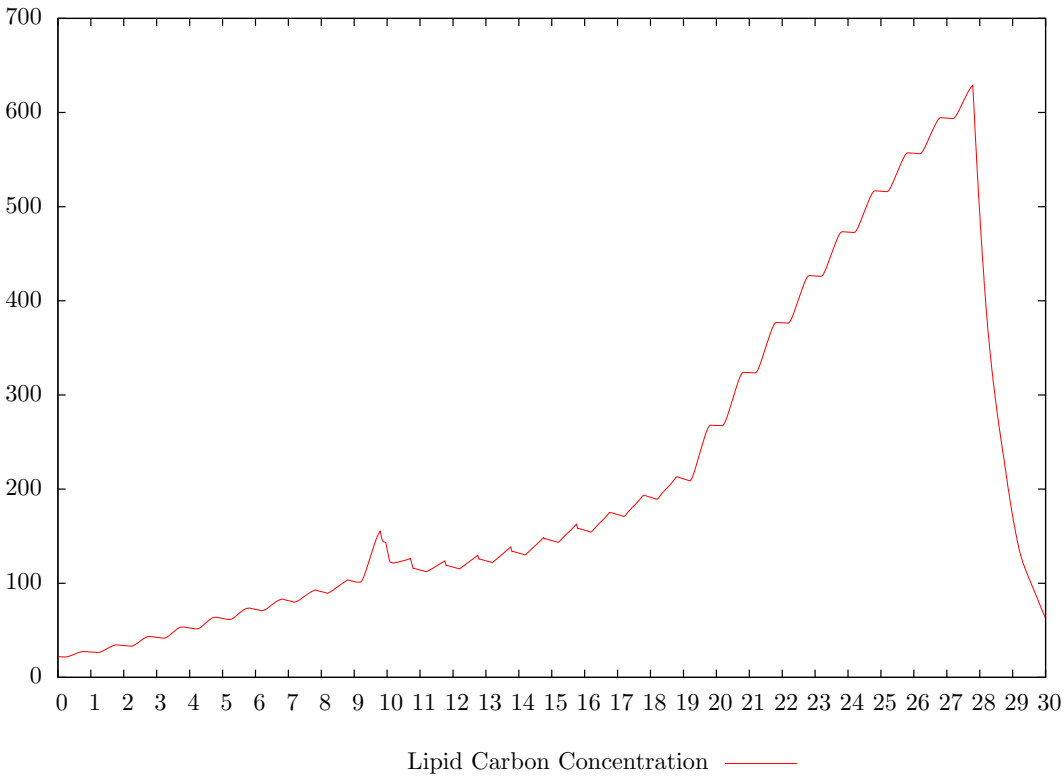

Figure 2.6.16: Extreme Nitrogen. η_L (Lipid carbon concentration)

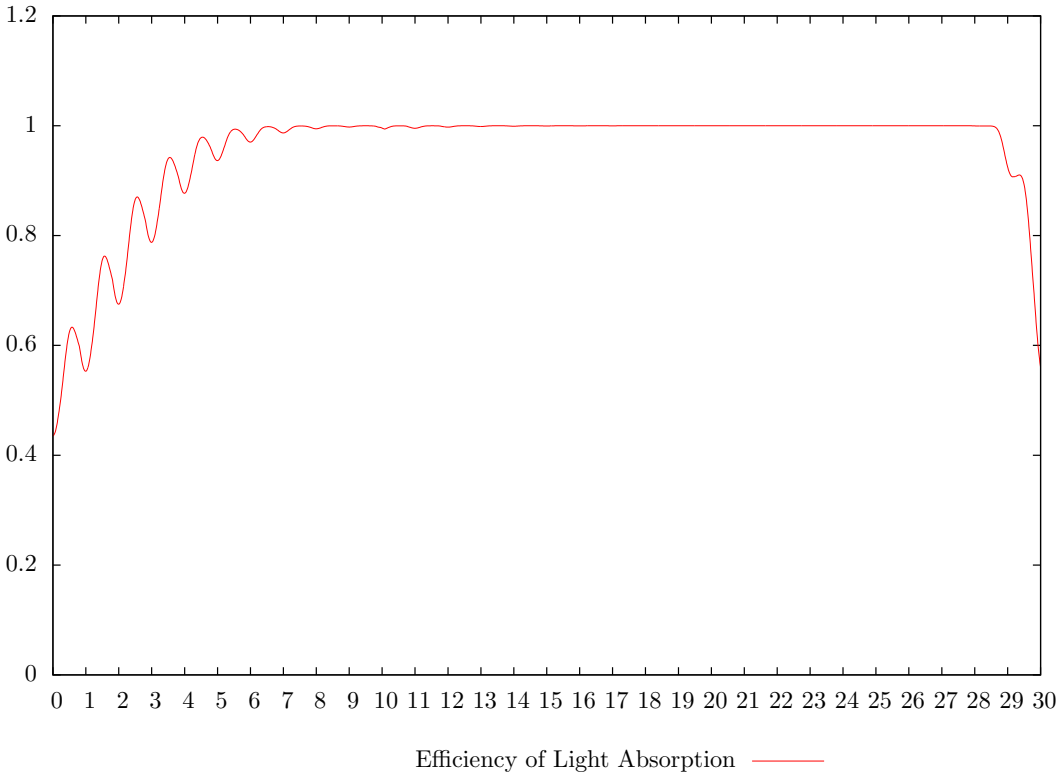

2.7 Robustness of Solutions

A general concern with open loop optimal controls is their lack of robustness with respect to modelling uncertainties and noise. We thus consider the performance of the optimal open loop control obtained for Problem P in the previous section when it is applied to a disturbed dynamic model of the raceway. We consider 4 disturbance types as follows.

1. The values of $I_0(t)$ as defined in (2.2.4) are multiplied by 0.3 on a specific day (which may correspond to this day being cloudy).
2. The values of $T(t)$ as defined by (2.2.3) are multiplied by 0.3 on a specific day.
3. Both the changes in types 1 and 2 applied together on a specific day
4. The theoretical maximum specific growth rate, $\tilde{\mu}$, is multiplied by 0.7 over the entire time horizon, which corresponds to the algae being stressed [91].

Disturbance types 1–3 are applied on Days 4 and 28. We now apply the optimal control calculated for the undisturbed model to the disturbed one. This turns out to have a relatively minor impact on the yield of the process with objective values in the range of 97.51% and 100.01% of the original optimal yield for Problem P. While the efficiency of light absorption (η_L) drops slightly on the days when the disturbances are active, it also recovers fairly quickly afterwards (see Figures 2.7.1 and 2.7.2). Predictably, Disturbance type 4 has a more significant impact on the yield. When the optimal control calculated for the undisturbed model is applied to the disturbed one, the resulting yield is only 68% of the original optimal value. However, even the optimised open loop control calculated for the disturbed model gives a yield which is only 74% of the original. Hence optimal solution of Problem P still performs quite well in the context of this disturbance. Overall, open loop optimal controls calculated for Problem P appear to be quite robust with respect to a range of disturbances.

Figure 2.7.1: Day 4 disturbance type 3 (Efficiency of light absorption)

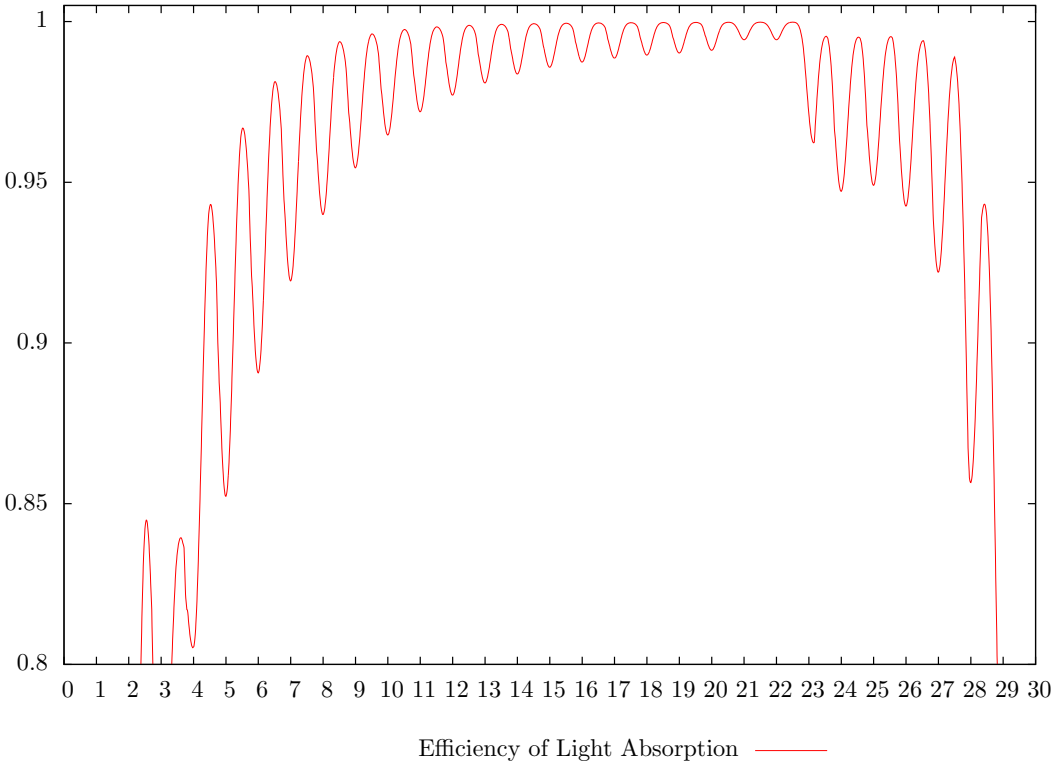

Figure 2.7.2: Day 28 disturbance type 3 (Efficiency of light absorption)

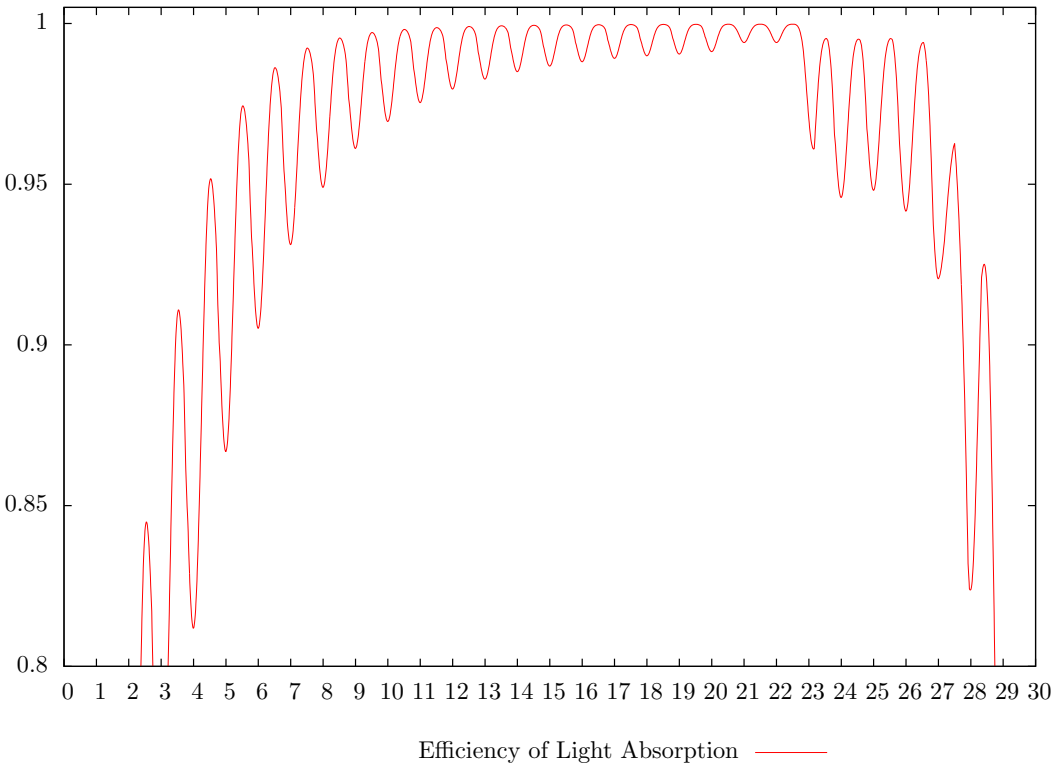

2.8 Optimal Closed Loop Control

As noted in Muñoz-Tamayo *et al.* [91], a practical alternative to an open loop optimal control computation is the design of a closed loop controller which maintains the operation of the raceway near an optimal quasi set point (note that an actual set point does not exist in the usual sense due to the daily fluctuation of insolation and temperature). In this section, we formulate and solve a simple closed loop optimal control problem and demonstrate the performance of the resulting closed loop optimal control.

For a closed loop formulation, the controls f_{in} and s_{in} should be defined in terms of quantities that can be measured easily. Clearly, both $I_0(t)$ and $T(t)$ fall into this category. It is also possible to estimate the light intensity at the bottom of the raceway, $I_L(t)$, if a point source of artificial light is used during the night [91]. Thus we propose the following affine feedback control functions

$$f_{in} = z_2 I_0 + z_3 I_L + z_4 T + z_5, \tag{2.8.1}$$

$$s_{in} = z_6 I_0 + z_7 I_L + z_8 T + z_9, \tag{2.8.2}$$

where z_2-z_9 are coefficients to be optimised. As for Problem P, we also require the constraints

$$0 \leq z_1 \leq 5, \tag{2.8.3}$$

$$0 \leq f_{in} \leq 0.8333, \ t \in [0, 720], \tag{2.8.4}$$

$$0 \leq s_{in} \leq 100, \ t \in [0, 720]. \tag{2.8.5}$$

The optimal feedback control problem can now be formulated as determining the optimal values of z_1-z_9 which will maximise the objective (2.4.1) with integrand (2.4.4) subject to the dynamics (2.3.16), the initial conditions given in (2.4.2) [47, 91], and constraints from (2.8.3)–(2.8.5). This constitutes an optimal parameter selection problem subject to all time state inequality constraints (2.8.4) and (2.8.5). While all time state inequality constraints can be difficult to handle, the MISER software has a built in algorithm [51, 52] to deal with them and it is also set up to deal with pure optimal parameter selection problems. The solution determined by MISER gives $s(0) = 5$ with

$$f_{in} = 2.09397261 \times 10^{-4} I_0 - 5.07177158 \times 10^{-4} I_L + 1.87050051 \times 10^{-2} T + 2.12531628 \times 10^{-4}, \tag{2.8.6}$$

$$s_{in} = -1.54036112 \times 10^{-2} I_0 - 6.80976078 \times 10^{-3} I_L + 42.6185859 T + 71.7318223 \tag{2.8.7}$$

and a corresponding yield of 6798.4 gC (25.930 tons ha^{-1} a^{-1}). Clearly, this is significantly lower

than the optimal yield of 9701.5 gC (37.003 tons ha^{-1} a^{-1}) obtained for the open loop optimal control Problem P since the closed loop control structure does not allow for a large f_{in} near the end of the time horizon to flush out the product (see Figure 2.8.1). Nevertheless, the closed loop control drives the system to an efficient quasi setpoint which then allows continued high productivity into the future if so desired. Indeed, Figure 2.8.3, shows that the efficiency of light absorption, η_L is driven to and maintained at a very high level by the optimal closed loop control. Productivity rates for both the open and closed loop optimal controllers are shown in Figure 2.8.4. For further illustration, we extend the simulation of the dynamics (2.3.16) to 60 days, using the optimal feedback control (2.8.6) and (2.8.7). This results in a total yield of 17628 gC over 60 days (33.617 tons ha^{-1} a^{-1}), i.e., a lipid production of 10829 gC (41.303 tons ha^{-1} a^{-1}) from Day 30 to Day 60. While this exceeds the 0-30 day yield resulting from the open loop optimal control, it has to be remembered that these two scenarios start with different initial conditions. Ultimately, the operator needs to decide whether a 30 day batch operation is more profitable than a continuous quasi setpoint operation beyond 30 days or not.

To test the robustness of the closed loop optimal controls, we apply the same range of disturbances we used in the open loop case to the closed loop system but with the time horizon extended to 60 days. In the case of reduced I_0 and T, we also introduce a similar reduction of these functions on Day 58 of the simulation. Results of these tests are marginally more favourable than for the open loop control tests over 30 days, with the yields saying in the range of 98.6-100.3% of the original when I_0 and T are reduced and close to 70% of the original when $\tilde{\mu}$ is reduced to 70% of its original value for all of the 60 days.

Figure 2.8.1: Open Loop vs Closed Loop f_{in} (Inflow rate)

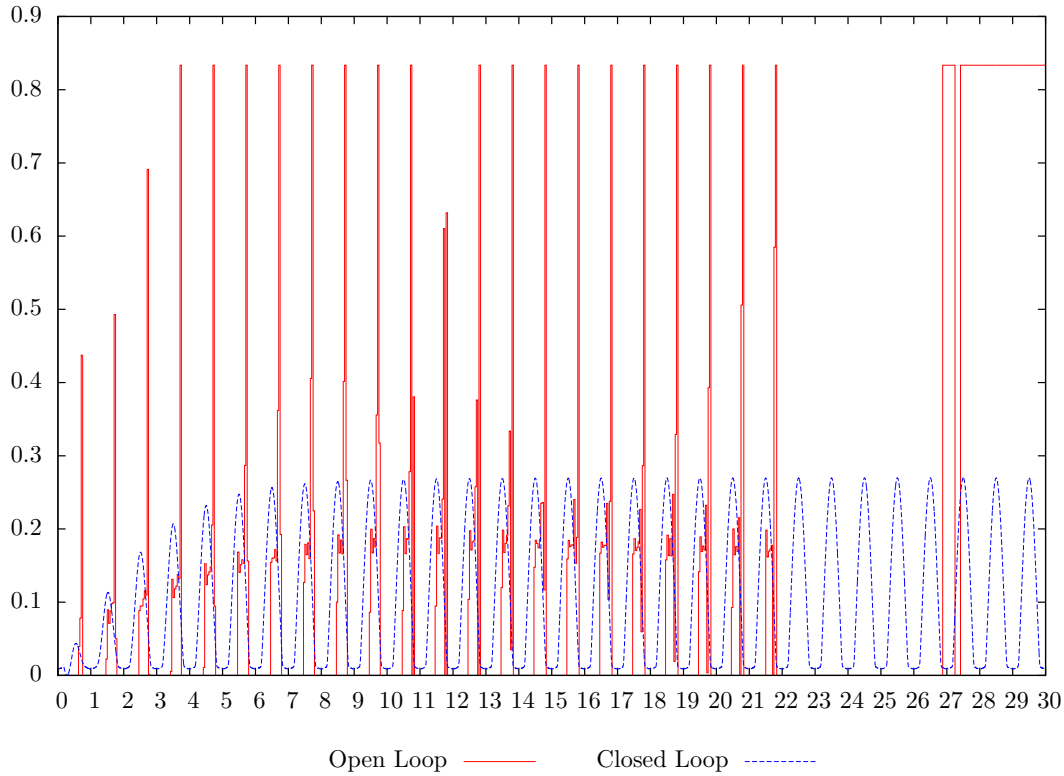

Figure 2.8.2: Open Loop vs Closed Loop f_{in} (Influent nitrogen concentration)

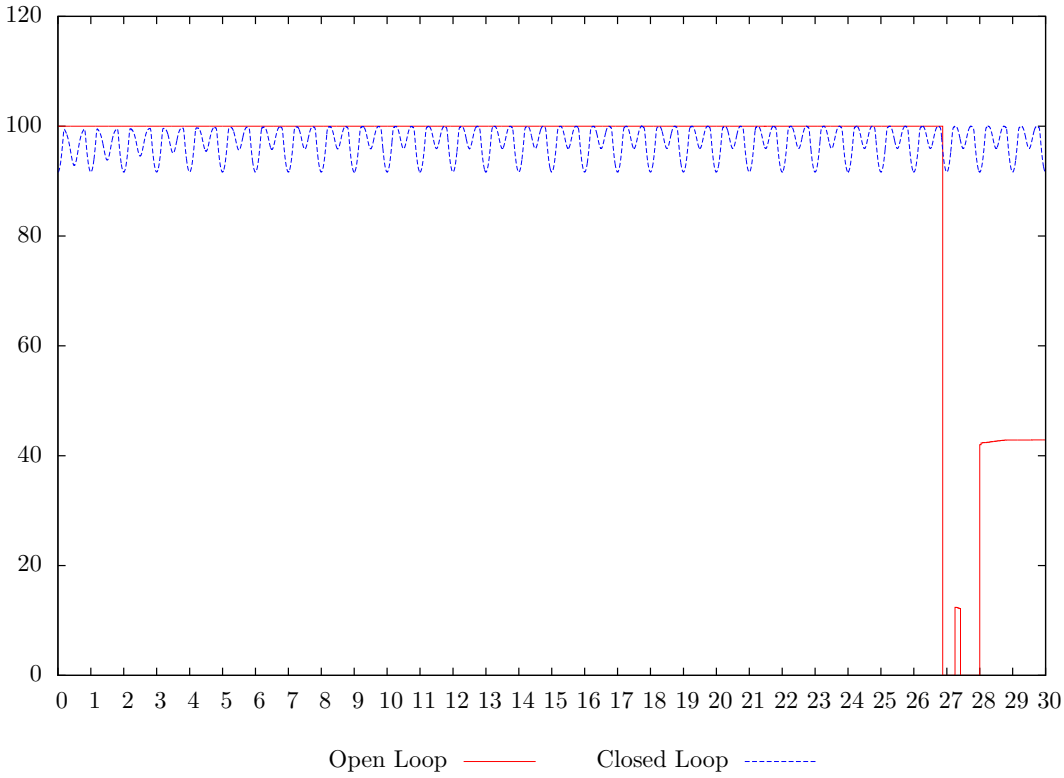

Figure 2.8.3: Open Loop vs Closed Loop η_L (Efficiency of light absorption)

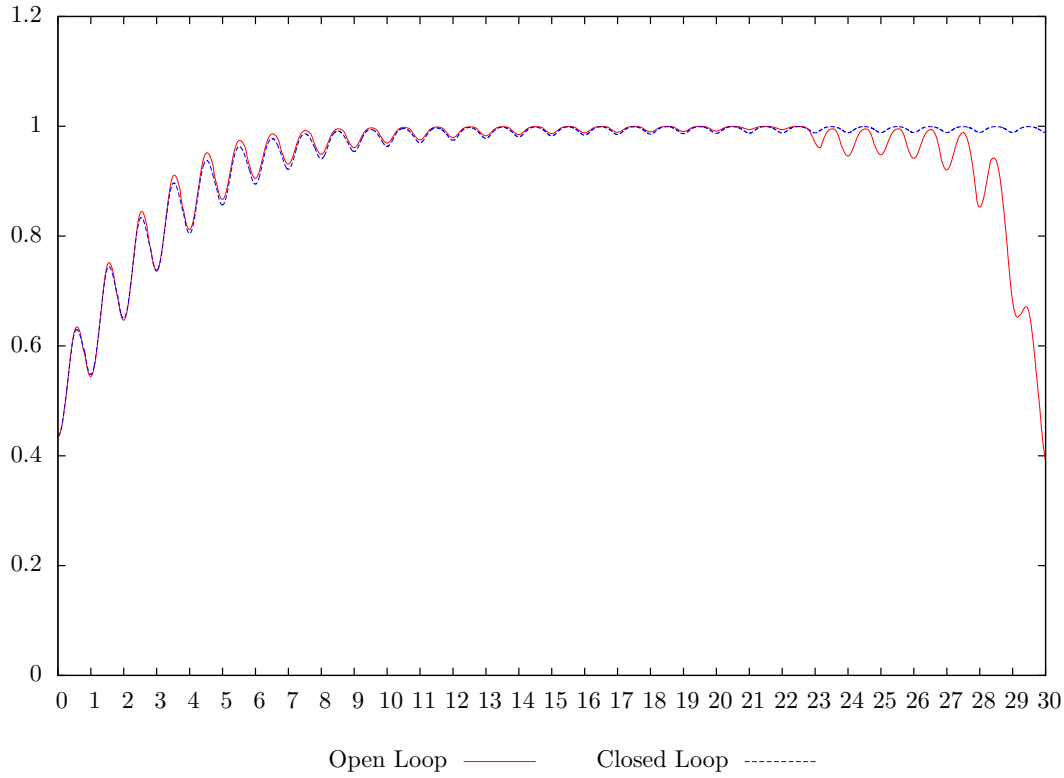

Figure 2.8.4: Open Loop vs Closed Loop (Cumulative Productivity)

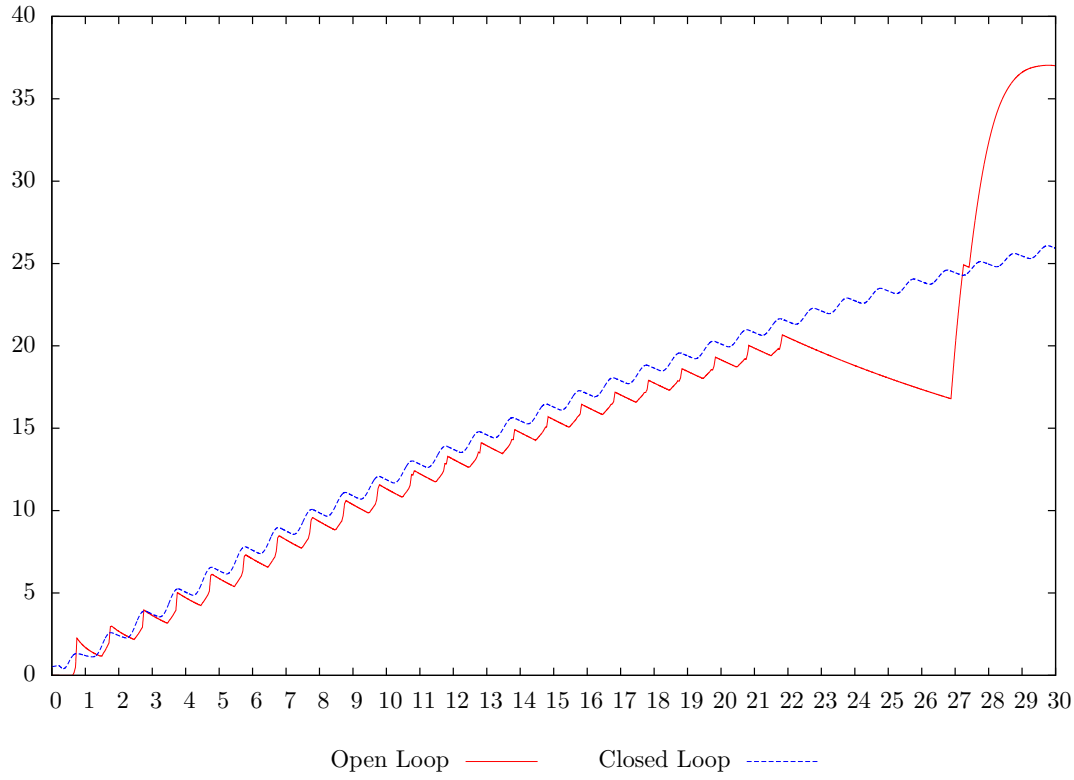

2.9 Optimal Raceway Depth

Figure 2.9.1: L as a Decision Variable, Fixed A_s. f_{in} (Inflow Rate)

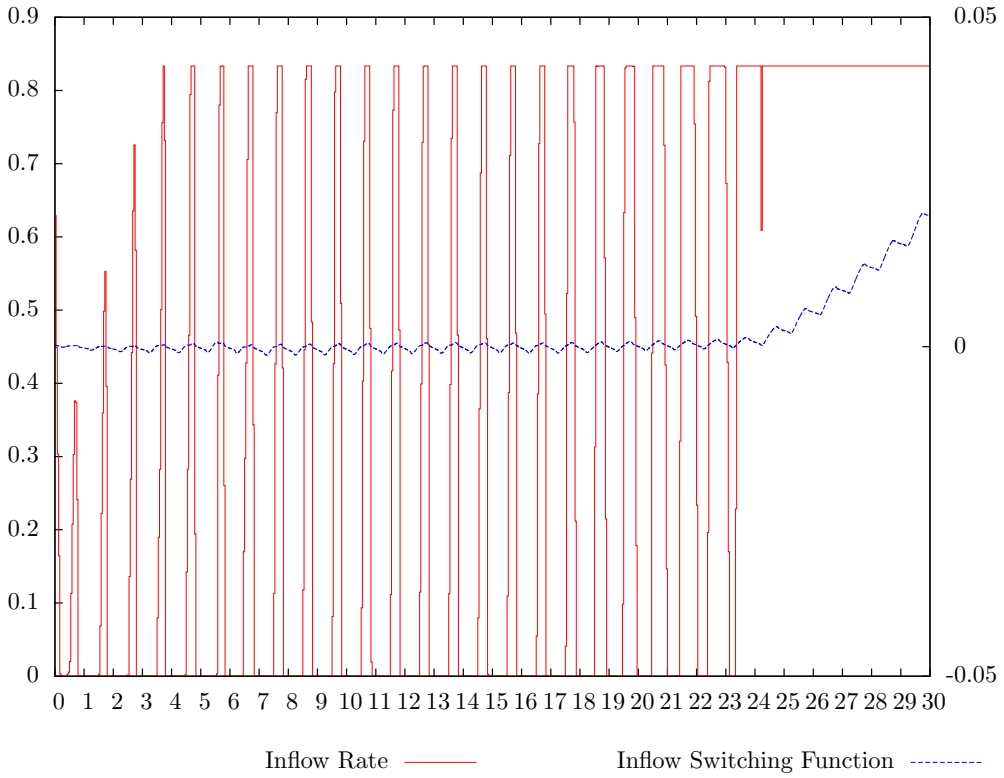

In this section, we allow the raceway depth, L, to be a decision variable to see if this can improve the yield of the process. To avoid confusion with the impact of other variables, we consider once more the original formulation of the problem with fixed nitrogen inflow concentration $s_{in} = 50$ and with a fixed initial extracellular nitrogen concentration $s(0) = 2$. We need to set upper and lower bounds for L. Choosing a minimal depth of 3cm and a maximal depth of 3m gives

$$0.03 \leq L \leq 3. \tag{2.9.1}$$

We use the MISER options of: number of knots in the partition for the control = 721, tolx = 10^{-7}, tolpsi = 10^{-7}, hmax = 10^{-4}, maxite = 1000, epsopt = 10^{-5}, epscon = 10^{-5}, imerit = 2, and ilql = 2 as well as using the NLPQLP optimiser [109].

Our objective is to maximise lipid production by determining an optimal f_{in} and L and we find that corresponding optimal solution results in $L = 0.03$ metres, i.e. the minimum allowed depth with a lipid yield of 10967 gC, which is a 44.6% improvement over the base case result.

Figure 2.9.2: L as a Decision Variable, Fixed A_s. s (Extracellular Nitrogen Concentration)

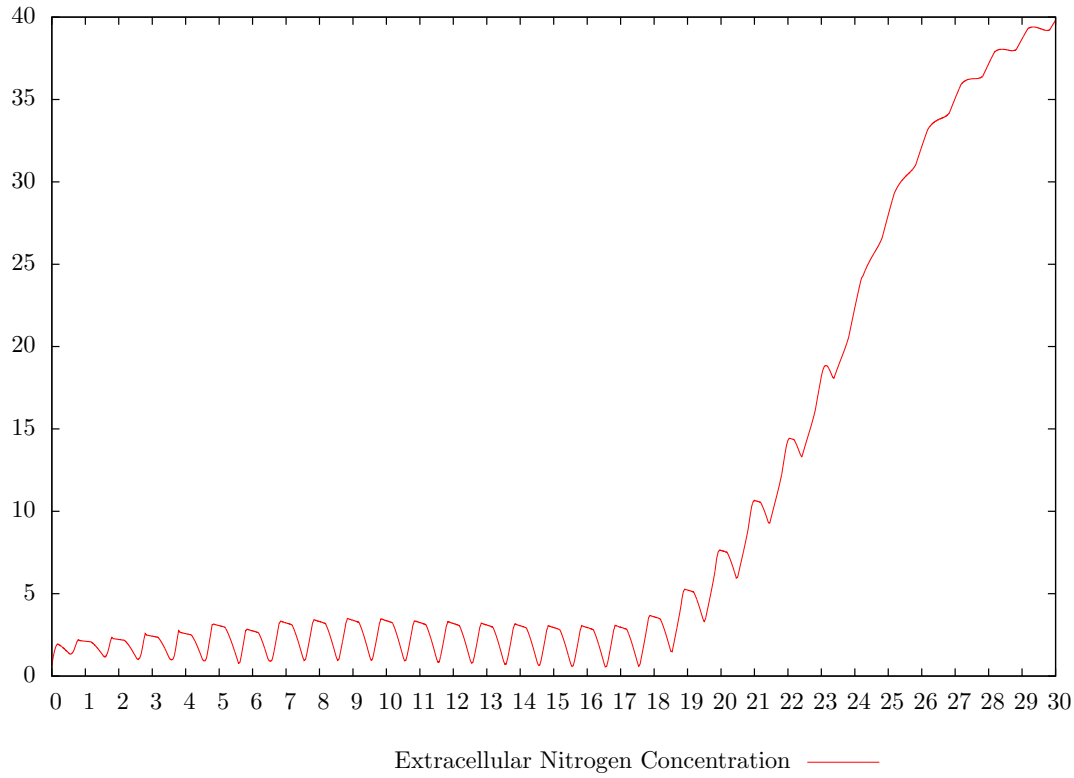

Figure 2.9.3: L as a Decision Variable, Fixed A_s. q_n (Nitrogen quota)

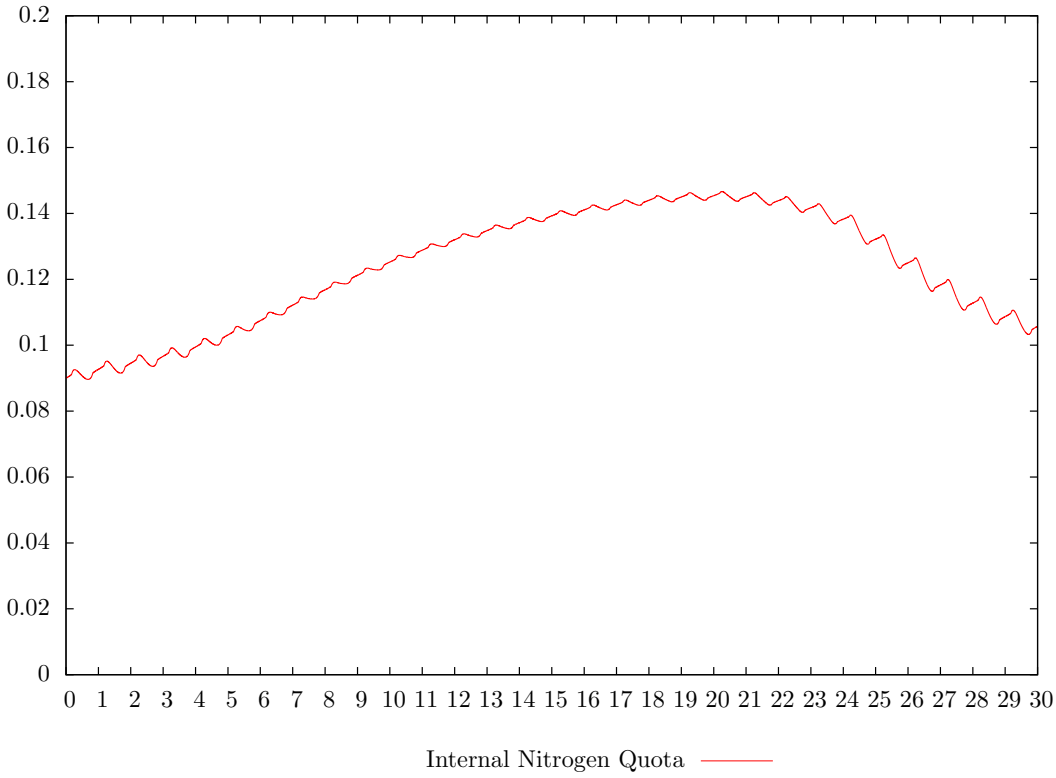

Figure 2.9.4: L as a Decision Variable, Fixed A_s. x (Carbon biomass concentration)

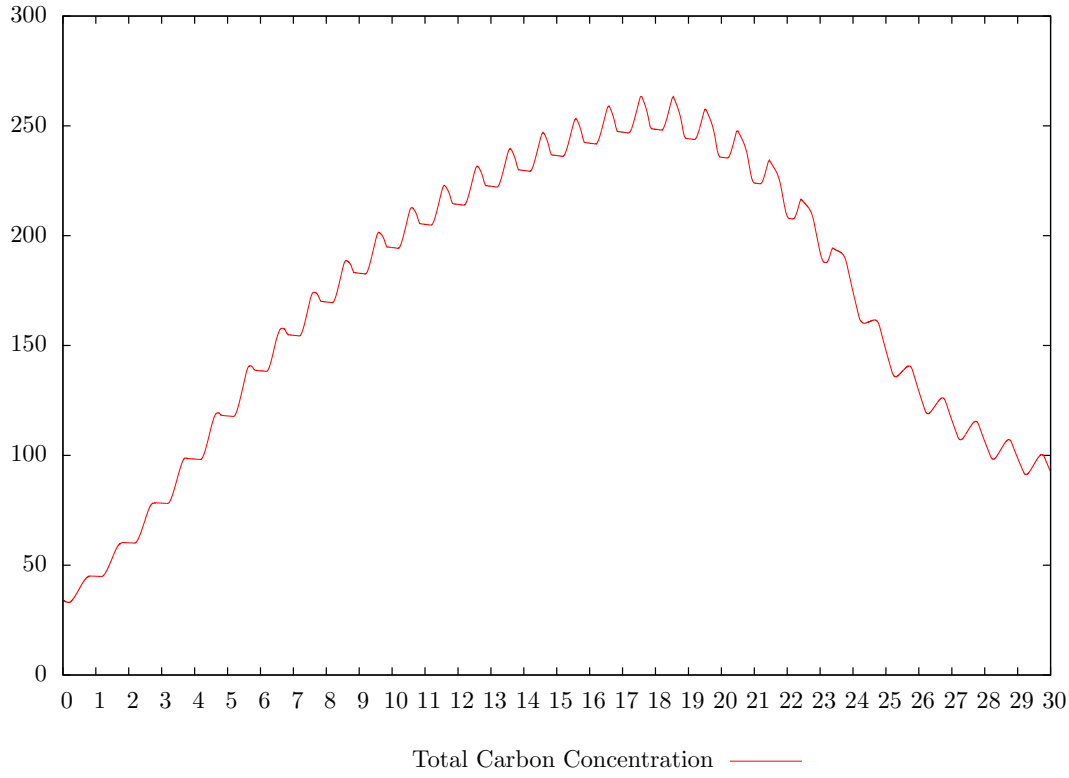

Given the nature of the process and the fact that we are dealing with a fixed volume V, this is hardly surprising since a shallow pond will make the best utilisation of available light. However the surface area has to increase tenfold over that of the base case and a shallow pond is likely to have significantly more evaporation. Rather than maintaining a fixed volume, a more practical limitation for raceway ponds is the available surface area, $A_s = V/L$. Using the original values of $V = 17.1\text{m}^3$ and $L = 0.3\text{m}$ we have $A_s = 57\text{m}^2$. We thus consider another version of the problem where A_s is fixed, L is a decision variable and the resulting volume is given by $V = A_s L$. The optimal lipid yield for this version of the problem is 10317 gC (39.351 tons ha^{-1} a^{-1}), a 36.0% improvement over the base case with a corresponding optimal depth $L = 1.8238$ m. What we find with this solution is a significant increase in the total volume and it also appears that the maximum bound on the inflow rate f_{in} is now limiting the performance of the process, as there is simply not enough time to flush the product from the raceway. If we increase this upper bound in proportion with the increased volume, we now find that the optimal depth becomes $L = 3$ with a corresponding yield of 13877 gC (52.928 tons ha^{-1} a^{-1}), a 83.0% improvement over the base case. While the yields resulting from a fixed surface area and a variable depth appear to be a significant improvement over the original result, most of this is simply due to maintaining the same initial values of $s(0)$, $q_n(0)$, $x(0)$, $x_l(0)$,

Figure 2.9.5: L as a Decision Variable, Fixed A_s. x_l (Lipid carbon concentration)

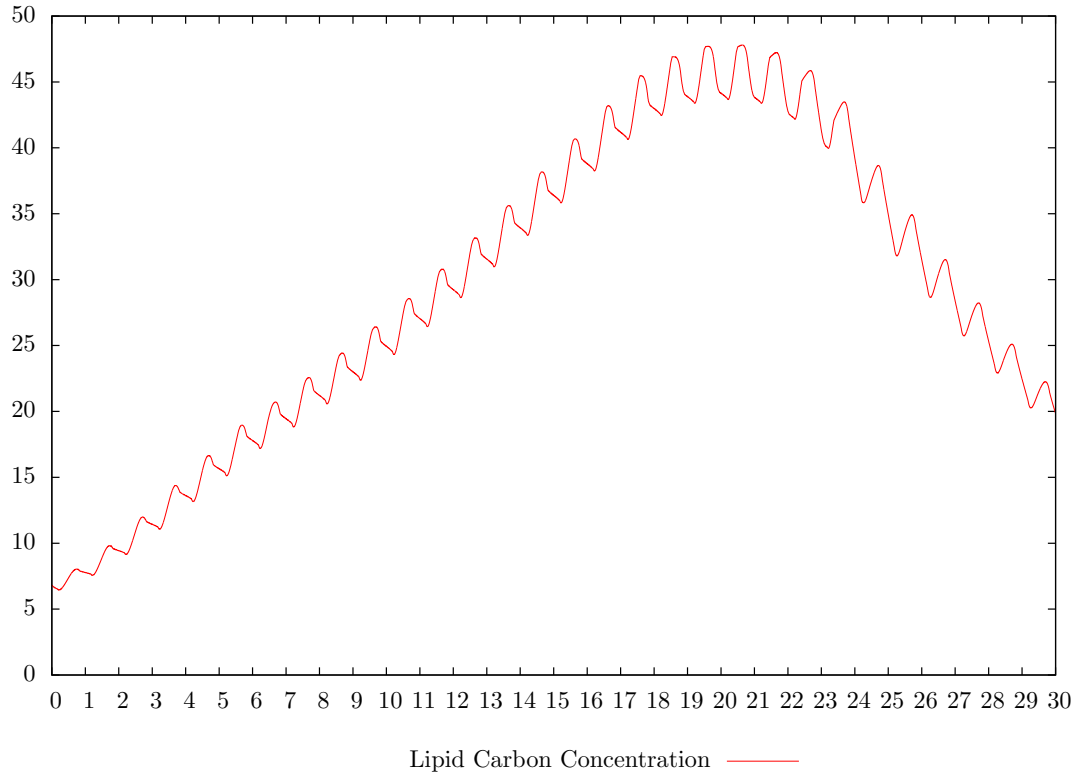

$x_f(0)$, $\bar{I}(0)$, and $C_{hl}(0)$ with a significant larger volume, i.e. a lot more biomass and nitrogen is already present at the start of the process. In fact, the efficiency of light absorption for these cases turns out to be quite low.

As a final revision we thus consider a fixed surface area A_s with L to be a decision variable, but with a fixed amount of resources (nitrogen, biomass, etc.) at t=0. This can be achieved by dividing the previous initial values of $s(0)$, $x(0)$, $x_l(0)$, $x_f(0)$, and $C_{hl}(0)$ by the change in volume which is equivalent to multiplying them by $0.3/L$. Fortunately, MISER3 does allow the appearance of the decision variable L in the initial conditions. This version of the problem results in an optimal yield of 8093.0 gC (30.868 tons ha^{-1} a^{-1}) which is an improvement of 6.7% over the base case yield. The corresponding optimal depth is 0.98770m. Figures 2.9.1–2.9.9 show the optimal f_{in}, state variables and efficiency of light absorption for this case. It is interesting to note that this case does not exhibit a period of nitrogen starvation that was present for our previous results. Light is being absorbed quite efficiently since the larger volume allows for lower algal concentration, lending in turn to better light penetration of the pond.

Figure 2.9.6: L as a Decision Variable, Fixed A_s. x_f (Functional carbon concentration)

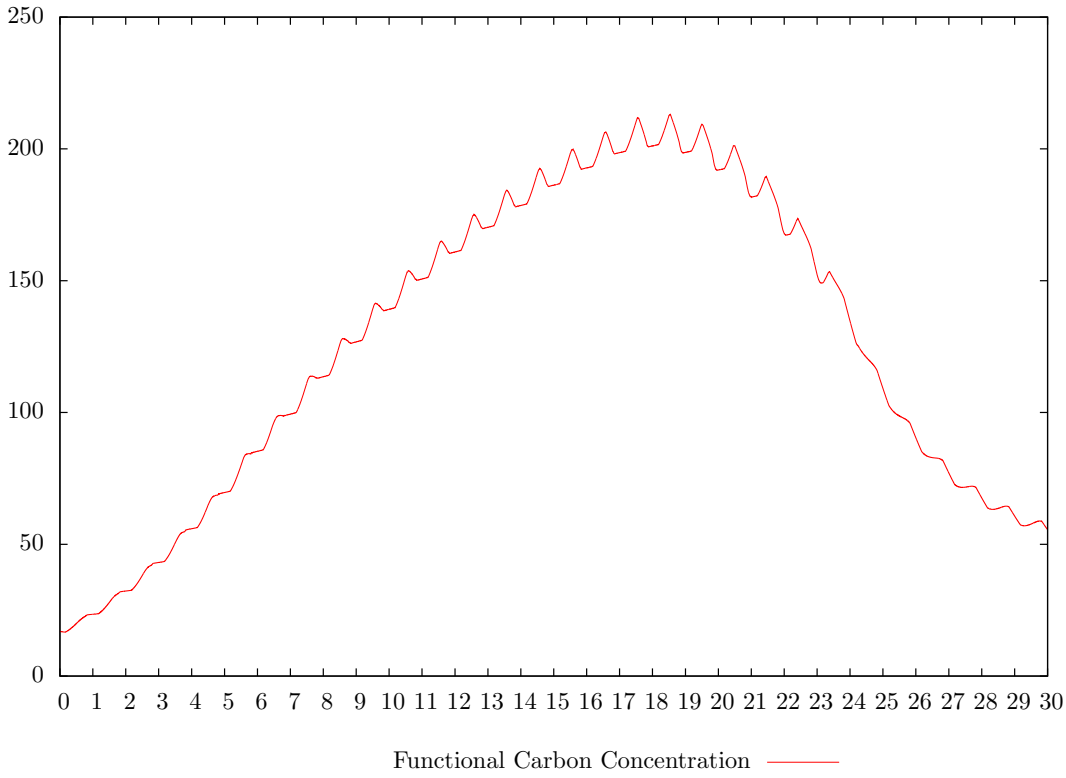

Figure 2.9.7: L as a Decision Variable, Fixed A_s. $\bar{I}$ (Average light intensity)

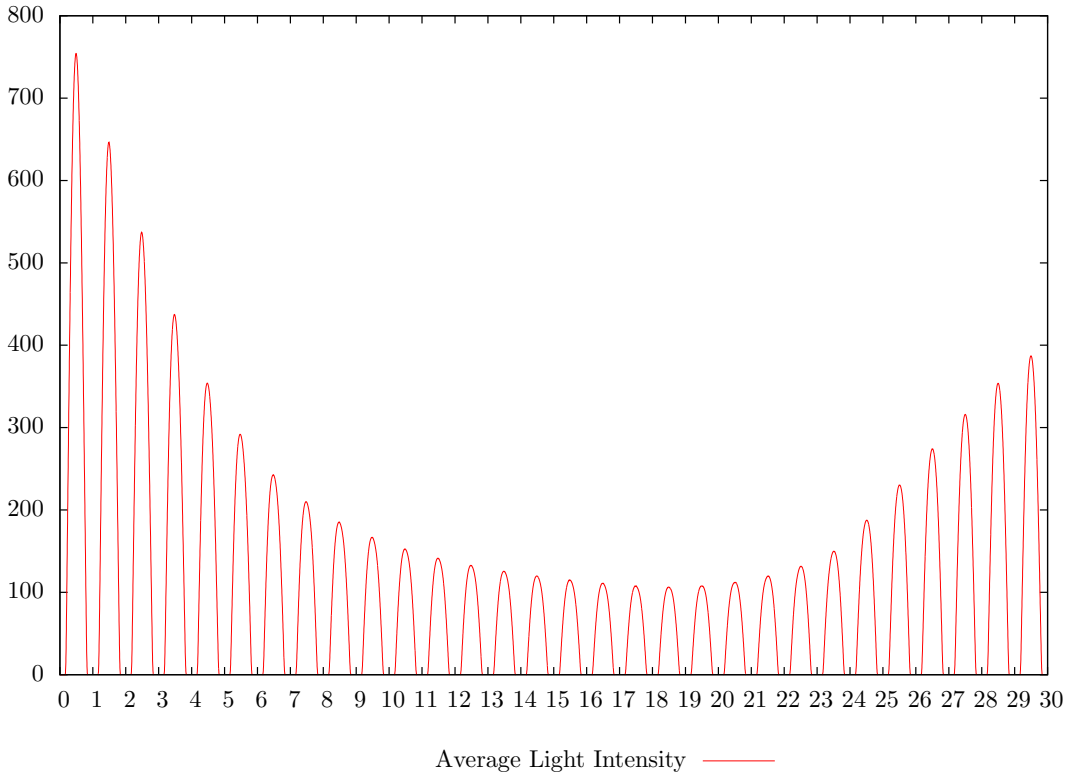

Figure 2.9.8: L as a Decision Variable, Fixed A_s. C_{hl} (Chlorophyll concentration)

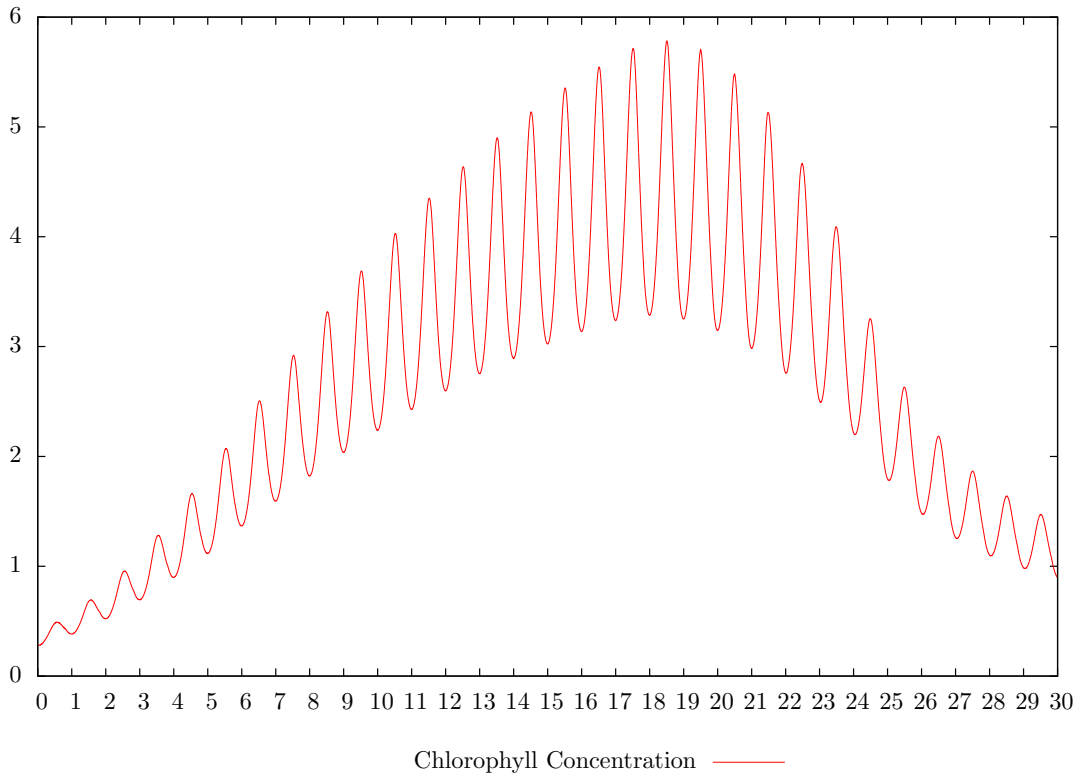

Figure 2.9.9: L as a Decision Variable, Fixed A_s. η_L (Efficiency of light absorption)

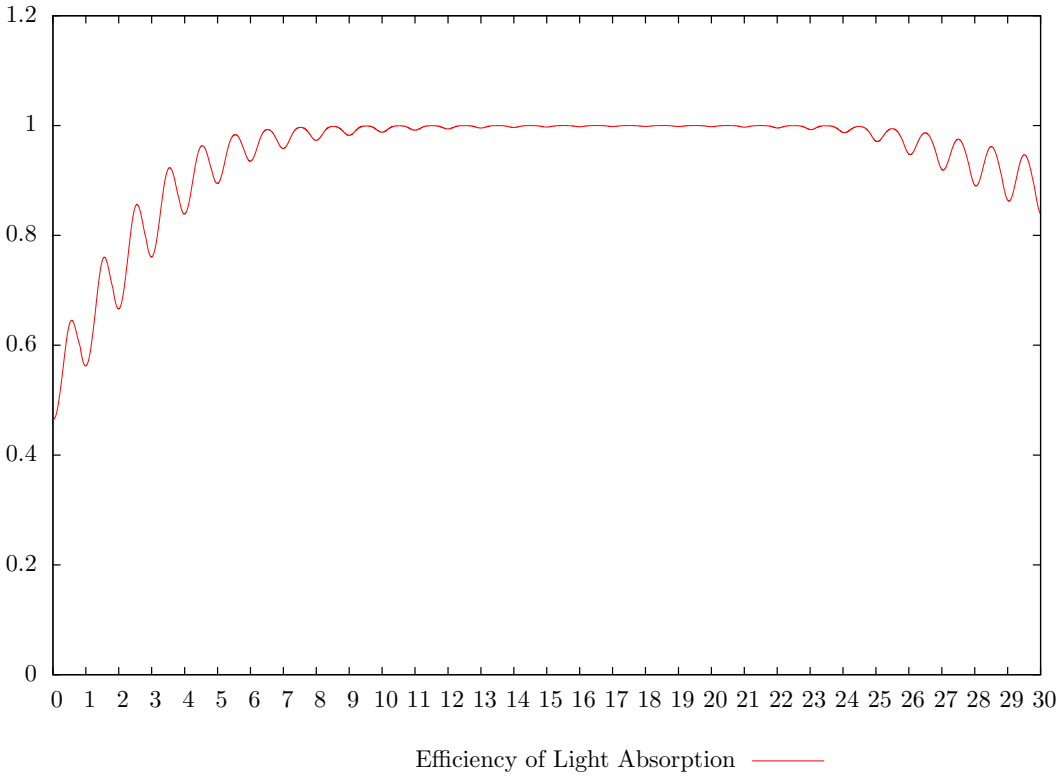

2.10 Conclusions

We have considered an existing dynamic algae growth model [91] which consists of 7 state variables and is described by a system of ordinary differential and algebraic equations. Our main focus here in is on the computation of open loop optimal controls with the main aim of maximising lipid production. We start with transformation of the system into a standard ordinary differential equation format. We also consider a slightly more general version of the problem where the influent nitrogen concentration as well as the initial extracellular nitrogen concentration are allowed to be variable. Numerical results show that significant improvements in lipid production are theoretically possible.

The existing model offers significant scope for further numerical studies. For example, the depth of a raceway pond could be altered over time to further improve productivity. This feature can be incorporated into the existing model with an additional control function to model the outflow and an additional state function to keep track of the total volume. We investigate this idea in Chapter 3. Part of the purpose of the optimal control formulation and 30 day time horizon used for the model in Muñoz-Tamayo *et al.* [91] was to see if the optimal control solution would approach some kind of (periodic) steady state and then derive a quasi-optimal closed loop control on the basis of this. However, our open loop optimal control results consistently show an extended high inflow period near the end of the 30 day period due to the need to harvest the microalgae. This is because an open loop control problem over a fixed time horizon defines the operation as a batch process. Thus the question of whether a batch operation or a continuous operation will ultimately yield a better rate of production arises. This issue is addressed in some detail for a different dynamic model in Bayen *et al.* [5]. However, the techniques used there cannot be used for the present microalgae model due to it's greater complexity and extensive numerical studies are required instead. Our work in Chapter 4 goes some way to addressing this question.

Chapter 3

Changing the Pond Depth

3.1 Introduction

Algae bioreactors come in many different forms, ranging from natural lake systems in large scale operations [14] to fully sealed glass tubes in a laboratory setting [13, 132] to maximise light penetration. A good compromise between the need for high growth rates and reasonable capital costs is given by open raceway ponds with paddle wheels typically used to keep the water circulating. Raceways ponds come in various sizes, with the larger ones often consisting of plastic lined channels dug out of the ground. Many studies considering algae growth for potential biofuel production consider smaller scale raceway ponds with a depth of around 30 cm [6, 91]. Ideally, ponds should be as shallow as possible so that algae cells have maximum exposure to light. However, for a given pond volume, very shallow ponds require a very large surface area which significantly increases capital costs and it also leads to very high rates of evaporation. Hence, a depth of 30 cm is generally considered to be a good compromise in practice [6, 13].

The growth of micro algae in raceway ponds has been modelled mathematically by a number of publications [50, 80, 96]. In the previous chapter, we have adopted a comprehensive model first published in [91]. This model consists of a set of differential algebraic equations (DAEs) to describe the algae growth process over a 30 day batch operation in a pond of 30cm depth. The only control considered in this model is the inflow of water containing a given concentration of nitrogen. Since the pond volume is fixed, the inflow automatically results in an equivalent outflow of pond water from which the algae can then be harvested. By converting the DAEs to an equivalent system of ordinary differential equations (ODEs) and employing computational optimal control methods, we were able to show that an optimal yield of 7584.4 gC equivalent of lipids could be produced

[47]. The computed optimal control strategy involved a rapid initial growth of cells, followed by a period of nutrient (nitrogen) starvation to build up lipids within the cells and finally a 'wash out' to harvest the algae. Upon suggestion from one of the reviewers of this work, we then considered the depth of the pond to be an additional decision variable while keeping the surface area constant. Note that maintaining the initial algal and nutrient concentrations in this scenario always results in the depth going to its upper bound, since this will result in the largest initial algal mass which can still be grown and harvested later. However, we also found in this case that the growth phase does not occur optimally with low utilisation of available light due to the excessive pond depth. A more practical scenario can be obtained by keeping the initial algal and nutrient mass in the pond the same as for the original model so that a greater depth and therefore volume would simply result in a lower initial concentration of both algae and nutrients. With this scenario, we found that the a pond depth of just over 90 cm along with an associated optimal control of inflow would increase lipid yield by around 6.7% over that from the original model [47].

The question of what raceway pond depth is best has been considered by a number of publications. In [59], experiments were conducted with paddle driven ponds having depths of 20, 30 and 40cm. The authors found that the most biomass was obtained with a 20cm pond depth and also noted that this resulted in the best settleability of algae (which aids the harvesting process) and requires the least amount of energy to circulate the pond water. In contrast, [108] considered a different experimental set up using a side entry axial flow impeller rather than a paddle wheel. This generally requires less energy and results in better mixing of the pond. The authors found that a pond depth of 1 metre resulted in better productivity than the typical depth of 30cm, giving some support to the numerical results we obtained in our previous work. In [6], ponds in a range of different climatic environments are considered. Both pond depth and the so called hydraulic retention time (HRT) are considered as decision variables, where the HRT essentially determines how much of the pond is drained at a fixed time every day in order to harvest the algae. The authors demonstrate good algal mass yield improvements if both pond depth and HRT are varied appropriately in different seasons. Note that it is difficult to compare these results and others in literature directly, as they are conducted in different environments with different algae species. For example, our adopted mathematical model of the process assumes that the pond is uniformly mixed and it is not concerned with the means by which this mixing occurs.

Our aim in this chapter is to explore another option of varying the pond depth. Since the pond depth at any instant has a significant impact on the light penetration down into the pond, we want to explore whether adjusting the pond depth during the batch process can further increase

the total lipid yield. Varying pond depth can be achieved by having a distinct outflow rate of pond water rather than simply assuming that the outflow is equal to the inflow. We thus have two control variables (inflow and outflow) instead of just one. This also requires the addition of a another differential equation to describe the dynamics of the pond depth. Once again converting the modified system of DAEs to an equivalent system of ODEs, we then apply computational optimal control methods to determine optimal inflow and outflow regimes. It is shown that these increase the lipid yield of the process by more then 67% over the base case model where only inflow is varied. This chapter is largely based on [48].

3.2 Problem Formulation

The raceway model under consideration is based on the mass balance equations for a completely mixed reactor at a constant volume given in [91]. We now assume that the pond depth, L, is a function of time t, where t is measured in hours. We also assume that the pond surface area, A_s, remains fixed. This means that the volume of the pond, $V = LA_s$, now also depends on t and all occurrences of V in the original dynamics are replaced by LA_s. The original model assumed that any inflow f_{in} to the pond would spill over to keep V constant and f_{in} was considered as the only control variable. We create a second control variable f_{out} to represent the chosen outflow rate. A simple differential equation then describes the dynamics of L. Combining this with the original model, we obtain the following modified dynamics for the current problem.

$$\begin{aligned}
\dot{s} &= f_{in}s_{in}/(LA_s) - f_{out}s/(LA_s) - \rho x,\\
\dot{q_n} &= \rho - (\mu - R)q_n,\\
\dot{x} &= (\mu - f_{out}/(LA_s) - R)x,\\
\dot{x_l} &= \beta q_n \mu x - \gamma \rho x - r_0\phi_T x_l - f_{out}x_l/(LA_s),\\
\dot{x_f} &= (\alpha + \gamma)\rho x - r_0\phi_T x_f - f_{out}x_f/(LA_s),\\
\dot{L} &= (f_{in} - f_{out})/A_s,
\end{aligned} \tag{3.2.1}$$

where the meaning of the dynamic variables and their units are described in Table 2.1. The derivatives are with respect to time and t = 0 corresponds to midnight of the first day. The control variables are f_{in} and f_{out}, the feeding flow (inflow) and extraction flow (outflow) rates respectively. The functions μ, ρ, R, ϕ_T represent average growth rate, nitrogen uptake rate, overall respiration rate, and temperature effect, respectively, and these are defined in Chapter 2. The values of the

model constants α, β, γ, r_0, A_s and s_{in} are based on [91] and given in Table 2.2.

The dynamics defined by (3.2.1) and (2.2.3)–(2.2.16) again constitute a system of differential algebraic equations of index 1. We use the same approach as that outlined in Section 2.3 to convert it to a system of ordinary differential equations. We may once again write the system of DAEs in the form

$$\dot{\mathbf{x}}_1(t) = \mathbf{f}_1(t, \mathbf{x}_1(t), \mathbf{x}_2(t)), \tag{3.2.2}$$

$$0 = \mathbf{f}_2(t, \mathbf{x}_1(t), \mathbf{x}_2(t)), \tag{3.2.3}$$

where

$$\mathbf{x}_1 = [s, q_n, x, x_l, x_f, L]^\top, \tag{3.2.4}$$

$$\mathbf{x}_2 = \left[\bar{I}, C_{hl}\right]^\top, \tag{3.2.5}$$

$$\mathbf{f}_1(t, \mathbf{x}_1(t), \mathbf{x}_2(t)) = \left[\dot{s}, \dot{q_n}, \dot{x}, \dot{x_l}, \dot{x_f}, \dot{L}\right]^\top, \tag{3.2.6}$$

$$\mathbf{f}_2(t, \mathbf{x}_1(t), \mathbf{x}_2(t)) = [f_{21}, f_{22}]^\top, \tag{3.2.7}$$

$$f_{21} = \frac{I_0}{\xi L}(1 - \exp(-\xi L)) - \bar{I}, \tag{3.2.8}$$

$$f_{22} = \frac{x q_n}{(g_1 - g_2 T) + g_3 \bar{I} \exp(-g_4 T)} - C_{hl}. \tag{3.2.9}$$

$$\tag{3.2.10}$$

The latter two equations follow from (2.2.13) and (2.2.16). We have

$$\begin{bmatrix} \mathbf{I} & 0 \\ \frac{\partial \mathbf{f}_2}{\partial \mathbf{x}_1} & \frac{\partial \mathbf{f}_2}{\partial \mathbf{x}_2} \end{bmatrix} \begin{bmatrix} \dot{\mathbf{x}}_1 \\ \dot{\mathbf{x}}_2 \end{bmatrix} = \begin{bmatrix} \mathbf{f}_1 \\ -\frac{\partial \mathbf{f}_2}{\partial t} \end{bmatrix}. \tag{3.2.11}$$

Since $\frac{\partial \mathbf{f}_2}{\partial \mathbf{x}_2}$ is again of full rank, the matrix in (3.2.11) is invertible and we may write

$$\begin{bmatrix} \dot{\mathbf{x}}_1 \\ \dot{\mathbf{x}}_2 \end{bmatrix} = \begin{bmatrix} \mathbf{I} & 0 \\ \frac{\partial \mathbf{f}_2}{\partial \mathbf{x}_1} & \frac{\partial \mathbf{f}_2}{\partial \mathbf{x}_2} \end{bmatrix}^{-1} \begin{bmatrix} \mathbf{f}_1 \\ -\frac{\partial \mathbf{f}_2}{\partial t} \end{bmatrix}. \tag{3.2.12}$$

Letting $\mathbf{x}(t) = [\mathbf{x}_1(t), \mathbf{x}_2(t)]^\top$ (3.2.12) may be written as

$$\dot{\mathbf{x}}(t) = \begin{bmatrix} \mathbf{I} & 0 \\ \frac{\partial \mathbf{f}_2}{\partial \mathbf{x}_1} & \frac{\partial \mathbf{f}_2}{\partial \mathbf{x}_2} \end{bmatrix}^{-1} \begin{bmatrix} \mathbf{f}_1 \\ -\frac{\partial \mathbf{f}_2}{\partial t} \end{bmatrix}. \tag{3.2.13}$$

Note that, by virtue of (3.2.8) and (3.2.9), we have

$$\begin{bmatrix} \mathbf{I} & 0 \\ \frac{\partial \mathbf{f}_2}{\partial \mathbf{x}_1} & \frac{\partial \mathbf{f}_2}{\partial \mathbf{x}_2} \end{bmatrix} = \begin{bmatrix} 1 & 0 & 0 & 0 & 0 & 0 & 0 & 0 \\ 0 & 1 & 0 & 0 & 0 & 0 & 0 & 0 \\ 0 & 0 & 1 & 0 & 0 & 0 & 0 & 0 \\ 0 & 0 & 0 & 1 & 0 & 0 & 0 & 0 \\ 0 & 0 & 0 & 0 & 1 & 0 & 0 & 0 \\ 0 & 0 & 0 & 0 & 0 & 1 & 0 & 0 \\ 0 & 0 & 0 & 0 & 0 & \frac{\partial f_{21}}{\partial L} & -1 & \frac{\partial f_{21}}{\partial C_{hl}} \\ 0 & \frac{\partial f_{22}}{\partial q_n} & \frac{\partial f_{22}}{\partial x} & 0 & 0 & 0 & \frac{\partial f_{22}}{\partial \bar{I}} & -1 \end{bmatrix} \text{ and } \begin{bmatrix} \mathbf{f}_1 \\ -\frac{\partial \mathbf{f}_2}{\partial t} \end{bmatrix} = \begin{bmatrix} \dot{s} \\ \dot{q_n} \\ \dot{x} \\ \dot{x_l} \\ \dot{x_f} \\ \dot{L} \\ -\frac{\partial f_{21}}{\partial t} \\ -\frac{\partial f_{22}}{\partial t} \end{bmatrix}.$$

Using SymPy [84] to determine the inverse of this matrix, we may write (3.2.13) as

$$\dot{\mathbf{x}}(t) = \begin{bmatrix} \dot{s} \\ \dot{q_n} \\ \dot{x} \\ \dot{x_l} \\ \dot{x_f} \\ \dot{L} \\ \frac{-\left(\frac{\partial f_{21}}{\partial t}\right) - \left(\frac{\partial f_{21}}{\partial C_{hl}}\frac{\partial f_{22}}{\partial t}\right) - \left(\frac{\partial f_{21}}{\partial C_{hl}}\frac{\partial f_{22}}{\partial q_n}\dot{q_n}\right) - \left(\frac{\partial f_{21}}{\partial C_{hl}}\frac{\partial f_{22}}{\partial x}\dot{x}\right) - \left(\frac{\partial f_{21}}{\partial C_{hl}}\frac{\partial f_{21}}{\partial L}\frac{\partial f_{22}}{\partial \bar{I}}\dot{L}\right)}{\frac{\partial f_{21}}{\partial C_{hl}}\frac{\partial f_{22}}{\partial \bar{I}} - 1} + \dot{L}\frac{\partial f_{21}}{\partial L} \\ \frac{-\left(\frac{\partial f_{21}}{\partial t}\frac{\partial f_{22}}{\partial \bar{I}}\right) - \left(\frac{\partial f_{21}}{\partial L}\frac{\partial f_{22}}{\partial \bar{I}}\dot{L}\right) - \left(\frac{\partial f_{22}}{\partial t}\right) - \left(\frac{\partial f_{22}}{\partial q_n}\dot{q_n}\right) - \left(\frac{\partial f_{22}}{\partial x}\dot{x}\right)}{\frac{\partial f_{21}}{\partial C_{hl}}\frac{\partial f_{22}}{\partial \bar{I}} - 1} \end{bmatrix}, \tag{3.2.14}$$

which is a system of first order ODEs as required. Initial values for $\bar{I}(0)$ and $C_{hl}(0)$ are the same as those we derived in Chapter 2. Again, note that this transformation preserves the original dynamics and guaranties satisfaction of the algebraic equations. The resulting system of ODE's is now suitable for implementation with MISER.

The initial conditions for the state variables are the same as in Chapter 2 [47, 91].

$$\begin{aligned} s(0) &= 2, \\ q_n(0) &= 0.09, \\ x(0) &= 110, \\ x_l(0) &= 22, \\ x_f(0) &= 55, \\ L(0) &= 0.3, \\ \bar{I}(0) &= 0, \\ C_{hl}(0) &= 0.909. \end{aligned} \tag{3.2.15}$$

The problem of maximising lipid production is given by

$$\max_{\substack{f_{in} \\ f_{out}}} \int_0^{t_f} f_{out}(t) x_l(t) dt, \tag{3.2.16}$$

subject to the dynamics of the transformed system of DAEs (3.2.1), the initial conditions (3.2.15) and the control variable bounds

$$\begin{aligned} 0 \leq f_{in}(t) \leq 0.8333, \\ 0 \leq f_{out}(t) \leq 0.8333. \end{aligned} \tag{3.2.17}$$

To compare the results from this problem with the base case problem in Chapter 2, we consider a time horizon of 30 days which corresponds to $t_f = 720$.

3.3 Results

The base case problem with $f_{in} = f_{out}$ and a constant depth of $L = 0.3$ over the entire time horizon that we solved in Chapter 2 yields 7584.4 gC (grams of carbon) of lipids (28.928 tons ha^{-1} a^{-1}). The new problem is solved with MISER (with the options of: number of knots in the partition for the control = 721, tolx = 10^{-9}, tolpsi = 10^{-9}, hmax = 10^{-4}, maxite = 1000, epsopt = 10^{-8}, epscon = 10^{-9}, imerit = 2, and ilql = 1 as well as using the NLPQLP optimiser [109]). We assume a piecewise constant parameterisation of f_{in} and f_{out} over a fixed partition of $[0, t_f]$ with 1 hour intervals. This results in a yield of 12706 gC of lipids (48.462 tons ha^{-1} a^{-1}) which is a significant increase of 67%. Our result also represents a significant increase of approximately 108% over that found by [91] (approximately 6100 gC or 24 tons ha^{-1} a^{-1}).

Figure 3.3.1: Variable Pond Depth. f_{in}

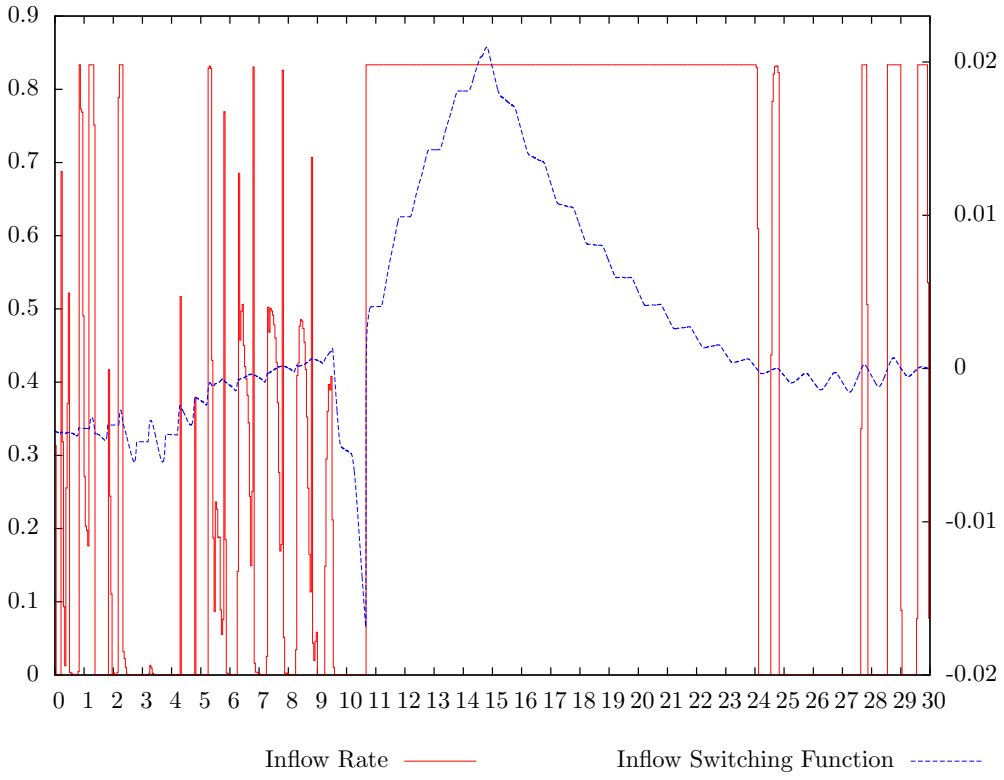

The numerical solution for this problem is very close to satisfying the first order optimality conditions dictated by the minimum principle [101]. Briefly, the Hamiltonian function of the problem, H, may be written as

$$H = K_1 f_{in} + K_2 f_{out} + K_3. \tag{3.3.1}$$

The K_1, K_2, and K_3 terms contain the various state variables. Owing to the complexity of the transformed dynamics, we choose not to write out the complete expressions for K_1, K_2, and K_3 here, but they are readily computable within the existing subroutines we use in MISER. As H is linear in both of the control variables, maximising the Hamiltonian function requires that each control takes on the upper bound (0.8333) when its switching function is positive, the lower bound (0) when its switching function is negative, and may be between the bounds (singular) when its switching function is zero. Figures 3.3.1 and 3.3.2 both show conditions are satisfied over most of the time horizon. Note that since the partition for the piecewise constant control is fixed, we cannot determine the exact optimal switching times so the conditions are not satisfied exactly when the controls go from one bound to another.

Figure 3.3.2: Variable Pond Depth. f_{out}

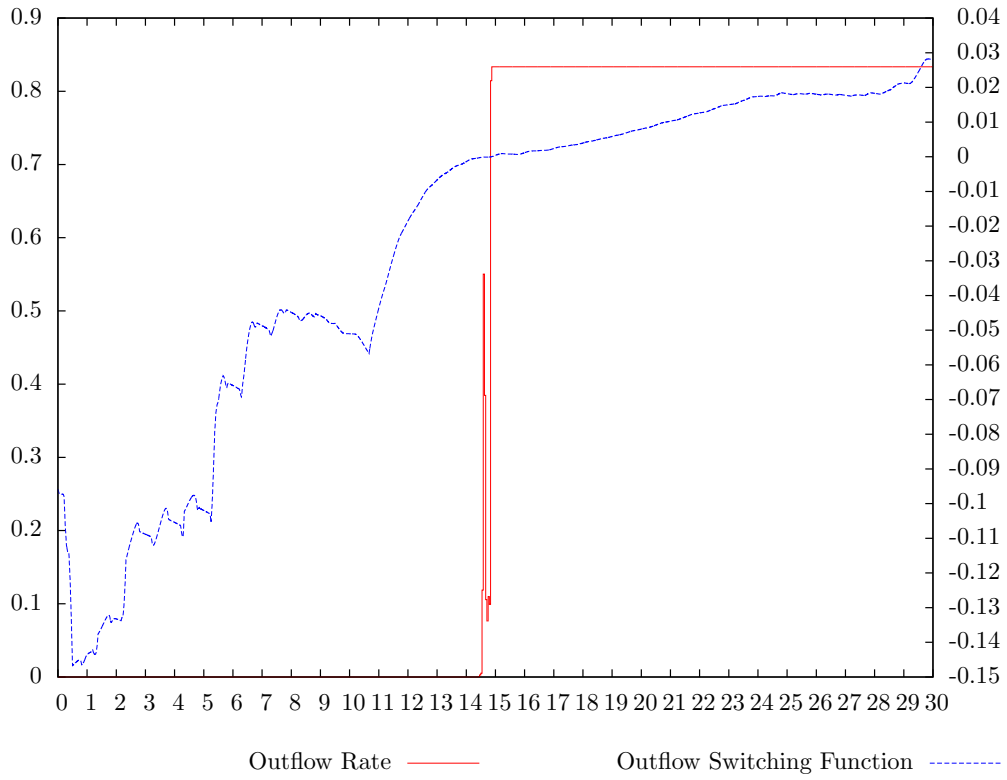

In Figures 3.3.2–3.3.4 we see that the outflow remains zero for the first half of the time horizon so that the intermittent inflow builds up the depth of the pond to almost 2.5 metres. Figure 3.3.5 shows a brief nitrogen starvation period between days 9 and 11, much earlier than what we see for the optimised base case model in Chapter 2, see Figure 2.6.3. Because of this, we see a significant increase in lipid carbon concentration, x_l, over the same period in Figure 3.3.6. After the starvation period, the inflow goes to its upper bound which increases the depth (Figure 3.3.3), until the outflow, f_{out} (Figure 3.3.1), comes in at it's upper bound on day 15. This balances the depth until inflow is reduced to zero for most of the remaining time period after day 24. Outflow remains at its upper bound after this time to harvest as much algae as possible.

The efficiency of light absorption shown in Figure 3.3.7 and the average light intensity, $\bar{I}$, shown in Figure 3.3.4 demonstrate a significant increase of light absorption over the total time period from what is shown for the corresponding base case problem in Chapter 2, see Figures 2.5.12 and 2.5.9, respectively. The deeper pond allows for more algal growth which is then able to utilise the available light more efficiently.

Another interesting feature born out by these results can be noted by the comparison of Figures 2.5.5 and 3.3.8. The internal nitrogen quota, q_n, tends to remain fairly constant for the base

Figure 3.3.3: Variable Pond Depth. L

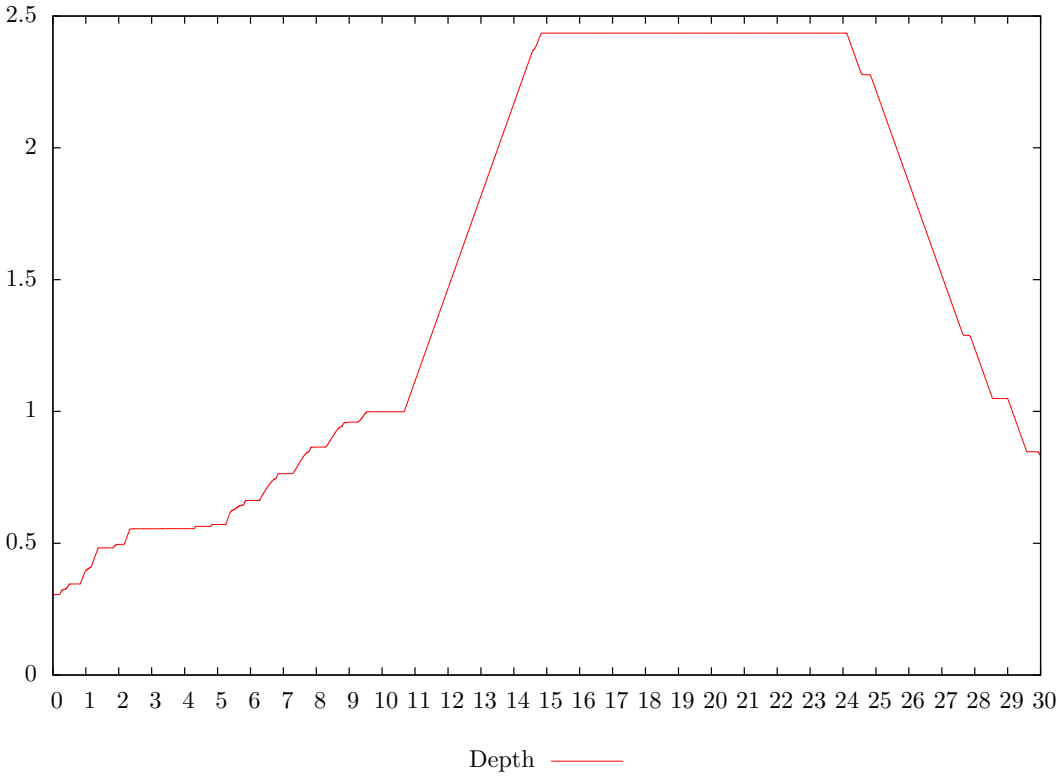

case result. For the results of Chapter 3, q_n increases somewhat and overall is greater than for the base case. Further to our discussion in Chapter 2, it would appear that lipid growth is stimulated more directly by a lower external nitrogen concentration, s, than by the internal nitrogen quota, q_n.

Figure 3.3.4: Variable Pond Depth. $\bar{I}$

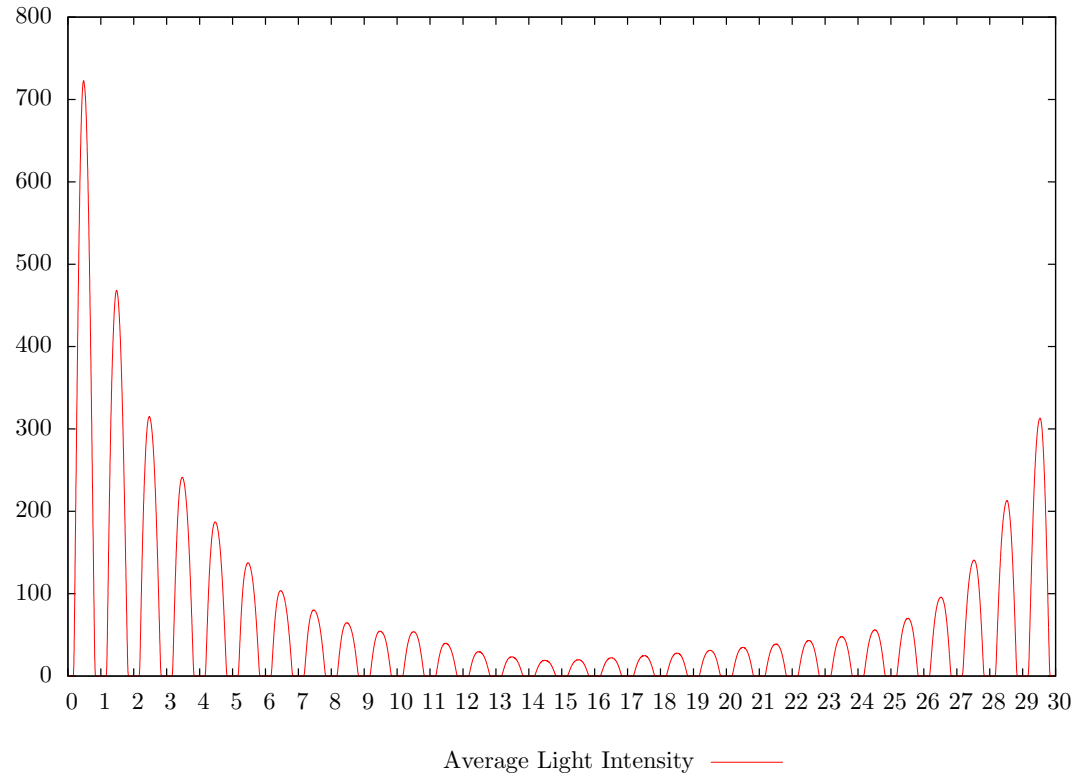

Figure 3.3.5: Variable Pond Depth. s

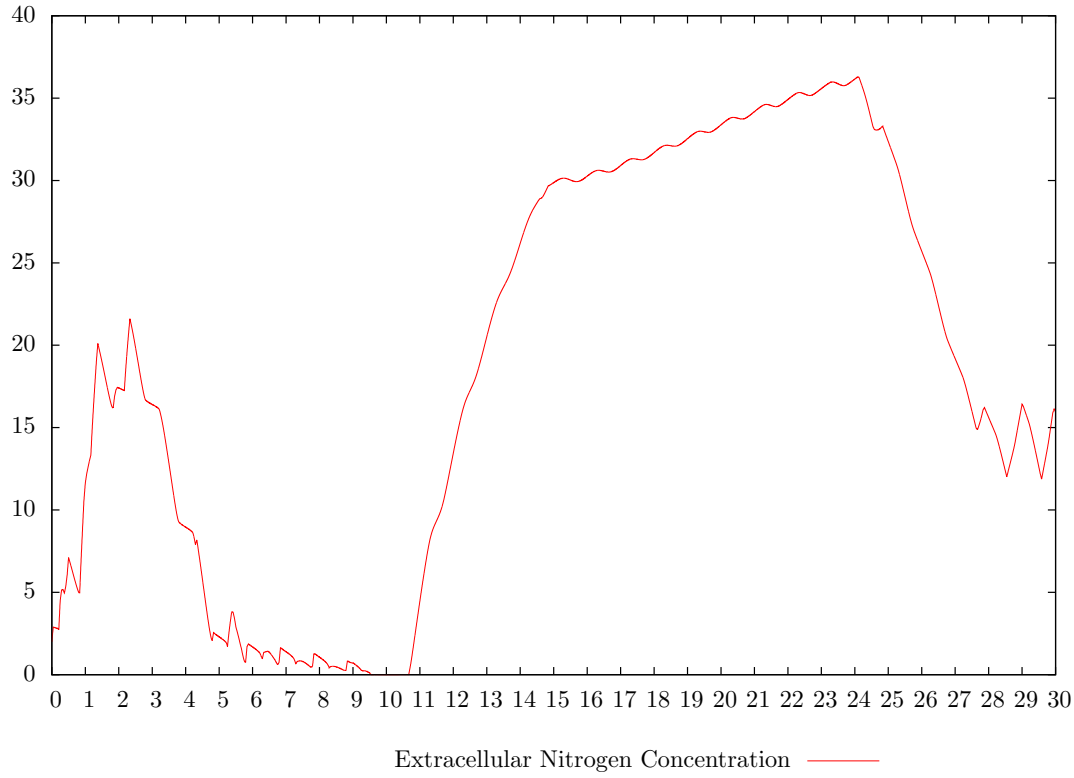

Figure 3.3.6: Variable Pond Depth. x_l

Figure 3.3.7: Variable Pond Depth. η_L

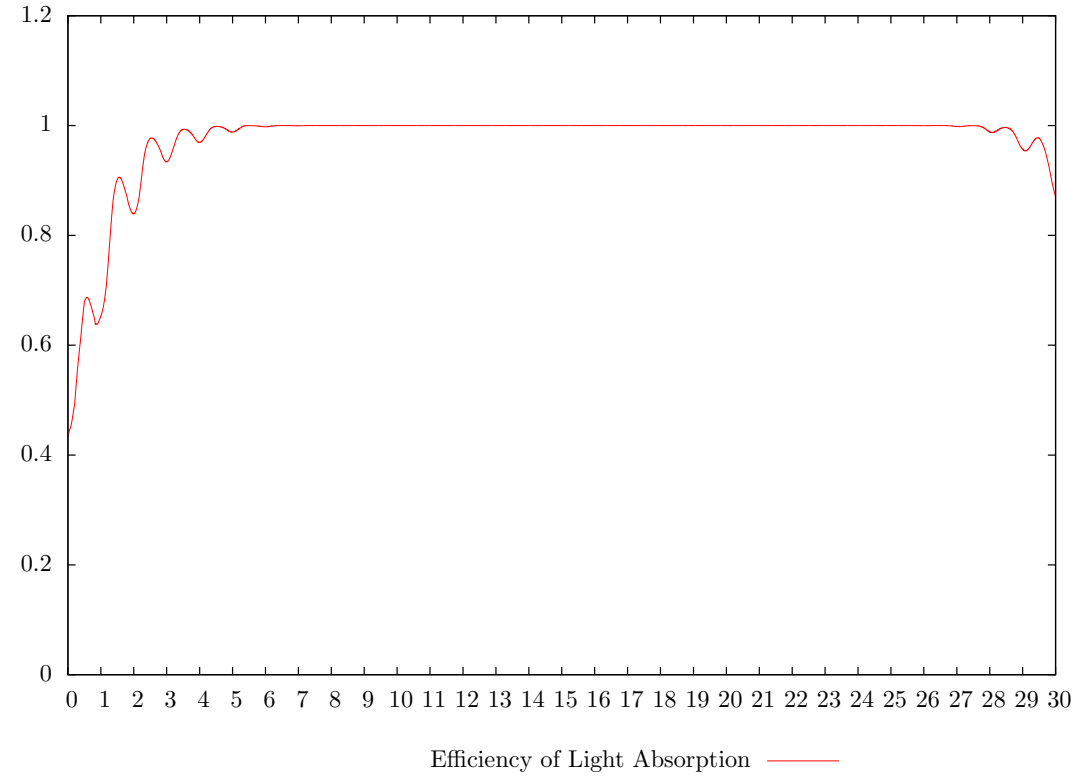

Figure 3.3.8: Variable Pond Depth. q_n

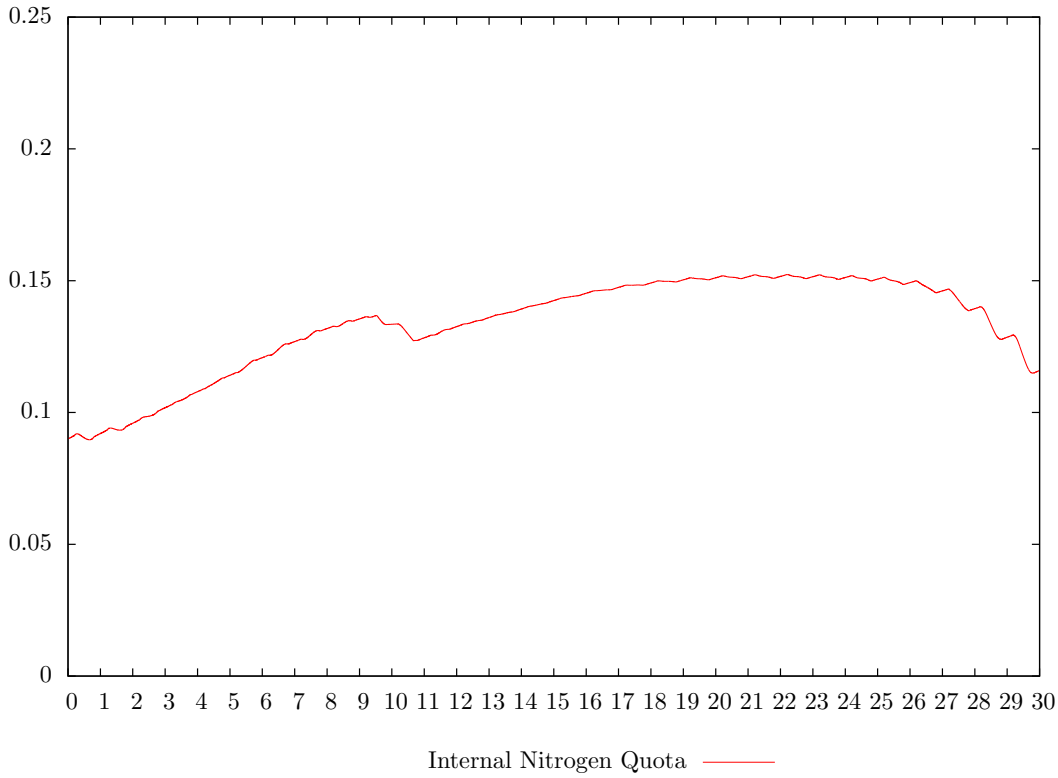

Figure 3.3.9: Variable Pond Depth. x

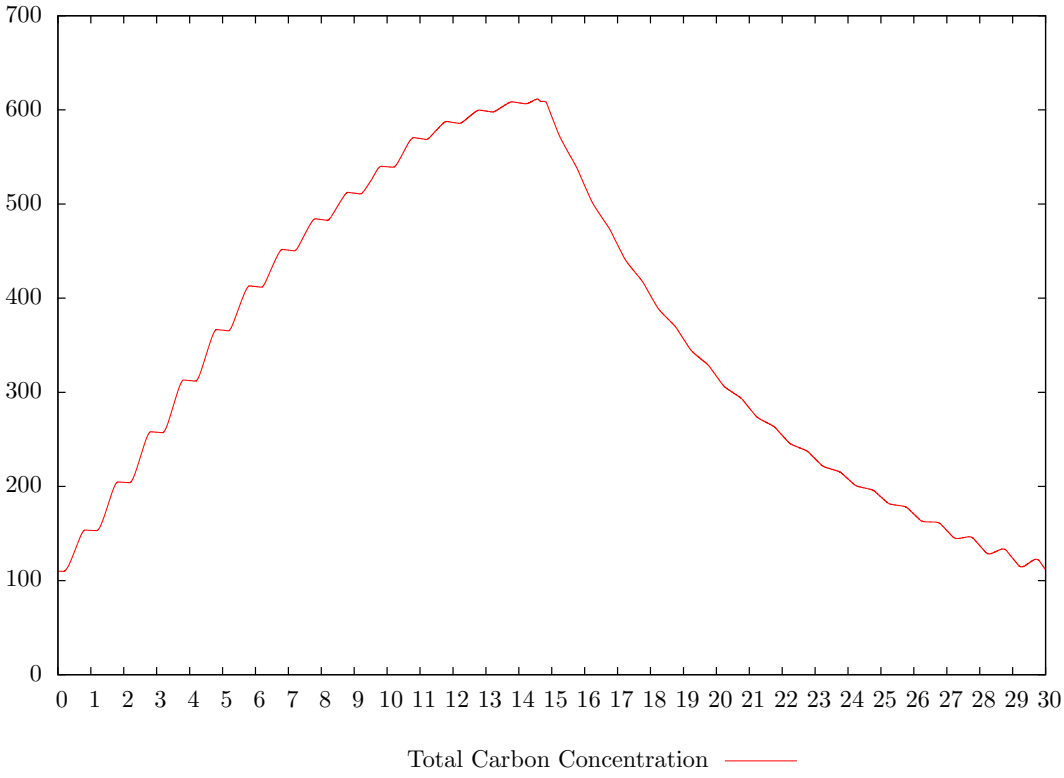

Figure 3.3.10: Variable Pond Depth. x_f

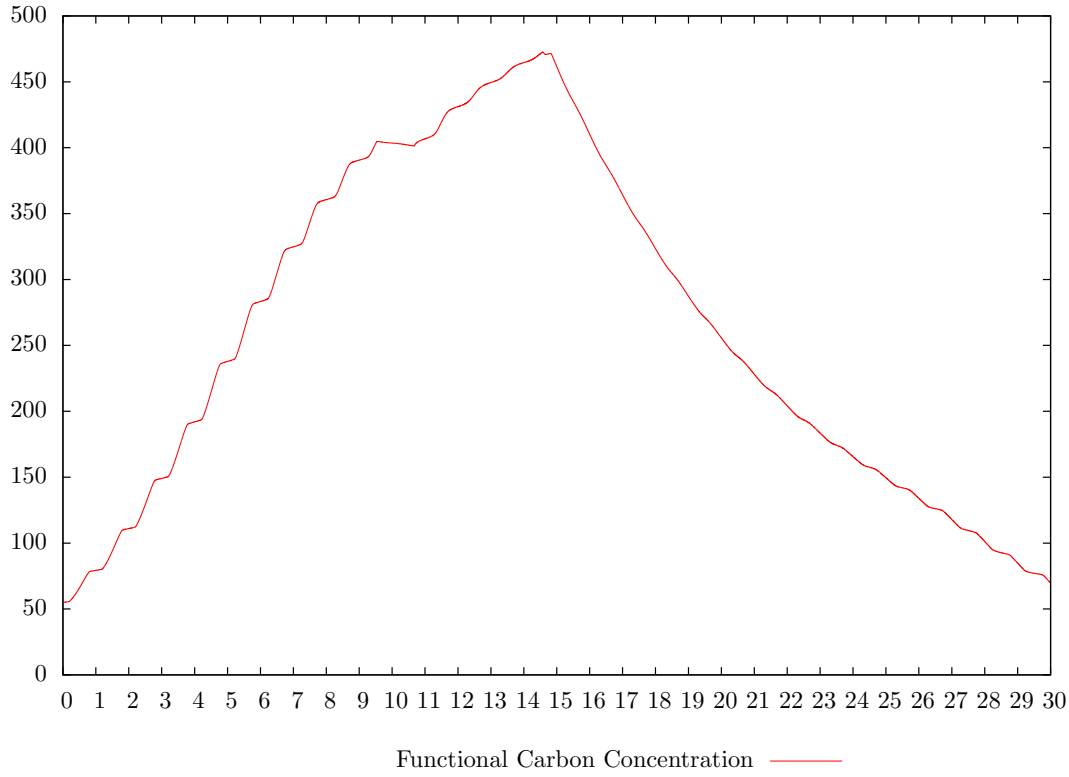

3.4 Conclusion

The model of algae growth in a raceway pond given in [91] is modified to contain the additional feature of variable pond depth. To achieve this, we use a new state variable to model depth as well as an additional control to represent variable outflow. We apply the numerical optimal control of MISER to this model and see that the lipid yield of the process is increased by 67% for the modified model.

Note that this is purely a numerical study and it is unlikely that the demonstrated yields gains can be reproduced in an actual pond. For example, our adopted model assumes that the process is not limited by the available carbon dioxide as there is no CO_2 driven limit on growth. One could address this shortcoming by applying a similar physical structure as that suggested in [96], but this would result in much more complex mathematical model, and thus a much longer computation time. Furthermore, the 2.5 metre pond depth that we observe in our optimal solution may not be practically feasible as tall side walls could have a significant shadowing effect on the available light. The representation of fixed daily temperature and irradiance is also somewhat unrealistic, but other typical light and temperature profiles for different seasons and global positions could be readily adopted.

Nevertheless, numerical results suggest that the variable depth option has some significant potential for yield improvement and should be considered further in future studies.

Chapter 4

Optimizing a microalgae raceway model with periodic boundary conditions

4.1 Introduction

For the base case algal raceway pond model in Chapter 2, we were able to generate an open loop optimal control f_{in} which resulted in a lipid yield equivalent to 28.928 tons ha^{-1} a^{-1}. The resulting optimal strategy involves a build up of total biomass, followed by a starvation period in order to promote the growth of lipids, and a final flush or wash out period to harvest these lipids. As noted Chapter 2, the downside of this high yield is a raceway pond depleted of algae at the end of the time horizon.

In this chapter we investigate a different strategy of operating the raceway pond. With the aim of a continuing algae growth and harvesting operation, we not only optimise the yield but also impose periodic boundary conditions on the state of the system so that it returns to its initial configuration at the end of the time horizon. Mathematically, this requires the addition of appropriate terminal state constraints to the model and also treating the start and end state values as decision variables. While a formal proof for the existence of an optimal periodic solution [5] is too difficult for the given dynamics, we are able to show numerically that such a solution exists and that it results in good lipid yields.

Finally we consider the practicality of the optimal periodic solution by formulating another

optimal control problem where we aim to drive the model from a given initial state to the optimal periodic boundary state. Numerical results for this problem appear to suggest that the optimal periodic state can not be reached in finite time. While this clearly limits the practicality of the optimal periodic solution, it still represents an important benchmark for future studies. This chapter is largely based on [46].

4.2 New Problem Formulation

Table 4.1: MISER periodic optimal initial conditions

State	Definition	Units	Value
s^*	Nitrogen concentration initial condition	gN m^{-1}	2.79046
q_n^*	Nitrogen quota initial condition	gN$(gC)^{-1}$	0.13082
x^*	Carbon biomass concentration initial condition	gC m^{-3}	743.10323
x_l^*	Lipid carbon optimal periodic concentration initial condition	gC m^{-3}	162.07085
x_f^*	Functional carbon initial condition	gC m^{-3}	542.05475

Table 4.2: AMPL periodic optimal initial conditions

State	Definition	Units	Value
s^*	Nitrogen concentration initial condition	gN m^{-1}	6.09022
q_n^*	Nitrogen quota initial condition	gN$(gC)^{-1}$	0.13105
x^*	Carbon biomass concentration initial condition	gC m^{-3}	716.58193
x_l^*	Lipid carbon optimal periodic concentration initial condition	gC m^{-3}	156.74079
x_f^*	Functional carbon initial condition	gC m^{-3}	523.45648

As noted in the previous section, we would like to formulate a new problem so that the raceway pond finishes in the same state in which it begins the process, thus allowing for ongoing operations. As the daily insolation and temperature profiles are assumed to repeat, it is reasonable to fix the time horizon to a single day, i.e. $t_f = 24$ in the notation of Chapter 2. We briefly consider longer time horizons in Section 4.4. Furthermore, we wish to find an optimal start/end state for the process. These aims can be conveniently achieved by regarding the initial values of the states as decision variables, i.e.

$$\begin{aligned} s(0) &= z_1, \\ q_n(0) &= z_2, \\ x(0) &= z_3, \\ x_l(0) &= z_4, \\ x_f(0) &= z_5 \end{aligned} \tag{4.2.1}$$

Figure 4.2.1: (MISER) 1 day period - f_{in}

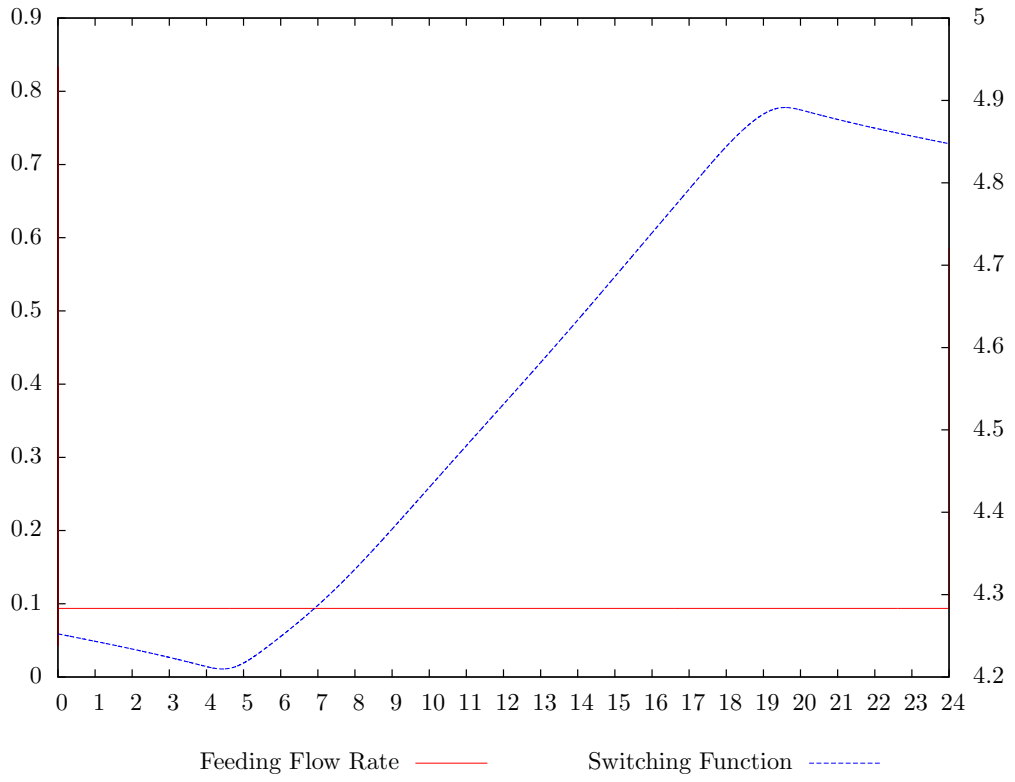

and by imposing the following set of terminal state constraints

$$\begin{aligned} s(t_f) &= z_1, \\ q_n(t_f) &= z_2, \\ x(t_f) &= z_3, \\ x_l(t_f) &= z_4, \\ x_f(t_f) &= z_5, \end{aligned} \tag{4.2.2}$$

where $z_1, z_2, \ldots, z_5$ are decision variables. The Initial condition for $\bar{I}$ and C_{hl} follow from (2.3.17) and (2.3.18):

$$\begin{aligned} \bar{I}(0) &= 0, \\ C_{hl}(0) &= \frac{z_3 z_2}{g_1 - g_2 T(0)}, \end{aligned} \tag{4.2.3}$$

and terminal constraints are not required as both of these states continually maintain their dependence on the other states due to the transformed dynamics (2.3.16).

Note that the dynamics are quite sensitive to the choice of $z_1, z_2, \ldots, z_5$. For this reason we

Figure 4.2.2: (AMPL) 1 day period - f_{in}

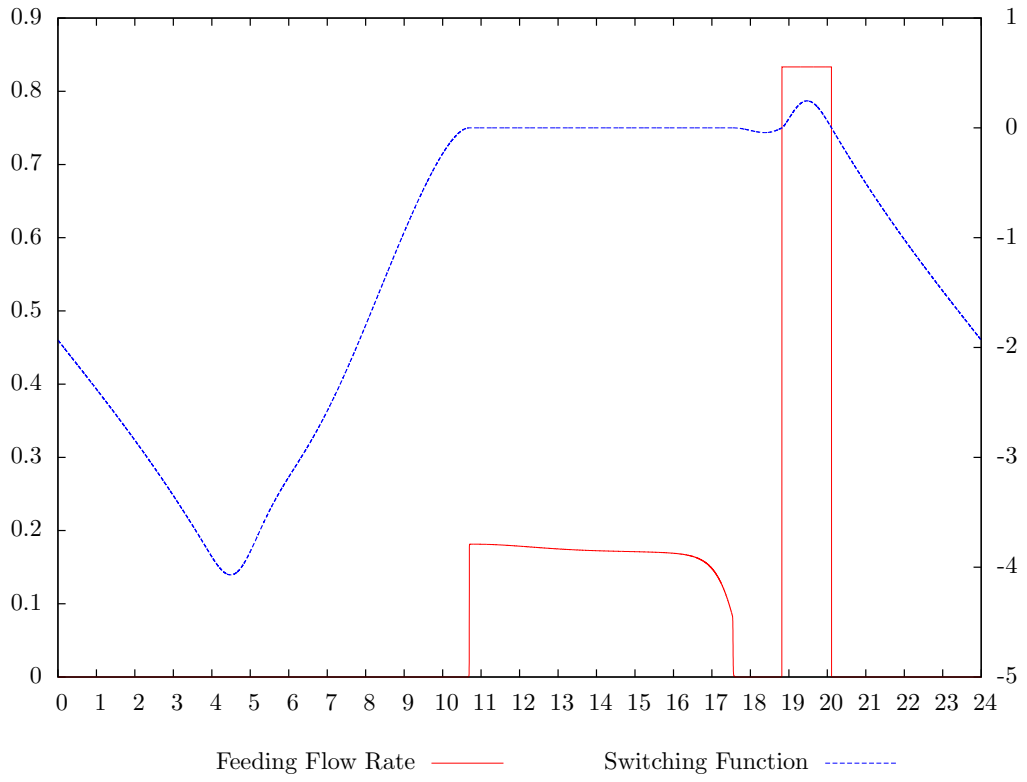

need to impose some bounds for the decision variables $z_1, z_2, \ldots, z_5$. As a guide, we look at the approximate maximum and minimum values reached by each state variable over the time horizon in our previous results in Chapter 2. Hence, we adopt the following bounds.

$$\begin{aligned} 0 \leq z_1 \leq 30, \\ 0.05 \leq z_2 \leq 0.2, \\ 85 \leq z_3 \leq 1250, \\ 14 \leq z_4 \leq 350, \\ 44 \leq z_5 \leq 600. \end{aligned} \tag{4.2.4}$$

Note that in the solutions presented below, none of the bounds in (4.2.4) are active.

Consider the problem of finding $z_1, z_2, \ldots, z_5$, s_{in}, and f_{in} to maximise the objective (2.4.1) with integrand (2.4.4) (maximising lipids) subject to the dynamics (2.3.16), the initial conditions (4.2.1), and the constraints (2.4.3), (4.2.2), and (4.2.4). We then employed the MISER optimal control software (with the MISER options of: number of knots in the partition for the control = 25, tolx = 10^{-9}, tolpsi = 10^{-9}, hmax = 10^{-4}, maxite = 1000, epsopt = 10^{-9}, epscon = 10^{-9},

Figure 4.2.3: (MISER) 1 day period - s

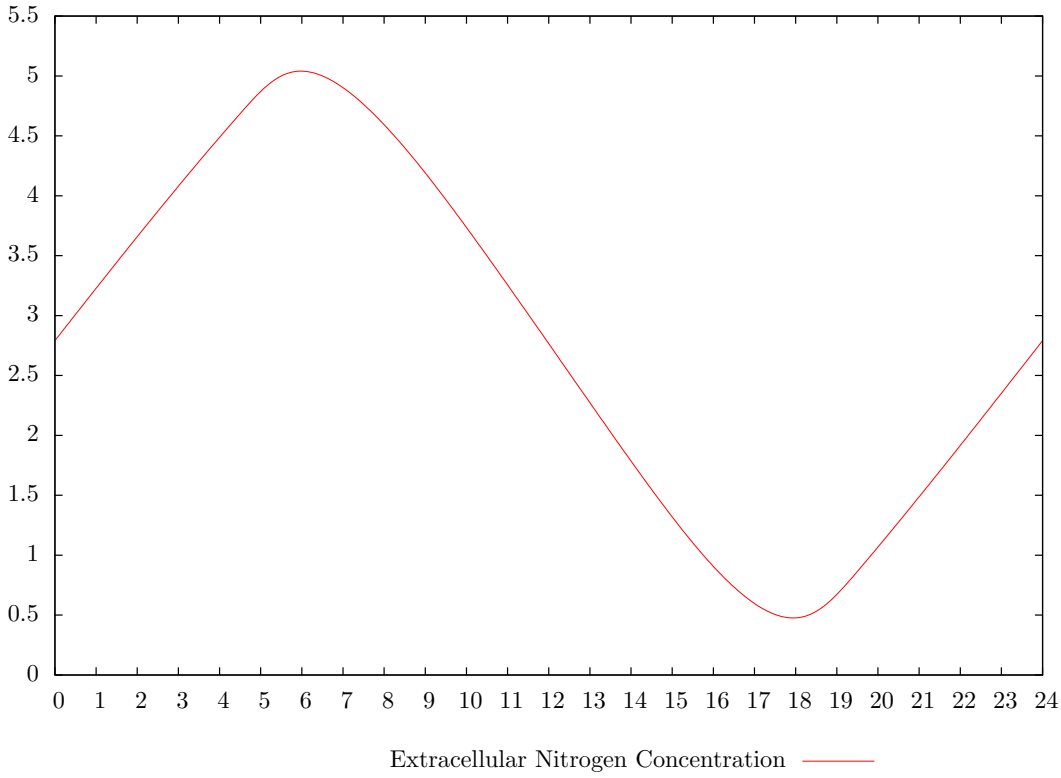

imerit = 2, and ilql = 1 as well as using the NLPQLP optimiser [109]) to solve this problem numerically, allowing for piecewise constant control functions f_{in} and s_{in} consistent with a partition of $[0, t_f]$ into 24 subintervals. We consider the subinterval of both uniform length (1 hour ass for the computations in Chapter 2) or varying length (via a time scale transformation [106]). Several solutions were obtained by starting with varying initial guesses of the optimisation parameters. The best feasible solution resulted in both controls taking on a constant value for the entire time horizon with $f_{in} = 0.09368$, $s_{in} = 100$ and the corresponding optimal $z_1, z_2, \ldots, z_5$ values given in Table 4.1. The corresponding optimal lipid yield is 41.745 tons ha^{-1} a^{-1} (10944.8 gC over 30 days) which is a significant improvement on our base case batch result in Chapter 2.

While a single control value for the entire time horizon has an obvious appeal in terms of ease of use and practical application, we were not convinced that we had obtained the best possible solution to the problem. This solution had arisen when we allowed for variable control knot points and our past numerical experience has been that the use of the associated time scale transformation often results in getting stuck in suboptimal local minimisers of the underlying mathematical programming problem. It turns out that while the obtained solution is feasible, it does not satisfy the requirements of the minimum principle. The Hamiltonian and switching functions of the problem are the same

Figure 4.2.4: (MISER) 1 day period - q_n

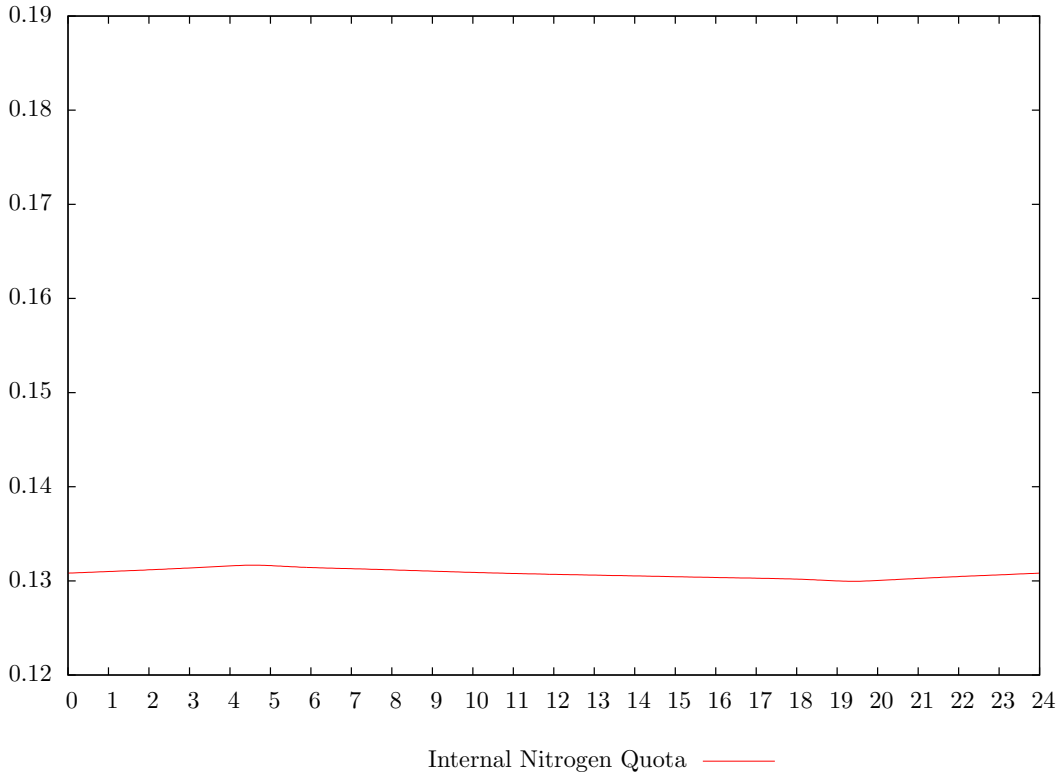

as those for the problem described in Section 2.4 given by (2.4.6) and (2.4.9), respectively. The solution obtained has $s_{in} = 100$ throughout. Maximising the Hamiltonian requires that f_{in} should take on its upper bound when its switching function is greater than 0 and it should take on the value zero when its switching function is less than 0. However, looking at Figure 4.2.1, we see that f_{in} is strictly between its bounds even though its switching function is positive throughout the time horizon. Graphs of the associated state variables are shown in Figures 4.2.3–4.2.7 and the efficiency of light absorption, is given by Figure 4.2.8.

Next, we try a different numerical solution strategy by formulating a discretised version of the problem in the AMPL [33] modelling environment and using the IPOPT [126] optimisation package (we employ the implicit Euler scheme to approximate the differential equations and the traditional trapezoidal rule to approximate the objective integral, use the AMPL options of timesteps = 24000, abs_boundtol = 1, as well as the IPOPT options of max_iter = 10000, acceptable_tol = 10^{-12}). Although this approach approximates the dynamics and objective integral less accurately, the step-size used still yields sufficiently accurate results for practical purposes. Given the MISER solution resulted in s_{in} going straight to its upper bound, we simply assumed $s_{in} = 100$ and allowed only f_{in} and $z_1, z_2, \ldots, z_5$ to be variable. The resulting optimal control f_{in} now has a bang-singular pattern

Figure 4.2.5: (MISER) 1 day period - x

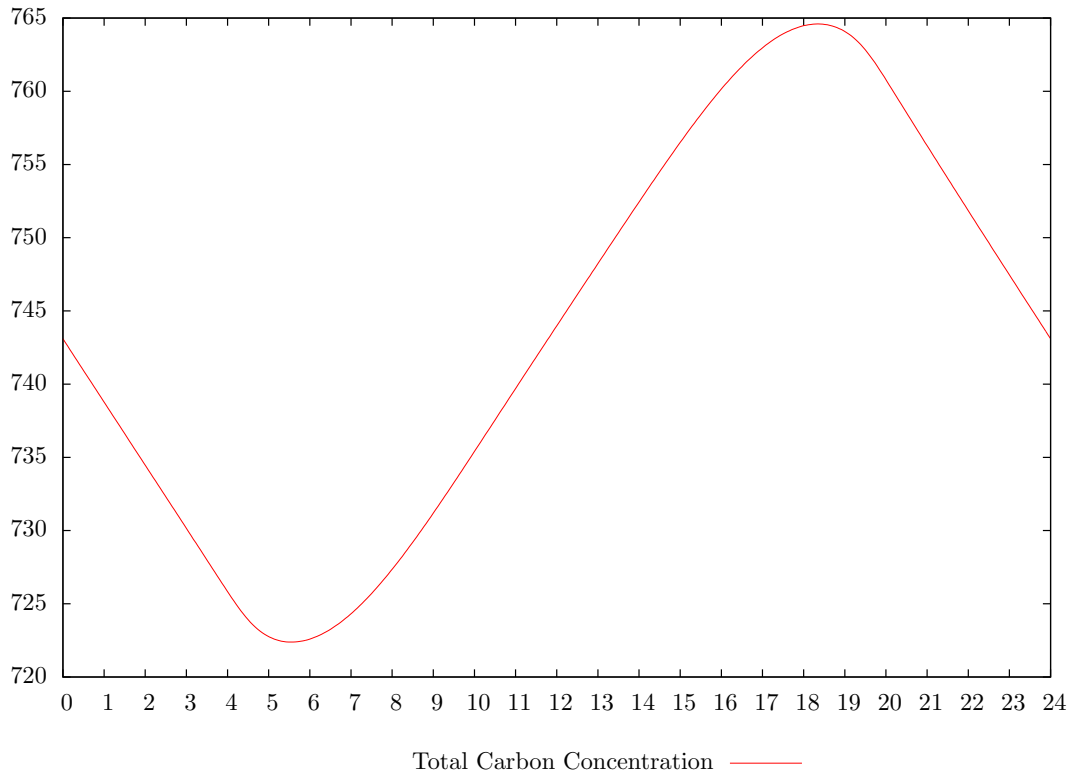

as shown in Figure 4.2.2. Note that the dotted curve in Figure 4.2.2 is the switching function for f_{in}. Its sign pattern confirms that the obtained solution satisfies the minimum principle. The optimal $z_1, z_2, \ldots, z_5$ values are given in Table 4.2. The corresponding optimal lipid yield of 42.029 tons ha^{-1} a^{-1} (11019.4 gC over 30 days) is a slight improvement again on that obtained with the suboptimal constant control calculated by MISER. Graphs of the associated state variables are shown in Figures 4.2.9–4.2.13 and the efficiency of light absorption, is given by Figure 4.2.14.

Note that both solutions obtained in this section satisfy all of the specified boundary conditions and are thus feasible. Even though the constant control solution obtained by MISER is not optimal in the strict sense of the minimum principle, its simple form makes it easier to use in practice and its lipid yield is not very different to that f the optimal result. Both sets of results exhibit a near complete utilization of the available insolation (see Figures 4.2.8 and 4.2.14). We thus continue to consider both solutions in the next section.

Figure 4.2.6: (MISER) 1 day period - x_l

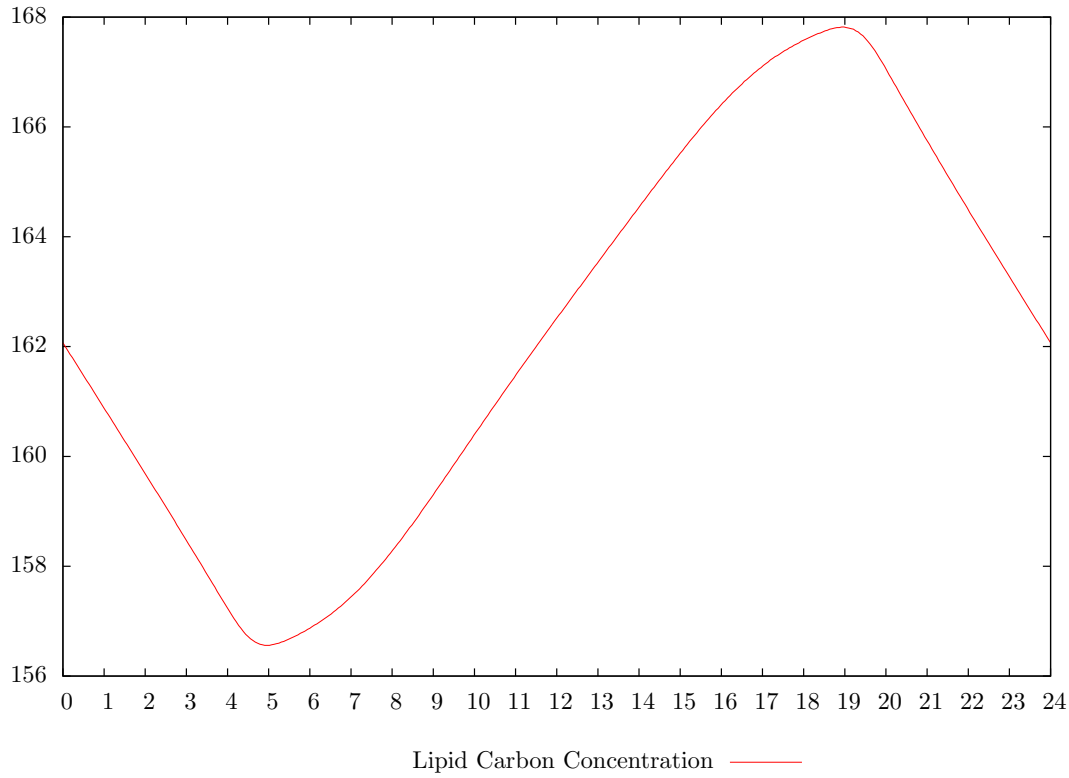

Figure 4.2.7: (MISER) 1 day period - x_f

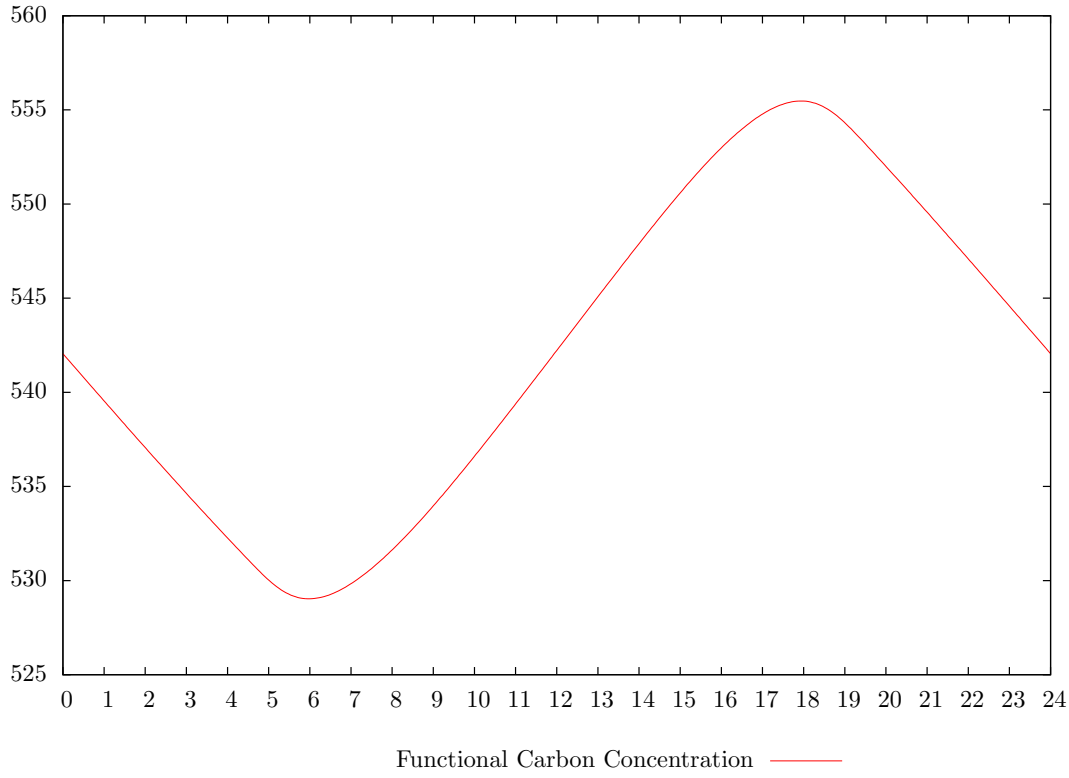

Figure 4.2.8: (MISER) 1 day period - η_L

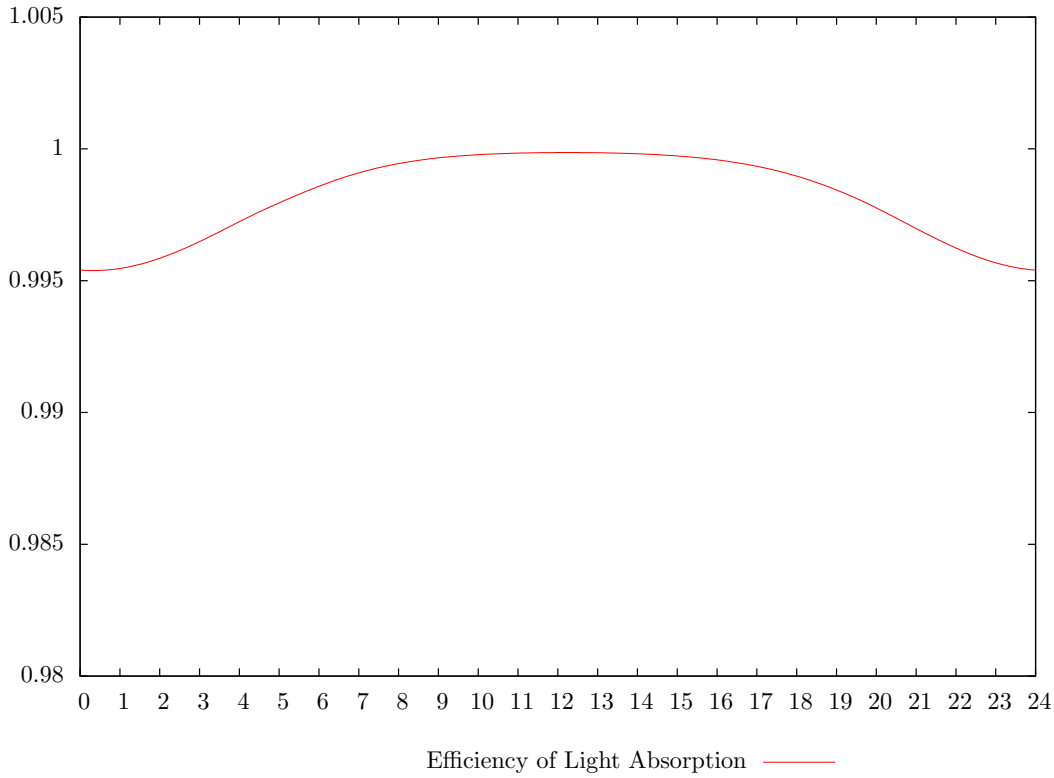

Figure 4.2.9: (AMPL) 1 day period - s

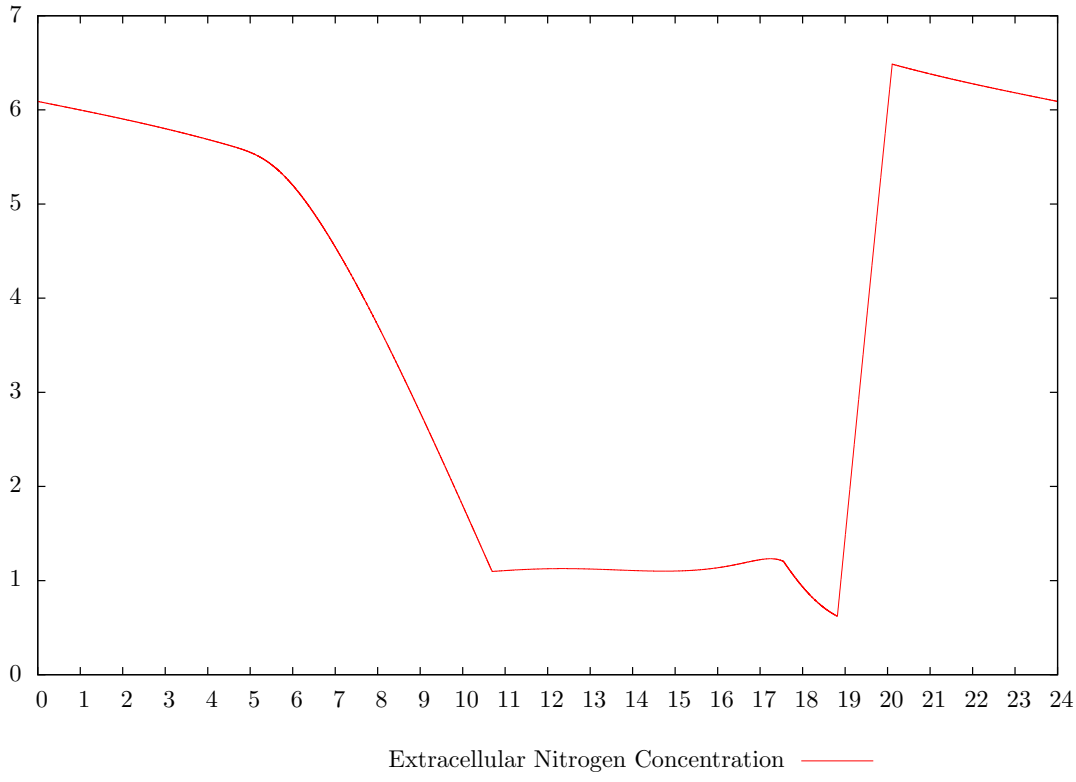

Figure 4.2.10: (AMPL) 1 day period - q_n

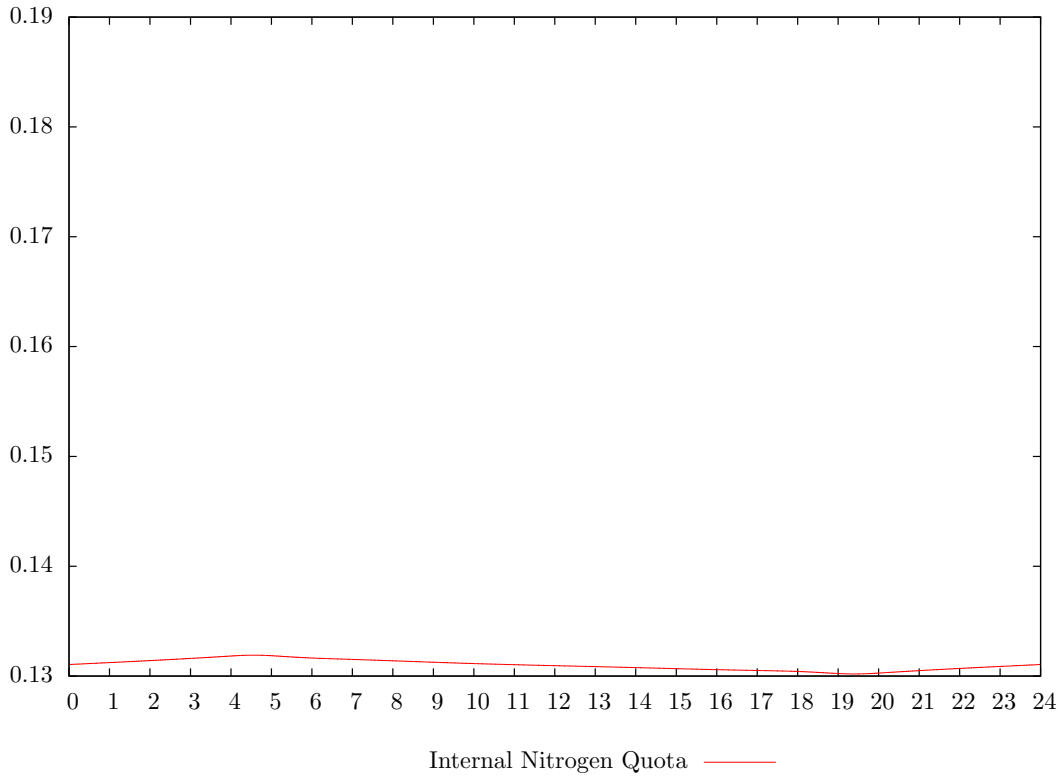

Figure 4.2.11: (AMPL) 1 day period - x

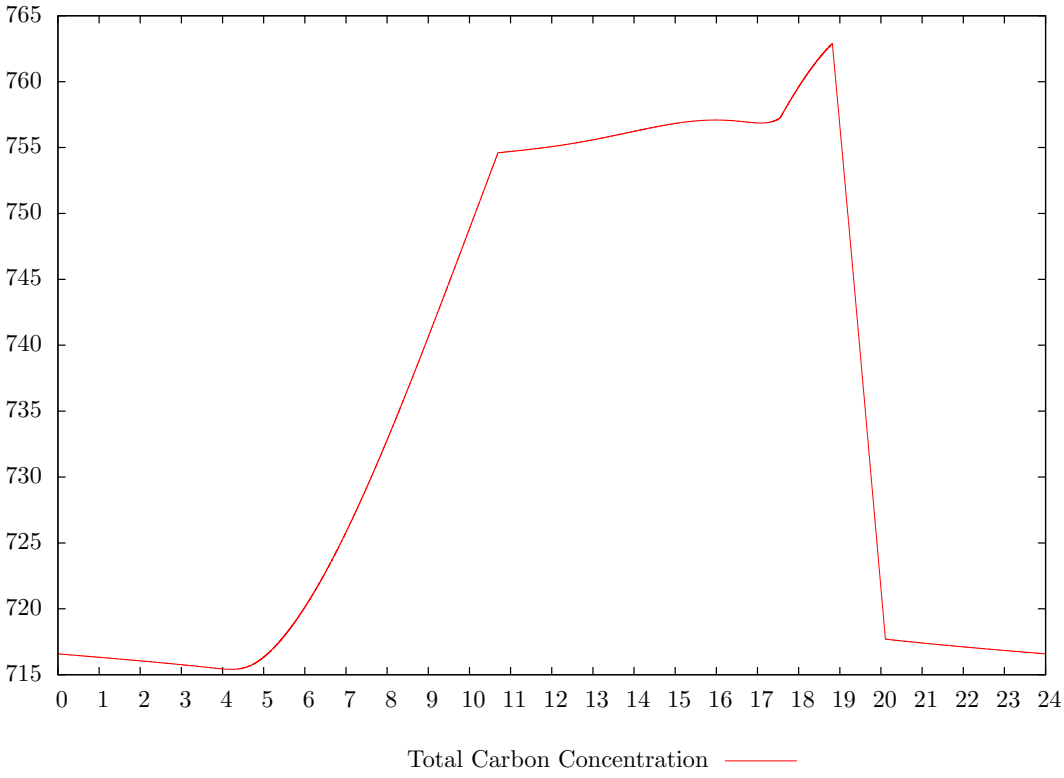

Figure 4.2.12: (AMPL) 1 day period - x_l

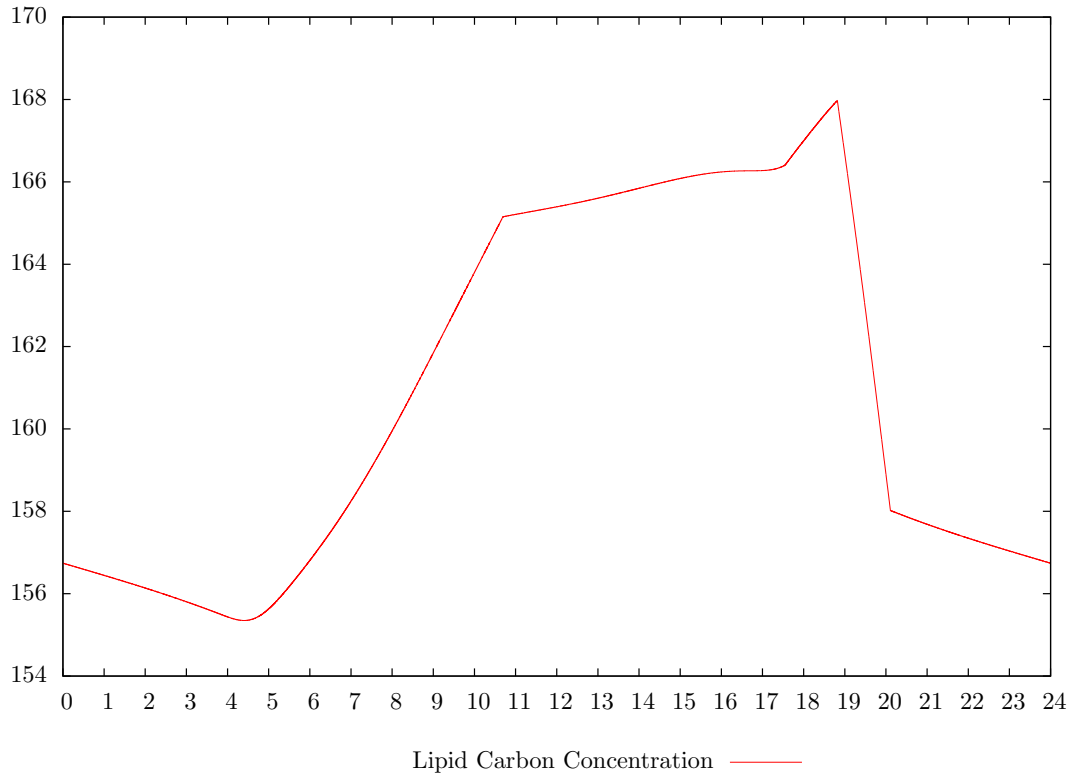

Figure 4.2.13: (AMPL) 1 day period - x_f

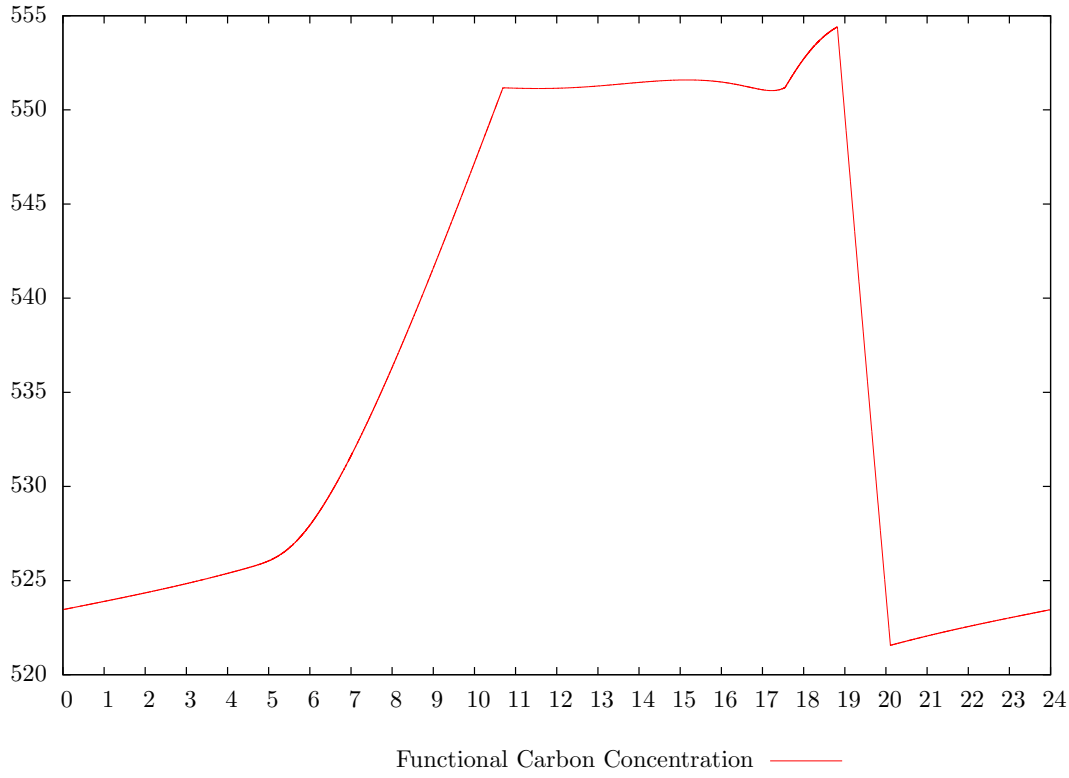

Figure 4.2.14: (AMPL) 1 day period - η_L

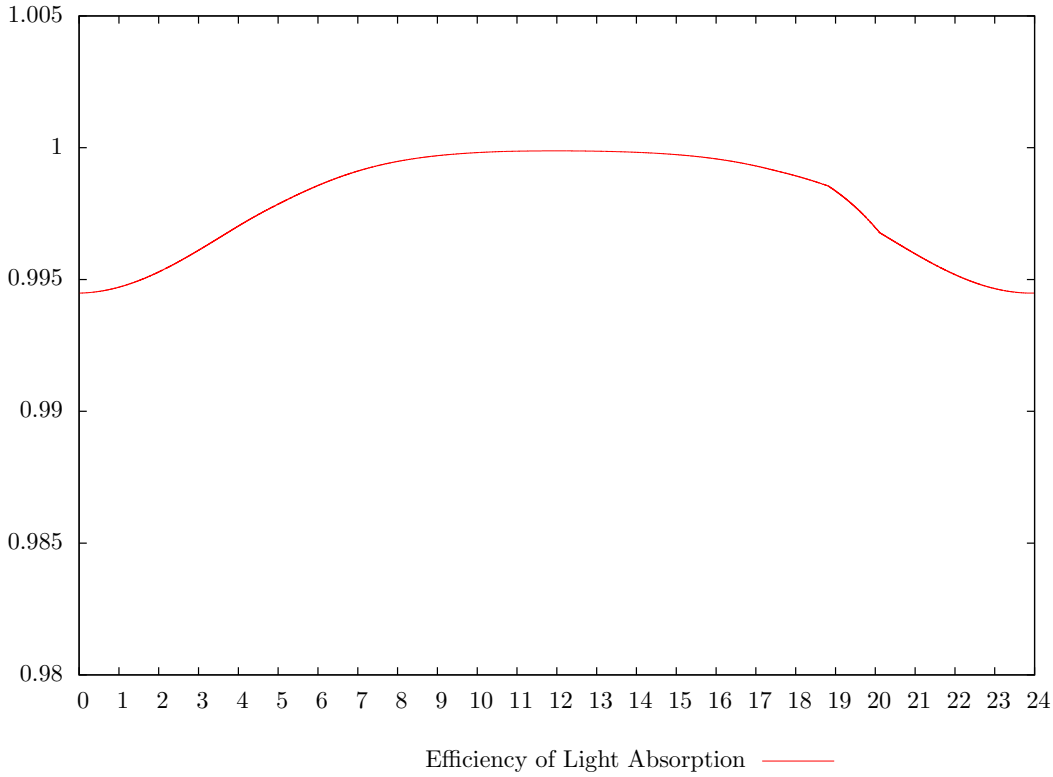

4.3 Initialization Problem

The periodic formulation of the problem in Section 4.2 assumes that it is possible to start the process with some optimised initial states. Thus the question of whether it is possible to drive the system to these states from a given starting point arises. We use s^*, q_n^*, x^*, x_l^*, and x_f^* to denote the optimal $z_1, z_2, \ldots, z_5$ in Tables 4.1 and 4.2, respectively. We also need to consider some reasonable initial values of $s(0)$, $q_n(0)$, $x(0)$, $x_l(0)$, and $x_f(0)$. For these, we simply go back to the values given for the original model, i.e. (2.4.2) as well as

$$s(0) = 2.0. \tag{4.3.1}$$

The aim is to reach the targets $s(t_f) = s^*$, $q_n(t_f) = q_n^*$, $x(t_f) = x^*$, $x_l(t_f) = x_l^*$, and $x_f(t_f) = x_f^*$ at some terminal time t_f. When we formulated a problem with these terminal constraints at $t_f = 720$ (30 days, the duration of our initial batch problem), MISER was unable to obtain a solution satisfying them. Hence, we formulated a different problem, where we now want to minimise the objective

$$\min_{\substack{f_{in} \\ s_{in}}} \left(\frac{s(t_f) - s^*}{s^*}\right)^2 + \left(\frac{q_n(t_f) - q_n^*}{q_n^*}\right)^2 + \left(\frac{x(t_f) - x^*}{x^*}\right)^2 + \left(\frac{x_l(t_f) - x_l^*}{x_l^*}\right)^2 + \left(\frac{x_f(t_f) - x_f^*}{x_f^*}\right)^2, \tag{4.3.2}$$

subject to the dynamics (2.3.16), the initial conditions (2.4.2) and (4.3.1), and the control bounds (2.4.3). Note again that associated state variables $\bar{I}$ and C_{hl} obey their own associated boundary conditions because they are dependant on q_n, x, and I_0, so they do not need to be part of the objective. If it is possible to reach the desired states exactly, we should find the objective function going to zero. We solve the problem with MISER beginning with $t_f = 720$ (30 days). The optimal objective value obtained is $4.89183858 \times 10^{-3}$ with the corresponding terminal states being at most 5.2792 percent off their desired value. As we increase the time horizon to 40, 50 and 60 days, we see that the objective value gets closer to zero, but never appears to reach it (see Table 4.3). Attempts to solve this same problem with the AMPL/IPOPT solution (with s^*, q_n^*, x^*, x_l^*, and x_f^*

Table 4.3: MISER initialization problem

Time Horizon	Objective Value	Maximum state deviation
30 days	$4.89183858 \times 10^{-3}$	5.2792%
40 days	$3.96110743 \times 10^{-4}$	1.4266%
50 days	$3.75673645 \times 10^{-5}$	0.5148%
60 days	$2.93231726 \times 10^{-5}$	0.4530%

representing the optimal $z_1, z_2, \ldots, z_5$ in Table 4.2) also did not result in a zero objective value. The numerical results appear to suggest that we cannot reach the desired periodic state value in finite time from the chosen initial state. Extensive numerical studies would be required to determine the existence of a set of initial states that would allow the model to reach the desired periodic state in finite time, but this is beyond the scope of the present study.

4.4 Conclusion

We have considered an optimal control model of an algae growth process with periodic boundary conditions with the view of an ongoing growth and harvesting operation. Numerical results show that solutions satisfying the periodic boundary conditions can be determined with the additional benefit of significantly improved yields compared to the previous batch model. While the optimised boundary conditions appear to be difficult to reach from typical initial conditions of the model, the results still represent useful benchmarks to guide the development of future practical control algorithms.

It is worth noting that the lipid yields resulting from the problem with periodic boundary conditions are only marginally better than that obtained from the feedback control formulation extended from 30 to 60 days in Section 2.8. As time progresses, one would expect the optimal feedback control to drive the system to some form of quasi-steady state which may also yield a reasonably good quality solution to the problem with periodic boundary conditions posed in this chapter.

Note that we have also solved the problem with periodic boundary conditions for different time horizon durations ($t_f = \{24,48,72,96,120,720\}$, corresponding to 1,2,3,4,5,and 30 days) to see whether yield could be further improved. We were not able to determine any substantial improvements in yield from this approach. The best improvement is approximately 1% above the 1 day result.

Chapter 5

Conclusions and Future Studies

In this thesis we have used computational optimal control methods to determine optimal strategies for operating raceway ponds in order to maximise the lipid yield of the harvested algae. We first solved a base case model with the only control being the inflow rate and numerically determined an optimal solution which yielded about 20% more lipids than the only other previously published result for this model. We then considered a range of different methods of operating the raceway pond allowing for both additional controls (inflow nutrient concentration and outflow in the case of variable raceway depth) and additional decision variables (initial and terminal conditions for various model states and fixed raceway depth) and found corresponding optimal solutions for these controls and decision variables. A range of significant lipid yield improvements of up to 67% over that for our own base case result were obtained. These results demonstrate clearly that there is still significant future potential to improve microalgae lipid production in raceway ponds. It is also worth noting that significant yield improvements were achieved for both batch and continuous operating models of raceway ponds.

We have by no means exhausted the full range of possible operating strategies for raceway ponds. For example, in the model where pond depth was varied over the time horizon, we kept the initial pond depth at 30cm to allow for an easier comparison of results to those of our base case model. However, it should be possible to also model the initial pond depth as a decision variable in this case. Similarly, we did not allow for variable pond depth when we proposed the models incorporating varying nutrient inflow or periodic boundary conditions, respectively. One can reasonably expect further improvements in lipid yields if these strategies were to be considered in combination.

We must, of course, acknowledge the obvious shortcomings of the basic approach taken in

this thesis. Since we have only considered a mathematical model of algal growth, it is unlikely that the optimal strategies we have derived would reproduce the same lipid yield improvements when applied to actual raceway ponds. Biological growth processes actually involve very complex chemical reactions. Modelling these in their entirety would result in models that are actually too time consuming to optimise or even simulate. On the other hand, mathematical biology is continually evolving and existing models are already able to capture most of the key features of the underlying processes in many instances. In the context of models of algal growth in raceway ponds, we considered a range of existing models and selected the one most suitable for our purposes [91]. While it captures most of key drivers and limitations of algal growth, it would be desirable in future studies to also include the impact of carbon dioxide on growth. It may be possible to adapt aspects of an existing model incorporating CO_2 such as [58] into the one considered here without significantly increasing its complexity. This would allow us to incorporate other objectives such as CO_2 mitigation into our model. A more complete model would also take into account the capital costs of building a raceway, discounted over its expected period of operation. Capital costs will depend on depth L but may also include additional factors such as the pond layout and equipment. Additionally, it would be desirable to also include the cost of harvesting the algae, which likely depends on the concentration of biomass in the outflow.

Another criticism which can be levelled at the existing model is the assumption of fixed daily temperature and irradiance profiles which are clearly unrealistic in practice. It would be interesting to replace these profiles with ones which vary between days (based on weather predictions) and then see how the optimal controls change in response. Techniques similar to those used for the operation of a solar car over a five day race [40] may be useful here. If a year round operation is to be considered, typical light and temperature profiles for other seasons should also be adopted.

Throughout the thesis, we have noted possible limitations of the alternative strategies we proposed. For example, we noted that a significant increase in pond depth may not be feasible if this introduces shadowing effects that are not catered for with the light propagation aspects of the existing model. It may be possible to overcome these shadowing effects if the pond walls are sloped rather than strictly vertical (indeed, for larger raceway ponds dug out of the ground, this is already the case). This will require some further model changes in terms of the relationships between volume, surface area, depth, and light propagation but, again, these should not add a great deal of complexity to the existing model.

Another interesting aspect of this thesis is the experience gained in the use of different computational optimal control methods. We employed both control parameterisation (via the MISER

package) and full discretisation/parameterisation (via the use of AMPL/IPOPT). The various versions of the problem we considered proved to be challenging for both of these methods. While a full discretisation is much easier to implement from a user point of view (for instance, conversion of the system of differential algebraic equations to one of ordinary differential equations is not required as the algebraic equations simply form an additional set of constraints in the fully discretised problem), we found that extending the time horizon of the problem to anything beyond 6 days would result in a discretised problem that was simply too large to be solved. The control parameterisation approach was able to deal with longer time horizons (up to 60 days) without too much difficulty, but it would often converge to suboptimal solutions from different initial guesses. Also, we would have liked to make more use control parameterisation in conjunction with a time scale transformation in order to better localise the optimal switching times of the bang-singular controls, but in most cases this also resulted in problems too large to solve or it would lead to premature convergence to poor locally optimal solutions. The insight given by the patterns of bang-singular optimal controls we have determined in this thesis may allow for more efficient parameterisations of the controls in future studies.

In conclusion, we hope that the results presented in this thesis will encourage researchers in algal growth to contemplate a much wider range of strategies of raceway pond operation than is currently being considered. There is clearly potential to significantly increase lipid yields in this field. We also hope that our results will encourage the wider adoption of mathematical modelling and computational optimal control methods for biological systems.

Bibliography

[1] H. A. Alalwan, A. H. Alminshid, and H. A. Aljaafari, "Promising evolution of biofuel generations. subject review," *Renewable Energy Focus*, vol. 28, pp. 127–139, 2019, ISSN: 1755-0084.

[2] K. Alloula, F. Monfreda, R. Thery, and J.-P. Belaud, "Converting dae models to ode models: Application to reactive rayleigh distillation," *Chemical engineering transactions*, vol. 32, 2013.

[3] B. D. Anderson and J. B. Moore, *Optimal control: linear quadratic methods*. Courier Corporation, 2007.

[4] N. Banihashemi and C. Y. Kaya, "Inexact restoration for euler discretization of box-constrained optimal control problems," *Journal of Optimization Theory and Applications*, vol. 156, no. 3, pp. 726–760, 2013.

[5] T. Bayen, F. Mairet, P. Martinon, and M. Sebbah, "Analysis of a periodic optimal control problem connected to microalgae anaerobic digestion," *Optimal Control Applications and Methods*, vol. 36, no. 6, pp. 750–773, 2015, ISSN: 1099-1514.

[6] Q. Béchet, A. Shilton, and B. Guieysse, "Maximizing productivity and reducing environmental impacts of full-scale algal production through optimization of open pond depth and hydraulic retention time," *Environmental science & technology*, vol. 50, no. 7, pp. 4102–4110, 2016.

[7] R. E. Bellman, *Dynamic programming*. Princeton, N.J.: Princeton, N.J. : Princeton Univ. Pr., 1957.

[8] O. Bernard, "Hurdles and challenges for modelling and control of microalgae for CO_2 mitigation and biofuel production," *Journal of Process Control*, vol. 21, no. 10, pp. 1378–1389, 2011.

[9] L. T. Biegler, "An overview of simultaneous strategies for dynamic optimization," *Chemical Engineering and Processing: Process Intensification*, vol. 46, no. 11, pp. 1043–1053, 2007.

[10] E. Birgin and J. Martínez, "Local convergence of an inexact-restoration method and numerical experiments," *Journal of Optimization Theory and Applications*, vol. 127, no. 2, pp. 229–247, 2005.

[11] E. A. Blanchard, R. Loxton, and V. Rehbock, "A computational algorithm for a class of non-smooth optimal control problems arising in aquaculture operations," *Applied Mathematics and Computation*, vol. 219, no. 16, pp. 8738–8746, 2013.

[12] M. A. Borowitzka, "Energy from microalgae: A short history," in *Algae for biofuels and energy*, M. A. Borowitzka, Ed., vol. 5, Springer, 2013, pp. 1–15.

[13] M. A. Borowitzka and N. R. Moheimani, *Algae for Biofuels and Energy*. Springer, 2013, vol. 5.

[14] M. A. Borowitzka and N. R. Moheimani, "Open pond culture systems," in *Algae for biofuels and energy*, M. A. Borowitzka, Ed., vol. 5, Springer, 2013, pp. 133–152.

[15] B. J. Boruff, N. R. Moheimani, and M. A. Borowitzka, "Identifying locations for large-scale microalgae cultivation in western australia: A gis approach," *Applied Energy*, vol. 149, pp. 379–391, 2015.

[16] K. E. Brenan, S. L. Campbell, and L. R. Petzold, *Numerical solution of initial-value problems in differential-algebraic equations*. Siam, 1996, vol. 14.

[17] L. Brennan and P. Owende, "Biofuels from microalgae - a review of technologies for production, processing, and extractions of biofuels and co-products," *Renewable and Sustainable Energy Reviews*, vol. 14, no. 2, pp. 557–577, 2010.

[18] C. Brennen, G Keady, and J Imberger, "A note on algal population dynamics," *J. Plankton Res*, vol. 23, pp. 1399–1411, 2018.

[19] J. S. Burlew *et al.*, "Algal culture from laboratory to pilot plant.," *Algal culture from laboratory to pilot plant.*, 1953.

[20] C. Büskens, "Direkte optimierungsmethoden zur numerischen berechnung optimaler steuerprozesse," Ph.D. dissertation, Diploma Thesis, University of Münster, 1993.

[21] C. Büskens, "Optimierungsmethoden und sensitivitatsanalyse fur optimale steuerprozesse mit steuer-und zustands-beschrankungen," *Westfalische Wilhelms-Universitat Munster*, 1998.

[22] C. Büskens and H. Maurer, "Nonlinear programming methods for real-time control of an industrial robot," *Journal of Optimization Theory and Applications*, vol. 107, no. 3, pp. 505–527, 2000.

[23] C. Büskens and H. Maurer, "SQP-methods for solving optimal control problems with control and state constraints: Adjoint variables, sensitivity analysis and real-time control," *Journal of Computational and Applied Mathematics*, vol. 120, no. 1-2, pp. 85–108, 2000, ISSN: 0377-0427. DOI: 10.1016/S0377-0427(00)00305-8.

[24] M. Cerucci, G. K. Jaligama, and R. B. Ambrose Jr, "Comparison of the monod and droop methods for dynamic water quality simulations," *Journal of Environmental Engineering*, vol. 136, no. 10, pp. 1009–1019, 2010, ISSN: 0733-9372.

[25] M. Chyba, T. Haberkorn, R. N. Smith, and S. Choi, "Design and implementation of time efficient trajectories for autonomous underwater vehicles," *Ocean Engineering*, vol. 35, no. 1, pp. 63–76, 2008.

[26] O. Ciferri, "Spirulina, the edible microorganism," *Microbiological reviews*, vol. 47, no. 4, p. 551, 1983.

[27] J. E. Cuthrell and L. T. Biegler, "Simultaneous optimization and solution methods for batch reactor control profiles," *Computers & Chemical Engineering*, vol. 13, no. 1-2, pp. 49–62, 1989.

[28] E. Denardo, *Dynamic programming : models and applications*. Mineola, N.Y: Dover Publications, 2003, ISBN: 9780486428109.

[29] M. R. Droop, "Vitamin b12 and marine ecology. iv. the kinetics of uptake, growth and inhibition in monochrysis lutheri," *J. Mar. Biol. Assoc. UK*, vol. 48, no. 3, pp. 689–733, 1968.

[30] M. R. Droop, "Vitamin b12 and marine ecology," *Helgoländer wissenschaftliche Meeresuntersuchungen*, vol. 20, no. 1-4, pp. 629–636, 1970.

[31] M. R. Droop, "25 years of algal growth kinetics a personal view," *Botanica Marina*, vol. 26, no. 3, pp. 99–112, 1983. DOI: https://doi.org/10.1515/botm.1983.26.3.99. [Online]. Available: https://www.degruyter.com/view/journals/botm/26/3/article-p99.xml.

[32] F. Fahroo and I. M. Ross, "Convergence of the costates does not imply convergence of the control," *Journal of guidance, control, and dynamics*, vol. 31, no. 5, pp. 1492–1497, 2008.

[33] R. Fourer, D. M. Gay, and B. W. Kernighan, "AMPL: A modeling language for mathematical programming," *Duxbury Press*, 2002.

[34] K. O. Geddes, B. W. Char, G. H. Gonnet, B. L. Leong, M. B. Monagan, *et al.*, *Maple V: Language reference manual*. Springer, 1993.

[35] P. E. Gill, W. Murray, and M. A. Saunders, "SNOPT: An SQP algorithm for large-scale constrained optimization," *SIAM review*, vol. 47, no. 1, pp. 99–131, 2005.

[36] B. H. H. Goh, H. C. Ong, M. Y. Cheah, W.-H. Chen, K. L. Yu, *et al.*, "Sustainability of direct biodiesel synthesis from microalgae biomass: A critical review," *Renewable and Sustainable Energy Reviews*, vol. 107, pp. 59 –74, 2019, ISSN: 1364-0321. DOI: https://doi.org/10.1016/j.rser.2019.02.012. [Online]. Available: http://www.sciencedirect.com/science/article/pii/S1364032119301054.

[37] K. F. Graham and A. V. Rao, "Minimum-time trajectory optimization of low-thrust earth-orbit transfers with eclipsing," *Journal of Spacecraft and Rockets*, vol. 53, no. 2, pp. 289–303, 2016.

[38] A. Griewank, "Who invented the reverse mode of differentiation," *Documenta Mathematica, Extra Volume ISMP*, pp. 389–400, 2012.

[39] F. Grognard, A. R. Akhmetzhanov, and O. Bernard, "Optimal strategies for biomass productivity maximization in a photobioreactor using natural light," *Automatica*, vol. 50, no. 2, pp. 359–368, 2014.

[40] E. Guerrero Merino and M. A. Duarte-Mermoud, "Online energy management for a solar car using pseudospectral methods for optimal control," *Optimal Control Applications and Methods*, 2015, ISSN: 1099-1514.

[41] R. Harder and H. Von Witsch, "Bericht über versuche zur fettsynthese mittels autotropher microorganismen," *Forschungsdienst Sonderheft*, vol. 16, pp. 270–275, 1942.

[42] R. Harder and H. Von Witsch, "The mass cultivation of diatoms," *Reports of the German Botanical Society*, vol. 60, pp. 146–52, 1942.

[43] C. Y.-F. Ho, B. W.-K. Ling, Y.-Q. Liu, P. K.-S. Tam, and K. L. Teo, "Optimal pwm control of switched-capacitor dc–dc power converters via model transformation and enhancing control techniques," *IEEE Transactions on Circuits and Systems I: Regular Papers*, vol. 55, no. 5, pp. 1382–1391, 2008.

[44] D. Hull, J. Speyer, and C. Tseng, "Maximum-information guidance for homing missiles," *Journal of Guidance, Control, and Dynamics*, vol. 8, no. 4, pp. 494–497, 1985.

[45] G. T. Huntington and A. V. Rao, "Optimal reconfiguration of spacecraft formations using the gauss pseudospectral method," *Journal of Guidance, Control, and Dynamics*, vol. 31, no. 3, pp. 689–698, 2008.

[46] T. Hurst and V. Rehbock, "Optimizing a micro-algae raceway model with periodic boundary conditions," *DCDIS Series B: Applications & Algorithms*, to appear.

[47] T. Hurst and V. Rehbock, "Optimal control for micro-algae on a raceway model," *Biotechnology Progress*, 2017, ISSN: 1520-6033. DOI: 10.1002/btpr.2532. [Online]. Available: https://aiche.onlinelibrary.wiley.com/doi/abs/10.1002/btpr.2532.

[48] T. Hurst and V. Rehbock, "Optimizing micro-algae production in a raceway pond with variable depth," *Journal of Industrial & Management Optimization*, 2021. DOI: 10.3934/jimo.2021027. [Online]. Available: https://www.aimsciences.org/article/doi/10.3934/jimo.2021027.

[49] I. I. Hussein and A. M. Bloch, "Optimal control of underactuated nonholonomic mechanical systems," *IEEE Transactions on Automatic Control*, vol. 53, no. 3, pp. 668–682, 2008.

[50] S. C. James and V. Boriah, "Modeling algae growth in an open-channel raceway," *Journal of Computational Biology*, vol. 17, no. 7, pp. 895–906, 2010.

[51] L. S. Jennings, M Fisher, K. L. Teo, and C Goh, *MISER 3: Optimal control software, Version 2.0. Theory and user manual*. Dept. of Mathematics, University of Western Australia, Nedlands, 2002.

[52] L. S. Jennings, K. L. Teo, V. Rehbock, and W. X. Zheng, "Optimal control of singular systems with a cost on changing control," *Dynamics and Control*, vol. 6, no. 1, pp. 63–89, 1996.

[53] M. I. Kamien and N. L. Schwartz, *Dynamic optimization: the calculus of variations and optimal control in economics and management*. Courier Corporation, 2012.

[54] C. Y. Kaya and J. L. Noakes, "Computational method for time-optimal switching control," *Journal of optimization theory and applications*, vol. 117, no. 1, pp. 69–92, 2003.

[55] C. Y. Kaya, "Inexact restoration for runge–kutta discretization of optimal control problems," *SIAM Journal on Numerical Analysis*, vol. 48, no. 4, pp. 1492–1517, 2010.

[56] C. Y. Kaya and J. Martínez, "Euler discretization and inexact restoration for optimal control," *Journal of Optimization Theory and Applications*, vol. 134, no. 2, pp. 191–206, 2007.

[57] C. Y. Kaya and J. L. Noakes, "Leapfrog for optimal control," *SIAM journal on numerical analysis*, vol. 46, no. 6, pp. 2795–2817, 2008.

[58] B. Ketheesan and N. Nirmalakhandan, "Modeling microalgal growth in an airlift-driven raceway reactor," *Bioresource technology*, 2013.

[59] B.-H. Kim, J.-E. Choi, K. Cho, Z. Kang, R. Ramanan, *et al.*, "Influence of water depth on microalgal production, biomass harvest, and energy consumption in high rate algal pond using municipal wastewater," *J Microbiol Biotechnol*, vol. 28, no. 4, pp. 630–637, 2018.

[60] C. A. Klausmeier, E. Litchman, and S. A. Levin, "Phytoplankton growth and stoichiometry under multiple nutrient limitation," *Limnology and Oceanography*, vol. 49, no. 4, pp. 1463–1470, 2004.

[61] J. Kromkamp and A. E. Walsby, "A computer model of buoyancy and vertical migration in cyanobacteria," *Journal of Plankton Research*, vol. 12, no. 1, pp. 161–183, 1990.

[62] A. Kumar, S. Ergas, X. Yuan, A. Sahu, Q. Zhang, *et al.*, "Enhanced co2 fixation and biofuel production via microalgae: Recent developments and future directions," *Trends in biotechnology*, vol. 28, no. 7, pp. 371–380, 2010.

[63] H. W. J. Lee, K. L. Teo, V. Rehbock, and L. S. Jennings, "Control parametrization enhancing technique for time optimal control problems," *Dynamic Systems and Applications*, vol. 6, pp. 243–262, 1997.

[64] H. W. J. Lee, K. L. Teo, V. Rehbock, and L. S. Jennings, "Control parametrization enhancing technique for optimal discrete-valued control problems," *Automatica*, vol. 35, no. 8, pp. 1401–1407, 1999.

[65] T. Legovic and A. Cruzado, "A model of phytoplankton growth on multiple nutrients based on the michaelis-menten-monod uptake, droop's growth and liebig's law," *Ecological Modelling*, vol. 99, no. 1, pp. 19–31, 1997.

[66] W.-H. Leong, J.-W. Lim, M.-K. Lam, Y. Uemura, and Y.-C. Ho, "Third generation biofuels: A nutritional perspective in enhancing microbial lipid production," *Renewable and sustainable energy reviews*, vol. 91, pp. 950–961, 2018, ISSN: 1364-0321.

[67] C. Li, K. L. Teo, B. Li, and G. Ma, "A constrained optimal pid-like controller design for spacecraft attitude stabilization," *Acta Astronautica*, vol. 74, pp. 131–140, 2012.

[68] R. Li, K. L. Teo, K. Wong, and G.-R. Duan, "Control parameterization enhancing transform for optimal control of switched systems," *Mathematical and Computer Modelling*, vol. 43, no. 11-12, pp. 1393–1403, 2006.

[69] Q. Lin, R. Loxton, and K. L. Teo, "Optimal control of nonlinear switched systems: Computational methods and applications," *Journal of the Operations Research Society of China*, vol. 1, no. 3, pp. 275–311, 2013.

[70] Q. Lin, R. Loxton, and K. L. Teo, "The control parameterization method for nonlinear optimal control: A survey," *Journal of Industrial and Management Optimization*, vol. 10, no. 1, pp. 275–309, 2014.

[71] Q. Lin, R. Loxton, K. L. Teo, and Y. H. Wu, "Optimal control computation for nonlinear systems with state-dependent stopping criteria," *Automatica*, vol. 48, no. 9, pp. 2116–2129, 2012.

[72] C. Liu, Z. Gong, B. Shen, and E. Feng, "Modelling and optimal control for a fed-batch fermentation process," *Applied Mathematical Modelling*, vol. 37, no. 3, pp. 695–706, 2013.

[73] C. Liu, Z. Gong, *et al.*, *Optimal control of switched systems arising in fermentation processes*. Springer, 2014, vol. 97.

[74] R. Loxton, Q. Lin, and K. L. Teo, "Switching time optimization for nonlinear switched systems: Direct optimization and the time-scaling transformation," *Pacific Journal of Optimization*, vol. 10, no. 3, pp. 537–560, 2014.

[75] R. Luus, "Optimal control by dynamic programming using grids points and region reduction," *Hung. J. Ind. Chem.*, vol. 17, pp. 523–524, 1989.

[76] R. Luus, "Optimal control by dynamic programming using systematic reduction in grid size," *International Journal of Control*, vol. 51, no. 5, pp. 995–1013, 1990.

[77] R. Luus, *Iterative dynamic programming*. Chapman & Hall/CRC: Boca Raton, FL, 2000.

[78] R. Luus and O. N. Okongwu, "Towards practical optimal control of batch reactors," *Chemical Engineering Journal*, vol. 75, no. 1, pp. 1–9, 1999.

[79] F. Mairet, O. Bernard, P. Masci, T. Lacour, and A. Sciandra, "Modelling neutral lipid production by the microalga isochrysis aff. galbana under nitrogen limitation," *Bioresource Technology*, vol. 102, no. 1, pp. 142–149, 2011.

[80] F. Mairet, O. Bernard, T. Lacour, and A. Sciandra, "Modelling microalgae growth in nitrogen limited photobiorector for estimating biomass, carbohydrate and neutral lipid productivities," *IFAC Proceedings Volumes*, vol. 44, no. 1, pp. 10 591–10 596, 2011.

[81] R. B. Martin, "Optimal control drug scheduling of cancer chemotherapy," *Automatica*, vol. 28, no. 6, pp. 1113–1123, 1992.

[82] T. M. Mata, A. A. Martins, and N. S. Caetano, "Microalgae for biodiesel production and other applications: A review," *Renewable and Sustainable Energy Reviews*, vol. 14, no. 1, pp. 217–232, 2010.

[83] MATLAB, *version 7.10.0 (R2010a)*. Natick, Massachusetts: The MathWorks Inc., 2010.

[84] A. Meurer, C. P. Smith, M. Paprocki, O. Čertík, S. B. Kirpichev, *et al.*, "Sympy: Symbolic computing in python," *PeerJ Computer Science*, vol. 3, e103, Jan. 2017, ISSN: 2376-5992. DOI: 10.7717/peerj-cs.103. [Online]. Available: https://doi.org/10.7717/peerj-cs.103.

[85] A. Miele, R. E. Pritchard, and J. N. Damoulakis, "Sequential gradient-restoration algorithm for optimal control problems," *Journal of Optimization Theory and Applications*, vol. 5, no. 4, pp. 235–282, 1970.

[86] A. Miele and T. Wang, "Dual properties of sequential gradient—restoration algorithms for optimal control problems," in *Optimization and Related Fields*, Springer, 1986, pp. 331–357.

[87] A. Miele, T. Wang, and V. K. Basapur, "Primal and dual formulations of sequential gradient-restoration algorithms for trajectory optimization problems," *Acta Astronautica*, vol. 13, no. 8, pp. 491–505, 1986.

[88] L. F. Møller and H. U. Riisgård, "Impact of jellyfish and mussels on algal blooms caused by seasonal oxygen depletion and nutrient release from the sediment in a danish fjord," *Journal of Experimental Marine Biology and Ecology*, vol. 351, no. 1-2, pp. 92–105, 2007, ISSN: 0022-0981.

[89] J. Monod, *Recherches sur la croissance des cultures bacteriennes*. Paris: Hermann, 1942.

[90] J. Monod, "The growth of bacterial cultures," *Annual Review of Microbiology*, vol. 3, no. 1, pp. 371–394, 1949. DOI: 10.1146/annurev.mi.03.100149.002103. eprint: https://doi.org/10.1146/annurev.mi.03.100149.002103. [Online]. Available: https://doi.org/10.1146/annurev.mi.03.100149.002103.

[91] R. Muñoz-Tamayo, F. Mairet, and O. Bernard, "Optimizing microalgal production in raceway systems," *Biotechnology Progress*, vol. 29, no. 2, pp. 543–552, 2013.

[92] M. Negoro, N. Shioji, K. Miyamoto, and Y. Micira, "Growth of microalgae in high co 2 gas and effects of so x and no x," *Applied biochemistry and biotechnology*, vol. 28, no. 1, p. 877, 1991.

[93] H. J. Oberle and W. Grimm, *BNDSCO: a program for the numerical solution of optimal control problems*. Inst. für Angewandte Math. der Univ. Hamburg Germany, 2001.

[94] R. V. O'Neill, D. L. Deangelis, J. J. Pastor, B. J. Jackson, and W. M. Post, "Multiple nutrient limitations in ecological models," *Ecological Modelling*, vol. 46, no. 3-4, pp. 147–163, 1989.

[95] A. Packer, Y. Li, T. Andersen, Q. Hu, Y. Kuang, *et al.*, "Growth and neutral lipid synthesis in green microalgae: A mathematical model," *Bioresource technology*, vol. 102, no. 1, pp. 111–117, 2011.

[96] A. K. Pegallapati and N. Nirmalakhandan, "Modeling algal growth in bubble columns under sparging with CO_2-enriched air," *Bioresource Technology*, vol. 124, pp. 137–145, 2012.

[97] L. Petzold, "Automatic selection of methods for solving stiff and nonstiff systems of ordinary differential equations," *SIAM journal on scientific and statistical computing*, vol. 4, no. 1, pp. 136–148, 1983.

[98] P. T. Pienkos and A Darzins, *The promise and challenges of microalgal-derived biofuels. biofuels bioprod biorefining 3: 431–440*, 2009.

[99] E. Polak, *Optimization: algorithms and consistent approximations*, ser. Applied mathematical sciences. New York: Springer-Verlag, 1997, vol. 124, ISBN: 9780387949710.

[100] E. Polak, "On the use of consistent approximations in the solution of semi-infinite optimization and optimal control problems," *Mathematical programming*, vol. 62, no. 1, pp. 385–414, 1993.

[101] L. S. Pontryagin, V. G. Boltyanskii, R. V. Gamkrelidze, and E. F. Mischenko, *The Mathematical Theory of Optimal Processes*. Wiley-Interscience, New York, 1962.

[102] W. Press, S. Teukolsky, W. Vetterling, and B. Flannery, "Section 18.1. the shooting method," in *Numerical Recipes: The Art of Scientific Computing (3rd ed.)* W. Press, Ed., Cambridge, UK New York: Cambridge University Press, 2007, ISBN: 9780521880688.

[103] O. Pulz and W. Gross, "Valuable products from biotechnology of microalgae," *Applied microbiology and biotechnology*, vol. 65, no. 6, pp. 635–648, 2004, ISSN: 0175-7598.

[104] A. V. Rao, D. A. Benson, G. T. Huntington, C. Francolin, C. L. Darby, *et al.*, "User's manual for GPOPS: A MATLAB package for dynamic optimization using the gauss pseudospectral method," *University of Florida report*, 2008.

[105] I. Rawat, R. R. Kumar, T. Mutanda, and F. Bux, "Biodiesel from microalgae: A critical evaluation from laboratory to large scale production," *Applied Energy*, vol. 103, pp. 444–467, 2013.

[106] V. Rehbock, K. L. Teo, L. S. Jennings, and H. W. J. Lee, "A survey of the control parametrization and control parametrization enhancing methods for constrained optimal control problems," in *Progress in Optimization: Contributions from Australasia*, A. Eberhard, R. Hill, D. Ralph, and B. M. Glover, Eds., vol. vol. 30, Boston, MA: Springer US, 1999, pp. 247–275, ISBN: 978-1-4613-3285-5. DOI: 10.1007/978-1-4613-3285-5_13. [Online]. Available: https://doi.org/10.1007/978-1-4613-3285-5_13.

[107] T. Ruby, "Optimization of hybrid power systems," Thesis, 2003.

[108] S. Sawant, H. Khadamkar, C. Mathpati, R. Pandit, and A. Lali, "Computational and experimental studies of high depth algal raceway pond photo-bioreactor," *Renewable Energy*, vol. 118, pp. 152–159, 2018.

[109] K. Schittkowski, "NLPQLP: A fortran implementation of a sequential quadratic programming algorithm with non-monotone line search-user's guide, version 2.0," *Department of Computer Science, University of Bayreuth*, 2004.

[110] K. Schittkowski, "NLPQL: A fortran subroutine solving constrained nonlinear programming problems," *Annals of operations research*, vol. 5, no. 2, pp. 485–500, 1986.

[111] A. Schwartz, E. Polak, and Y. Chen, *Homepage of RIOTS-the most powerful optimal control problem solver*. [Online]. Available: http://www.schwartz-home.com/RIOTS/.

[112] A. L. Schwartz, "Theory and implementation of numerical methods based on runge-kutta integration for solving optimal control problems," Ph.D. dissertation, University of California, Berkeley, 1996.

[113] H. Seki, M. Takahashi, Y. Hara, and S. Ichimura, "Dynamics of dissolved oxygen during algal bloom in lake kasumigaura, japan," *Water Research*, vol. 14, no. 2, pp. 179–183, 1980, ISSN: 0043-1354.

[114] W. Semmler, H. Maurer, and A. Bonen, "An extended integrated assessment model for mitigation and adaptation policies on climate change," in *Control systems and mathematical methods in economics*, Springer, 2018, pp. 297–317.

[115] Y. C. Sharma, B. Singh, and J. Korstad, "A critical review on recent methods used for economically viable and eco-friendly development of microalgae as a potential feedstock for synthesis of biodiesel," *Green chemistry*, vol. 13, no. 11, pp. 2993–3006, 2011.

[116] J. Sheehan, T. Dunahay, J. Benemann, and P. Roessler, "A look back at the us department of energy's aquatic species program: Biodiesel from algae," *National Renewable Energy Laboratory*, vol. 328, pp. 1–294, 1998.

[117] H. R. Sirisena and F. S. Chou, "Convergence of the control parameterization ritz method for nonlinear optimal control problems," *Journal of Optimization Theory and Applications*, vol. 29, no. 3, pp. 369–382, 1979.

[118] E. Smith, V. Rehbock, and N. Adams, "Deterministic modeling of whole-body sheep metabolism," *Journal of Industrial & Management Optimization*, vol. 5, no. 1, p. 61, 2009.

[119] U. Sommer, "A comparison of the droop and the monod models of nutrient limited growth applied to natural populations of phytoplankton," *Functional Ecology*, pp. 535–544, 1991, ISSN: 0269-8463.

[120] O. von Stryk, "User's guide for DIRCOL version 2.1: A direct collocation method for the numerical solution of optimal control problems," *Report, Lehrstuhl M2 Höhere Mathematik und Numerische Mathematik, Technische Universität München*, 1999.

[121] Y. Sun, G. Aw, K. L. Teo, and G. Zhou, "Portfolio optimization using a new probabilistic risk measure," *Journal of Industrial and Management Optimization*, vol. 11, no. 4, pp. 1275–1283, 2015.

[122] K. L. Teo, C.-J. Goh, and K.-H. Wong, *A unified computational approach to optimal control problems*, eng, ser. Pitman Monographs and Surveys in Pure and Applied Mathematics 55. Harlow, Essex, England: Longman Scientific & Technical, 1991, OCLC: 23653709, ISBN: 9780582078109.

[123] K. L. Teo, G. Jepps, E. J. Moore, and S. Hayes, "A computational method for free time optimal control problems, with application to maximizing the range of an aircraft-like projectile," *The ANZIAM Journal*, vol. 28, no. 3, pp. 393–413, 1987.

[124] A. Trimbee and E. Prepas, "The effect of oxygen depletion on the timing and magnitude of blue-green algal blooms: With 2 figures and 2 tables in the text," *Internationale Vereinigung für theoretische und angewandte Limnologie: Verhandlungen*, vol. 23, no. 1, pp. 220–226, 1988, ISSN: 0368-0770.

[125] I. G. Van Loosen, "Optimization techniques for constrained path problems," Thesis, 2007.

[126] A. Wächter and L. T. Biegler, "On the implementation of an interior-point filter line-search algorithm for large-scale nonlinear programming," *Mathematical Programming*, vol. 106, no. 1, pp. 25–57, 2006, ISSN: 1436-4646. DOI: 10.1007/s10107-004-0559-y. [Online]. Available: https://doi.org/10.1007/s10107-004-0559-y.

[127] "What Happened To Sapphire Energy?" *Algae World News*, Apr. 2017. [Online]. Available: https://news.algaeworld.org/2017/04/happened-sapphire-energy/.

[128] P. J. L. B. Williams and L. M. L. Laurens, "Microalgae as biodiesel & biomass feedstocks: Review & analysis of the biochemistry, energetics & economics," *Energy & Environmental Science*, vol. 3, no. 5, pp. 554–590, 2010.

[129] L. Xiao and X. Liu, "An effective pseudospectral optimization approach with sparse variable time nodes for maximum production of chemical engineering problems," *The Canadian Journal of Chemical Engineering*, vol. 95, no. 7, pp. 1313–1322, 2017.

[130] J. Yuan, Y. Zhang, J. Ye, J. Xie, K. L. Teo, *et al.*, "Robust parameter identification using parallel global optimization for a batch nonlinear enzyme-catalytic time-delayed process presenting metabolic discontinuities," *Applied Mathematical Modelling*, vol. 46, pp. 554–571, 2017.

[131] W. Zhong, Q. Lin, R. Loxton, and K. Lay Teo, "Optimal train control via switched system dynamic optimization," *Optimization Methods and Software*, pp. 1–25, 2019.

[132] G. C. Zittelli, L. Rodolfi, N. Bassi, N. Biondi, and M. R. Tredici, "Photobioreactors for microalgal biofuel production," in *Algae for biofuels and energy*, M. A. Borowitzka, Ed., vol. 5, Springer, 2013, pp. 115–131.